



# A Study of Ni/V Contamination and Interaction in Cracking Catalyst

**Thanong Hongdul**

**Master of Engineering Thesis in Chemical Engineering**

**Prince of Songkla University**

**2002**

Call No.	TP690.4 T42 2002 c.2
Bib Key	220642
	2.1 311.1. 2542


(1)


Thesis Title      A Study of Ni/V Contamination and Interaction in Cracking Catalyst

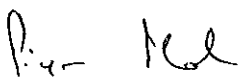
Author             Mr. Thanong Hongdul

Major Program    Chemical Engineering


Advisory Committee

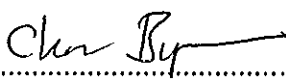
.....Chairman  
(Associate Professor Dr. Chakrit Tongurai)

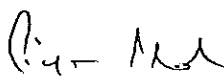
.....Committee  
(Dr. Charun Bunyakan)


.....Committee  
(Professor Dr. Piyasan Prasertthdam)


Examining Committee

.....Chairman  
(Associate Professor Dr. Chakrit Tongurai)

.....Committee  
(Dr. Charun Bunyakan)

.....Committee  
(Professor Dr. Piyasan Prasertthdam)

.....Committee  
(Dr. Sutham Sukmanee)

.....Committee  
(Associate Professor Dr. Sumpun Wongnawa)

The Graduate School, Prince of Songkla University, has approved this thesis as partial fulfillment of the requirement for the Master of Engineering degree in Chemical Engineering.



.....  
(Piti Trisdikoon, Ph.D.)

Associate Professor and Dean, Graduate School

ชื่อวิทยานิพนธ์	การศึกษาการปนเปื้อนและอันตรายของนิกเกิลและวานาเดียมของตัวเร่งปฏิกิริยาการแตกตัว
ผู้เขียน	นายทง ห่องดุษย์
สาขาวิชา	วิศวกรรมเคมี
ปีการศึกษา	2544

### บทคัดย่อ

ปัจจุบันสารปนเปื้อนในกระบวนการแตกตัวฟลูอิดไดซ์ มีสารปนเปื้อนเช่นนิกเกิล วานาเดียม โลหะอัลคาร์ไลน์เอิร์ท ในปริมาณที่สูง การตรวจสอบผลของการปนเปื้อนนั้นถูกจำกัดจากเวลาที่ใช้ในการศึกษาในระดับโรงงานขนาดเล็ก หรือความยากและไม่แม่นยำของการศึกษาในระดับห้องปฏิบัติการ การจำลองตัวเร่งปฏิกิริยาสมดุลงจากการปนเปื้อนโลหะตัวเร่งปฏิกิริยาใหม่สดจึงจำเป็นในการศึกษาพฤติกรรมของตัวเร่งปฏิกิริยาสมดุลง นำมาสู่จุดประสงค์ของงานวิจัยนี้ซึ่งทำขึ้นเพื่อประเมินเทคนิคในการปนเปื้อน นิกเกิล/วานาเดียม บนตัวเร่งปฏิกิริยาใหม่สดในกระบวนการแตกตัวฟลูอิดไดซ์ เพื่อให้ใกล้เคียงตัวเร่งปฏิกิริยาสมดุลง และศึกษาผลต่อสมบัติการแตกตัวโดยใช้หน่วยทดสอบทางจุลทรรศน์ภาพ

ภาวะที่เหมาะสมในการปนเปื้อนประกอบด้วย ให้ความร้อนตัวเร่งปฏิกิริยาที่อุณหภูมิ 600 องศาเซลเซียสเป็นเวลา 1 ชั่วโมง ปนเปื้อนนิกเกิล และ/หรือ วานาเดียม หลังจากนั้นนำไปลดความว่องไวโดยการผ่านด้วยไอน้ำอิมตัวที่อุณหภูมิ 800 องศาเซลเซียสเป็นเวลา 6 ชั่วโมง การปนเปื้อนนิกเกิลจะส่งผลในการเกิดปฏิกิริยาการตั้งไฮโดรเจนอย่างมากแต่พื้นที่ผิวจะลดลงค่อนข้างน้อย ส่วนการปนเปื้อนวานาเดียมแสดงให้เห็นว่าเกิดการทำลายโครงสร้างของซีโอไลต์เป็นอย่างมากอย่างรุนแรง และส่งผลให้พื้นที่ผิวลดลงมากหลังจากกระบวนการลดความว่องไวด้วยไอน้ำ วานาเดียมจะส่งผลต่อปฏิกิริยาการตั้งไฮโดรเจนน้อยกว่านิกเกิล การปนเปื้อนทั้งนิกเกิลและวานาเดียมพร้อม ๆ กันจะส่งผลให้เกิดปฏิกิริยาเร่งการทำลายโครงสร้างของซีโอไลต์ ซึ่งจะพบได้เมื่อตัวเร่งปฏิกิริยามีนิกเกิลและวานาเดียมในปริมาณที่สูง ผลที่ได้จากการทดลองนี้จะนำไปใช้ในการจำลองตัวเร่งปฏิกิริยาสมดุลง และศึกษาพฤติกรรมการปนเปื้อนโลหะต่อไป

Thesis Title	A Study of Ni/V Contamination and Interaction in Cracking Catalyst
Author	Mr. Thanong Hongdul
Major Program	Chemical Engineering
Academic Year	2001

### Abstract

These days, FCC's feedstocks have a high amount of impurities such as nickel, vanadium, and alkaline-earth metals. Previously, the investigations of metal contamination effects were limited to long term pilot scale studies or to the difficult and inaccurate bench-scale studies. Simulation of an equilibrium catalyst containing metal contamination was needed to study the equilibrium catalyst behavior. This work aims at evaluating nickel/vanadium impregnation techniques to gain an equivalent equilibrium catalyst from FCC fresh catalyst and investigating their effects on catalytic properties by micro-activity testing unit.

The satisfied metal impregnation techniques consisted of heat shock fresh catalyst at 600 °C for 1 hour, impregnation of nickel and vanadium, and then steam deactivation at 800 °C for 6 hours. Nickel contamination had a strong effect on dehydrogenation reaction and a slight effect on loss of surface area. Vanadium contamination showed a great destruction of zeolite structure and resulted in a high reduction of surface area after the deactivation process. Vanadium had less effect on dehydrogenation than nickel (1/5 times). Combined nickel and vanadium contamination resulted in a synergistic effect detrimental to zeolite structure, which was found at the high level of nickel and vanadium. These results were used to simulate the equilibrium catalyst and to study the metal contamination behavior.

## Acknowledgment

I would like to express deep gratitude to the following individuals and organizations:

To Associate Professor Dr. Chakrit Tongurai, my advisor, for his valuable guidance, encouragement and support throughout my work. His expertise is something that I admire and appreciate. I am very proud of having him as an advisor.

To Dr. Charun Bunyakan and Professor Dr. Piyasan Prasertdam, my co-advisor, for their helpful advice and support during my graduate research and education.

To Dr. Sutham Sukmanee and Associate Professor Dr. Sumpun Wongnawa, for their advice and the proof reading of my thesis.

To my friend, Mr. Sutha Onkam, for his valuable advice.

To all staff at Chemical Engineering Department, for their help during my graduate education.

To the Graduate School for the financial support of my thesis.

Finally, I would like to express my deepest appreciation to my parent and my sisters for their love and attention through out my life.

Thanong Hongdul

## Contents

	Page
Abstract	(3)
Acknowledgment	(5)
Contents	(6)
List of Tables	(9)
List of Figures	(10)
Chapter	
1. Introduction	1
1. Introduction	1
2. Literature Review	3
3. Objectives	43
4. Possible Achievements	43
5. Contents of Research	44
2. Experimentation	45
1. Feedstocks and catalysts	45
2. Equipment and Materials	46
3. Instruments	47
4. Experiment and Procedure	48
- Impregnation Method	48
- Experiment	48

	Page
5. Test Procedure and Test Conditions	50
3. Results and Discussion	56
1. Investigation of the appropriate condition for impregnation method	56
- The sequences of the impregnation method	56
2. Evaluation of the effect of Nickel, Vanadium, Nickel+Vanadium on catalyst surface area	57
3. Investigation of effect of nickel contamination on the catalytic properties	59
4. Investigation of effect of vanadium contamination on the catalytic properties	62
5. Effect of both nickel and vanadium on catalytic properties	67
4. Conclusions	76
Bibliography	78
Appendix	
A – The acid digestion process for zeolite	85
B – True boiling point distillation unit (TBP)	86
C – Hydrothermal deactivation (By CLY-1 Hydrothermal Aging Unit)	91
D – Micro-Activity Unit	95

	Page
E – Gas Chromatography set and Integrator (GC-14B)	105
F – Gas Chromatography set and Integrator (GC-14A)	111
G – Surface Area and Pore Size Analyzer	114
H – Table of result	127
Vitae	132



## List of Tables

Table	Page
1-1 Antimony Passivation at Low Nickel Level	34
1-2 Ranking of Elements for reduction of Hydrogen	42
2-1 Properties of gas oil	45
2-2 Catalysts used in experiments	46
3-1 Surface area and pore volume of catalyst from experiment 3.1.1	57
3-2 Percent of crystallinity reduction with metal content on catalyst E	75
D-1 Feed oil: gas oil (light cycle oil, LCO) obtained from RIPP	102
D-2 Blank test for checking liquid recovery	102
E-1 MAT operation report	110
H-1 Test the sequence of impregnation method	127
H-2 Effect of nickel on surface area	127
H-3 Effect of vanadium on surface area	128
H-4 Effect of nickel/vanadium on surface area	128
H-5 Effect of nickel on catalytic properties (Catalyst A)	129
H-6 Effect of nickel on catalytic properties (Catalyst E)	129
H-7 Effect of vanadium on catalytic properties (Catalyst A)	130
H-8 Effect of vanadium on catalytic properties (Catalyst E)	130
H-9 Effect of nickel/vanadium on catalytic properties (Catalyst E)	131

## List of Figures

Figure	Page
1-1 Reactor/Regenerator	5
1-2 Main fractionator	11
1-3 Gas concentration unit	13
1-4 Metals degrade surface area	18
1-5 Relative activity loss due to metals	23
1-6 Antimony passivates metals on FCC catalyst Data for 75 vol.%conversion of West Texas topped crude on equilibrium catalyst from HOC at 950°F	28
1-7 Effect of antimony on high nickel catalysts	35
1-8 Effect of Bismuth Level	36
1-9 Tin maintains catalyst surface area and MAT activity	39
2-1 Schematic for typical MAT unit	51
3-1 Effect of impregnation sequence on nickel content	56
3-2 Effect of nickel content on surface area	57
3-3 Effect of vanadium content on surface area	58
3-4 Vanadium deactivation mechanism	58
3-5 Effect of vanadium content on surface area	59
3-6 Effect of nickel content on percent H <sub>2</sub> (feed basis) and percent conversion	60

Figure	Page
3-7 Effect of nickel content on percent conversion and percent gasoline yield	60
3-8 Effect of nickel content on coke yield	61
3-9 Effect of nickel content on gas yield	62
3-10 Effect of vanadium content on percent H <sub>2</sub> (feed basis) and percent conversion	62
3-11 Effect of vanadium content on percent conversion and percent gasoline yield	63
3-12 Effect of nickel/vanadium on percent conversion (CAT A)	64
3-13 Effect of vanadium on percent conversion and relative surface area	64
3-14 Effect of vanadium on coke yield	65
3-15 Effect of vanadium on coke selectivity	65
3-16 Effect of vanadium on gas yield	66
3-17 Effect of vanadium on gas selectivity	66
3-18 Effect of nickel equivalent on percent H <sub>2</sub>	67
3-19 Effect of nickel equivalent on H <sub>2</sub> selectivity	68
3-20 Effect of nickel/vanadium on surface area	69
3-21 Effect of nickel/vanadium on percent relative surface area	70
3-22 Effect of nickel/vanadium on percent conversion	71
3-23 Effect of nickel/vanadium on percent gasoline yield	71

Figure	Page
3-24 Effect of nickel/vanadium on coke yield	72
3-25 Effect of nickel/vanadium on coke selectivity	73
3-26 Effect of nickel/vanadium on gas yield	74
B-1 True boiling point distillation unit	90
C-1 Hydrothermal aging unit	94
D-1 The process diagram of MAT unit	96
D-2 Microactivity test unit	104
E-1 Gas Chromatograph unit	107
E-2 Chromatogram of n-dodecane (n-C <sub>12</sub> )	108
E-3 Temperature profile during catalytic cracking	108
E-4 Chromatogram of gas oil (LCO) before react with catalyst	109
E-5 Chromatogram of liquid after reacted with catalyst	109
F-1 Calibration curve of hydrogen gas	113
G-1 SA 3100 analyzer front view	119
G-2 SA 3100 analyzer back view	120

## Chapter 1

### INTRODUCTION

#### Introduction

The upgrade of heavy fractions into gasoline and middle distillates is becoming a main focus, since the market demand of heavy fractions is steadily decreasing; especially one possible route of heavy fractions conversion called *Fluid Catalytic Cracking (FCC)*. However, resid-cracking leads to severe problems, one of the most important is the high metal, mainly nickel and vanadium content of these fractions. Nickel is a catalyst for dehydrogenation reactions. Vanadium—the predominant effect of vanadium is to induce catalyst deactivation by a progressive and destructive attack of the active zeolite components. Vanadium at low levels can also exhibit significant hydrogenation properties (Cardet et al., 1991). Due to their abilities to catalyze dehydrogenation reactions, these deposited metals soon after the product distribution obtained from FCC units if they are allowed to reach certain maximum levels. As the level of metal contaminants increases, the yields of carbon and hydrogen increase at the expense of gasoline production (Mitchell., 1980).

The laboratory evaluation of Fluid Catalytic Cracking (FCC) catalysts has evolved into a common method for measuring performance characteristics of experimental and commercial catalyst samples. By applying the Micro-Activity Test Unit (MAT Unit), the most common method virtually employed within every laboratory, the MAT procedure employed for such testing, is generally equivalent to

that employed for metals free evaluations. The most noticeable problem that needs to be addressed is that the feedstock used for many metal tolerance studies. Therefore, the condition that makes fresh catalyst like equilibrium catalyst in the refinery process was found out.

Department of Chemical Engineering, Prince of Songkla University was responsible for works to accommodate the future development of petroleum refining and petrochemical industries of Thailand; especially in southern of Thailand. Preliminary work was begun by evaluating the fresh and equilibrium catalysts collected from Chinese and Thai refineries, and also using feedstocks from Chinese and Thai refineries (Angkasuwan, 1999). Then the faculty is also interested in zeolite and catalyst such as Y zeolite (Tuntragul, 2000) USY zeolite (Ritthichai, 2001) and REY catalyst (Kritsanaphak, 2001). But the laboratory couldn't simulate the entire FCC unit because the feedstocks, used in the FCC unit have contaminant so that the catalyst was contaminated. The suitable procedure that makes the laboratory closed to the FCC unit is using the heavy feedstocks and the contaminated catalyst. In this research used the Fang Standard Gas Oil (boiling point 260-340<sup>o</sup>C) and sought the condition, made the fresh impregnation catalyst liked the contaminated catalyst.

## Literature Review

Fluid catalytic cracking unit (FCCU) is one of the most important conversion processes in the petroleum refinery. The main purpose of the unit is to convert high boiling petroleum fractions called *gas oil* to high-value, high-octane gasoline and heating oil. Gas oil is the portion of crude oil that boils in the 650-1050°F (330-550°C) range and contains a diversified mixture of paraffins, naphthenes, aromatics, and olefins (Sadeghbeigi, 1995). FCCU is primarily a gasoline maker but it can also be operated to produce large quantities of C<sub>3</sub>'s and C<sub>4</sub>'s or home heating fuel. The cat cracker is the principle source of light olefin feed to alkylation units. It also provides a great deal of the isobutane feed. FCCU's are a source of C<sub>3</sub>'s and C<sub>4</sub>'s for feed to petrochemical plants and source of LPG (Liquid Petroleum Gas) for use in home heating and cooking (Grace Davidson, 1993).

The operating flexibility of the FCCU allows it not only to satisfy its normal production requirements but also to crack additional feeds from other refinery units to help in balancing the total refinery operation. A cat cracker can readily adjust to a wide variety of feedstocks of differing quality. This allows refiner latitude in the selection of the crude oil that he will charge to his refinery (Grace Davidson, 1993).

### 1. Fluid Catalytic Cracking Unit (Joseph, 1997)

A modern fluid catalytic cracking unit consists of three main sections: The reactor/regenerator, the main fractionator and the gas recovery section (also known as

the gas concentration unit or the vapor recovery unit). In addition to these primary sections the feed is preheated in the feed preheat system, and the flue gas from the regenerator is processed in the flue gas system.

### **1.1 Feed Preheat System**

Oil feed to the reactor is first heated to the desired feed preheat temperature. This is usually done by heat exchange with intermediate heat removal pumparounds from the main fractionator. While feed preheat systems differ greatly from unit to unit, the feed will normally be heated by exchange with the light cycle oil, heavy cycle oil and/or bottoms pumparounds. Typically this will raise the feed temperature to 300-500°F. This is generally sufficient for most FCCUs. In some cases, however, a feed preheat furnace is included to further raise feed temperature prior to its injection into the riser.

### **1.2 Reactor/Regenerator System**

Following feed preheat, the hot feed is injected into the base of the riser where it contacts hot catalyst from the regenerator. Contact with the hot catalyst vaporizes the feed and the mixture of hot catalyst and oil vapors travels up the riser.

Cracking reactions occur as the oil vapor and catalyst flow up the riser. Overall these reactions are endothermic and thus, the temperature in the riser decreases as the reaction progresses. Typically, the temperature will fall 40-70°F from the feed injection zone to the riser outlet. Residence times in the riser are typically 1-4 seconds, and the vast majority of the cracking reactions occur during this brief period.

At the end of the riser, the product vapors and the catalyst flow through a riser termination device (RTD) which separates the catalyst from the hydrocarbon vapors.



A quick separation is essential since the "spent" catalyst leaving the riser actually retains considerable activity. If this catalyst were to remain in contact with the oil vapors, additional-and undesirable-reactions would occur.

Catalyst separated in the riser termination device is directed into the spent catalyst stripper. Hydrocarbon vapors from the RTD enter the reactor vessel.

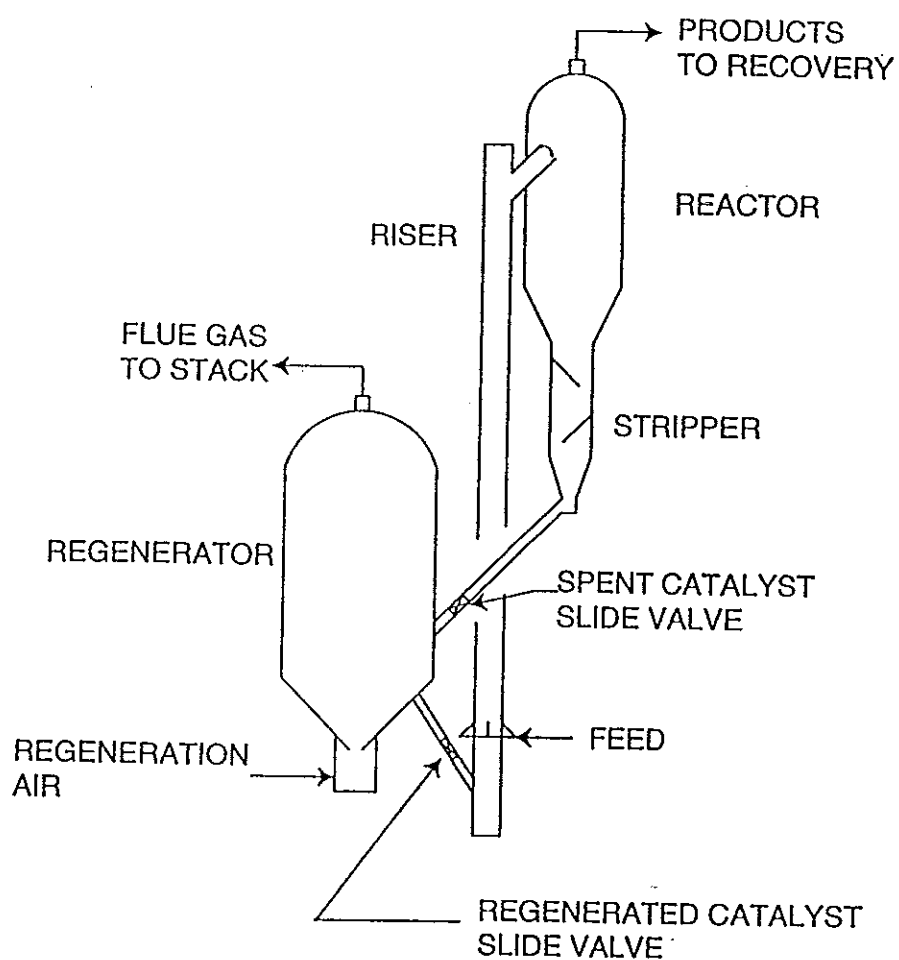


Figure 1-1 Reactor/Regenerator.

Source: Joseph W. Wilson, 1997: 11

In today's riser cracking units, the reactor vessel plays only a minor role in the actual cracking reactions. In fact, the reactions that do occur in this vessel are generally considered to be undesirable. The primary functions of the reactor vessel today are to provide some disengagement space between the riser termination device and the reactor cyclones and to contain both the RTD and the cyclones. Given this changed role, the term "reactor" is somewhat misleading. Some, in fact, prefer to use the term "disengager" when referring to this vessel.

The product vapors entering the reactor from the RTD are mixed with steam and hydrocarbon vapors leaving the spent catalyst stripper. This combined gas flow passes through the disengager and into the reactor cyclones. These may be single- or double-stage, but single-stage high efficiency systems are generally preferred for units with efficient riser termination devices.

The reactor cyclones remove any catalyst not separated by the RTD. This catalyst flows down the cyclone diplegs into the spent catalyst stripper. Vapors from the reactor cyclones flow through the reactor plenum and into the reactor overhead line.

Spent catalyst from the RTD and the reactor cyclones flows into the spent catalyst stripper. This catalyst still contains a considerable volume of product vapors. If not separated, these hydrocarbons will be carried into the regenerator where they will be burned. In the stripper, the catalyst is contacted with steam which displaces the hydrocarbon vapors. The bulk of the steam is injected at the bottom of the stripper and flows upward through the stripper while the spent catalyst flows downward. Most

strippers are equipped with a series of baffles to improve the mixing between steam and catalyst.

Steam and stripped hydrocarbons flow out through the top of the stripper and mix with product vapors leaving the riser termination device. The stripped catalyst exits from the bottom of the stripper and enters the spent catalyst standpipe. Depending on the unit design, steam may be injected into the standpipe to improve the flow of catalyst.

At the bottom of the spent catalyst standpipe the catalyst flows through the spent catalyst control valve. This is normally a slide valve. This valve serves to control the flow of catalyst from the stripper and thus the stripper bed level. From the spent catalyst standpipe the catalyst flows into the regenerator.

In the regenerator the spent catalyst is contacted with air from the main air blower. The catalyst and air are well-mixed in a fluid bed or fast fluid bed and the carbon (coke) deposited on the catalyst during the cracking reaction is burned off. The heat produced by the combustion of the coke deposits raises the temperature of the catalyst by 300-400°F. Flue gases leaving the regenerator catalyst bed pass through the regenerator cyclones where entrained catalyst is removed and returned to the regenerator bed. Flue gases leaving the cyclones pass through the regenerator plenum and into the flue gas system.

Hot regenerated catalyst leaves the regenerator through the catalyst withdrawal hopper and flows into the regenerated catalyst standpipe. As with the spent catalyst standpipe, this standpipe may require aeration to assure smooth catalyst flow. Air is the preferred medium for aeration of regenerated catalyst standpipes.

Catalyst leaving the regenerated catalyst standpipe flows through the regenerated catalyst control valve and into the base of the riser where it contacts the fresh feed. The regenerated catalyst control valve controls the quantity of hot catalyst entering the riser and thus, the riser outlet temperature.

### **1.3 Flue Gas System**

The regenerator flue gas passes through the flue gas slide valves, which control regenerator pressure, and into the flue gas line. In some cases, the flue gas flows directly to the stack where it is discharged into the atmosphere. In most units, however, the flue gas system contains additional equipment to recover energy (power recovery turbines, CO boilers and/or flue gas coolers) and to remove undesirable materials prior to discharge (third stage separators, electrostatic precipitators, flue gas scrubbers).

### **1.4 Main Fractionator**

Hydrocarbon products from the reactor cyclones flow through the reactor overhead line and into the bottom of the main fractionator. This tower is somewhat unusual since the tower feed is a superheated vapor which must be cooled before any liquid products can be condensed

In the bottom of the main fractionator (the desuperheating zone), the hot vapors from the reactor are contacted by cooled circulating tower bottoms liquid; the vapors are cooled and the bottoms product is condensed. This part of the tower is normally equipped with either shed deck or disc and donut style baffles, but structured grids have also been used successfully.

Circulating liquid plus the net bottom products are withdrawn from the bottom of the tower. This stream is cooled, usually by exchange with fresh feed and by steam production in the bottoms steam generator(s). The net product is separated from the circulating liquid stream, cooled further and sent to storage or other use. The circulating liquid stream is returned to the tower at the top of the desuperheating section.

Vapors from the superheating zone pass up through the tower where they are cooled further by circulating heavy cycle oil (HCO). This pumparound stream is normally cooled by heat exchange with fresh feed and reboilers in the gas concentration unit. The HCO pumparound may also be cooled by heat exchange with cold boiler feed water or by air or water trim coolers.

Following the HCO pumparound section, light cycle oil (LCO) is withdrawn from the tower and sent to the LCO stripper. In the LCO stripper, the product liquid is stripped by direct steam injection to control the quantity of low boiling hydrocarbons and thus, the product flash point. LCO from the bottom of the stripping tower is cooled and sent to storage.

Heat removal from the midsections of the main fractionator is by and LCO and/or heavy naphtha pumparound. The heat removed is used to preheat fresh feed, reboil towers' in the gas concentration unit or to preheat boiler feed water. In some main fractionators, there is a heavy catalytic naphtha (HCN) side draw above the light cycle oil. In these towers, the HCN is usually stripped in the steam stripper for flash point control.

The overhead products from the main fractionator consist of cat naphtha (gasoline), C<sub>3</sub> and C<sub>4</sub> LPG and dry gas (C<sub>2</sub> and lighter materials plus inerts carried into the reactor by the catalyst). This overhead gas is condensed in the partial condenser, and the gases and liquids are separated in the overhead separator drum. A portion of the condensed liquid is returned to the main fractionator as reflux, and the net overhead liquid is pumped to the gas concentration unit. Gases from the overhead drum flow to the wet gas compressor located in the gas concentration unit.

### 1.5 Gas Concentration Unit

The gas concentration unit (GCU) provides recovery of the C<sub>3</sub> and C<sub>4</sub> LPG produced in the FCC and separation of the lighter liquid products. Gas from the main fractionator overhead drum flows to the wet gas compressor. This is usually a two-stage machine. The first stage discharge is cooled and partially condensed in the interstage cooler and the liquid and gas streams are separated in the interstage separator drum. The liquid is pumped to the high pressure condensers and the gas flows to the second stage of the gas compressor.

The gas discharge from the second stage of the gas compressor is combined with the primary absorber bottoms liquid, the stripper overhead vapors and the liquid from the compressor interstage drum. This combined streamflows through the high pressure condensers and into the high pressure separator. Gas from the high pressure separator flows to the primary absorber column.

Overhead liquid from the main fractionator is pumped to the primary absorber serve as lean oil. In some cases, debutanizer bottoms liquid may also pumped to the primary absorber to increase the lean oil rate and thus, the propylene recovery.

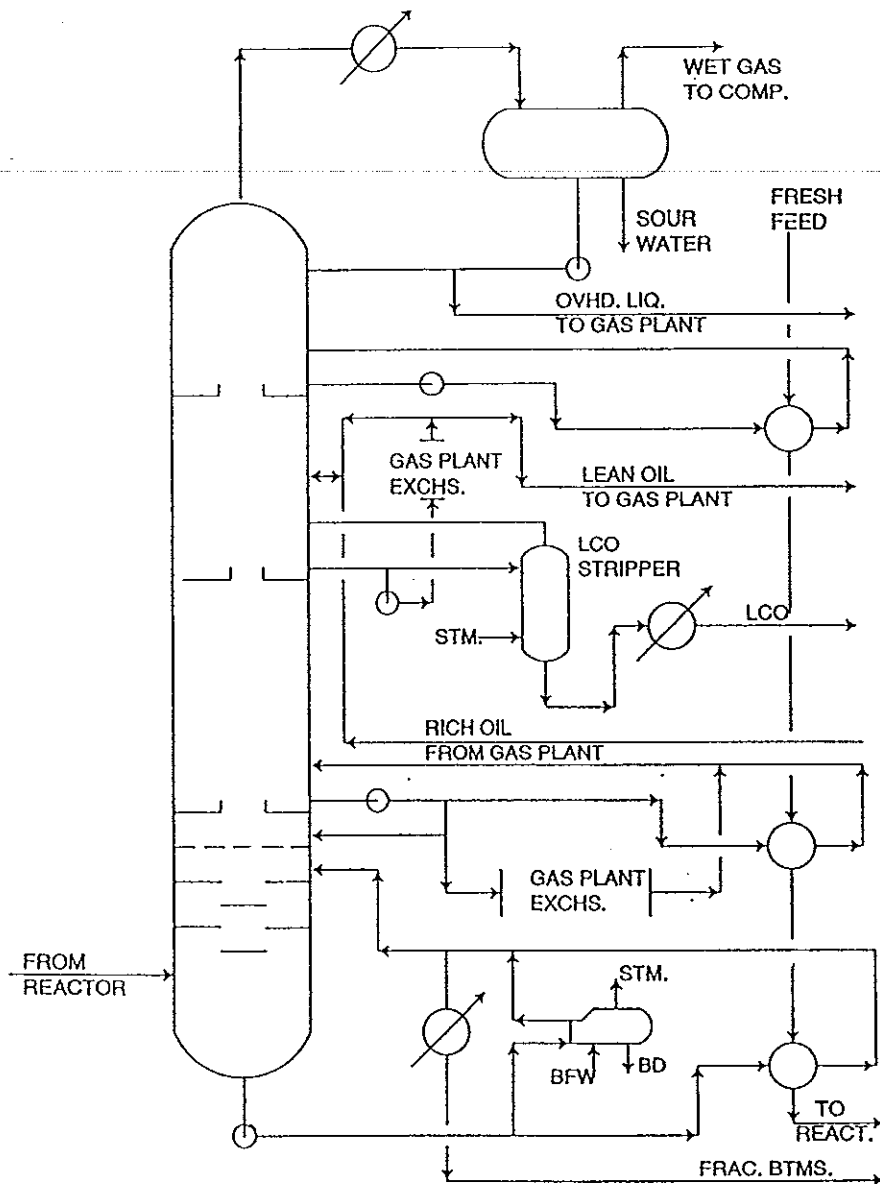


Figure 1-2 Main fractionator.

Source: Joseph W. Wilson, 1997: 15

$C_3$  &  $C_4$  LPG recovered in the primary absorber flow with the absorber bottoms to the high pressure condenser. Primary absorber overhead gas flows to the secondary or sponge absorber.

The sponge absorber is intended to capture gasoline range material (mostly C<sub>5</sub>S) lost to the gas in the primary absorber. Lean oil is either unstripped light cycle oil or unstripped heavy naphtha from the main fractionator. The lean sponge oil is cooled, first by exchange with the sponge absorber bottoms and then by air or water coolers. Rich sponge oil from the absorber is returned to the main fractionator where the absorbed gases are vaporized and returned to the GCU by way of the gas compressor. The absorber overhead flows to treating and from there to the refinery fuel gas system.

Liquid from the high pressure separator is pumped to the top of the stripper (de-ethanizer) tower. This tower removes ethane and lighter materials from the recovered liquid and is generally reboiled using heat from the main fractionator LCO or HCN pumparound. Gas leaving the top of the stripper flows to the high pressure condenser. The bottoms liquid, which contains the total liquid recovered in the GCU, is preheated by exchange with the debutanizer bottoms liquid and fed to the debutanizer column.

The butanizer separates the recovered liquids into LPG and naphtha. This is a conventional distillation column. Heat for the reboiler is supplied by the HCO pumparound from the main column. The overhead vapors are totally condensed and supercooled in the overhead condenser. A part of the condensed liquid is returned to the tower as reflux and the remainder is yielded as LPG product.

Bottoms from the debutanizer are cooled by exchange with the tower feed and then by air or water coolers. A portion of the cooled bottoms stream may be returned to the primary absorber as *recycle lean oil* and the remainder is yielded as the net gasoline product from the GCU.



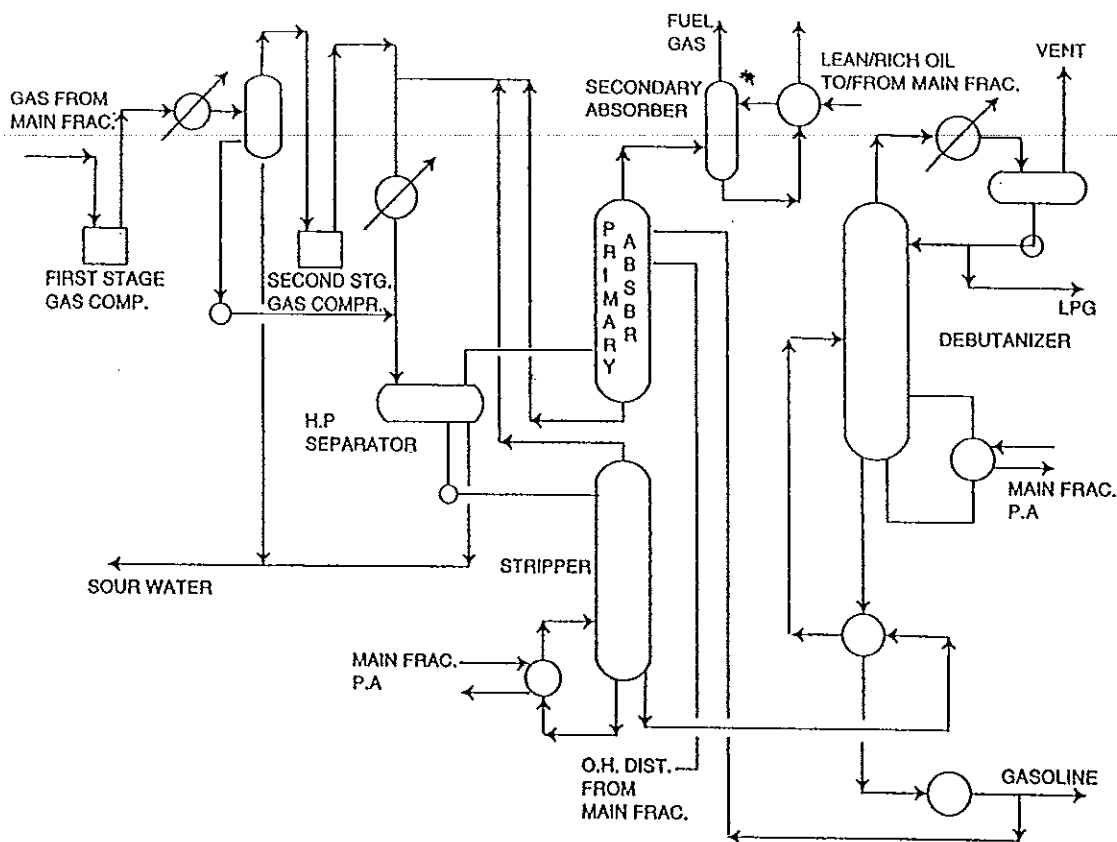


Figure 1-3 Gas concentration unit.

Source: Joseph W. Wilson, 1997: 17

In some cases, the LPG from the overhead of the debutanizer flows to a depropanizer where it is separated into separate C<sub>3</sub> and C<sub>4</sub> products. Similarly, the gasoline product can also be split into light and heavy fractions.

LPG produced in the FCCU contains both hydrogen sulfide and mercaptan compounds. These must be removed. Typically, the LPG is treated in an amine absorption tower to remove the H<sub>2</sub>S, and in a mercaptan extraction unit to remove the mercaptan sulfur.

The naphtha produced also contains mercaptans. These corrosive sulfur compounds are normally converted to disulfides in a sweetening unit.

## **2. Fluid Catalytic Cracking Catalyst Deactivation (Grace Davidson, 1993)**

Fluid catalytic cracking catalysts are deactivated by the coking process during the cracking reaction, by the effects of regeneration and by feedstock contaminants. Deactivation can be temporary or permanent in nature, depending on the type and cause of the deactivation process. This section will start with a review of catalyst activity loss due to the time, temperature and steam effects of regeneration. Catalyst coking and deactivation from feed contaminants are covered in following sections.

### **2.1 Thermal and Hydrothermal Deactivation (Grace Davidson, 1993)**

Thermal deactivation of catalyst is a permanent deactivation that occurs at very high temperatures such as those caused by feed reversals (feed accidentally going directly into a regenerator instead of up a riser) and excessive exposure to torch oil. Thermal deactivation effects are usually more severe than those caused by pure hydrothermal (steam) deactivation, although there is always some steam present in regenerators.

Activity loss from thermal effects is caused by melting of a catalyst's active structures. It can be detected by loss of pore volume, surface area and the formation of certain alumina phases. Analyses of equilibrium catalysts that have been thermally deactivated show the presence of significant amounts of materials such as cristobalite and mullite that are produced at temperatures in excess of 1800°F.

Hydrothermal deactivation, also a permanent loss of catalyst activity, is the more prevalent mechanism for activity loss during the regeneration cycle. Hydrothermal deactivation results from zeolite dealumination and subsequent crystallinity (and surface area) loss, as well as pore size shifts and surface area loss in the matrix.

Steam is always present in the FCCU regenerators. It represents about 15 to 25 V% of the gaseous mixture in typical single-stage regenerators. Steam time and temperature expels aluminum atoms from the zeolite structure, which causes a significant portion of them to collapse. Some zeolite actually “dealuminates” to a lower unit cell size without collapsing. The dealumination mechanism is similar to, though an uncontrolled version of the manufacturing step involving steam calcination of the Standard-Y zeolites to make USY.

Aging effects and catalyst deactivation can be minimized by using catalyst with “stable” components. Catalyst stability has many definitions; percent surface area retention, percent MAT retention and percent selectivity retention are some of the more common. Catalyst stability is an inherent catalyst property based on type and manufacture of catalyst components.

Coke-selective catalysts also have advantages if the unit is run with lower regenerator temperatures as a consequence. Lower regenerator temperatures result in a lower rate of deactivation.

The most important issue in maintaining catalyst activity is proper catalyst management, meaning an adequate fresh addition policy. When metals contaminants are not an issue, that is when unit activity is primarily dictated by thermal and

hydrothermal mechanisms, most units need at least a 1% of inventory per day replacement rate (2 tons/day for 200 ton catalyst inventory), or 0.2 lb. of fresh catalyst per barrel of feed.

## **2.2 Deactivation by Coking (Grace Davidson, 1993)**

Coke is necessary to cat cracker performance because it serves as a fuel to provide all the energy requirements of the process. Unfortunately, coke causes effective catalyst activity to decline as it deposits on the catalyst as a byproduct of the cracking reaction.

This is a temporary activity loss during the time that oil is in contact with the catalyst—commonly known as the “catalyst contact time.” Once coke is burned off in the regeneration step, intrinsic activity is restored unless permanent deactivation by other mechanisms occur. Deactivation by coking can be lessened both by limiting contact time between catalyst and feedstock and by efficient regeneration. Either process improves the activity and selectivity of the catalyst.

Most modern cat crackers are riser crackers with very short reaction times. Many FCCU's also are designed to provide rapid separation of cracked products and catalyst in disengagers to limit catalyst deactivation by coke, as well as to prevent undesirable cracking reaction. Units that do not have provisions for rapid separation of cracked products and catalyst can benefit by installation of such a system. Converting a reactor to allow rapid catalyst/cracked-product separation is a major unit modification.

## 2.3 Deactivation by Feedstock Contaminants (Magee and Mitchell Jr., 1993)

An important factor behind the growth of resid cracking is the development of heavy metal passivation technology. Compared to gas oils, resids usually contain high concentrations of heavy metals (nickel, vanadium, and iron) primarily in the form of porphyrin complexes and salts of organic acids. Under cracking conditions, metals, notably nickel and vanadium in gas oils as well as resids, deposit on the cracking catalyst and catalyze undesirable dehydrogenation reactions. High sodium levels poison acid sites of the cracking catalyst. Vanadium (and possibly sodium) under the conditions of the FCCU regenerator destroy the zeolitic component of the catalyst. Active metals reduce the yield of gasoline and increase the yields of hydrogen and coke. Since most cracking units can handle only limited amounts of hydrogen and coke, the level of active metals on the catalyst must be controlled in order to achieve maximum throughput and profit.

### 2.3.1 Chemistry of deactivation

Both nickel and vanadium function as dehydrogenation catalysts at FCC reactor condition. The dehydrogenation activity of vanadium is generally thought to be about one-fourth to one-fifth that of nickel.

Vanadium reacts destructively with the zeolitic component of the cracking catalyst causing loss of crystallinity, which is a more critical problem than its dehydrogenation activity. Nickel does not cause structural damage to the zeolitic cracking catalyst, but significantly alters product selectivity to increase coke and gas yields. High hydrogen production reduces gasoline volumetric yield and limits compressor throughput. When determined separately, the relative activity of

contaminant metals to degrade catalyst surface area are ranked as  $Ni < Fe < Na \ll V$  (Figure 1-4). Iron is usually associated with the catalyst primarily as a tramp metal. A small quantity is deposited by iron porphyrins which are present in the crude oil. With sodium removed by a properly working desalter, nickel and vanadium are primary contaminant metals of a typical FCC feedstock.

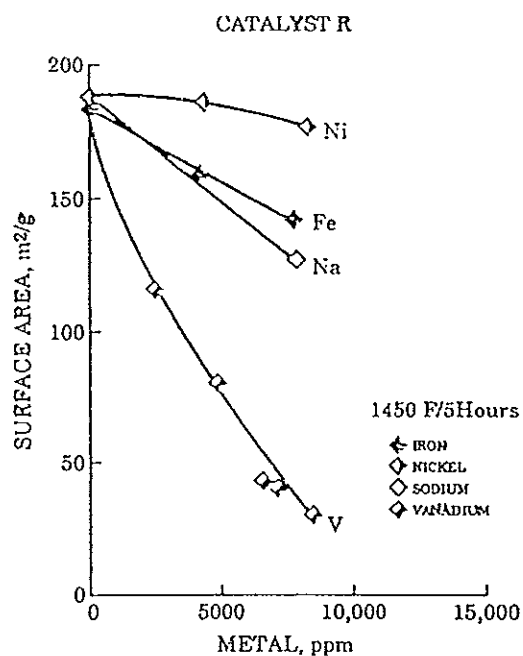


Figure 1-4 Metals degrade surface area.

Source: Richard and Patricia (Eds.: Magee and Mitchell Jr.), 1993: 341

### 2.3.2 Nickel (Sadeghbeigi, 1995)

There are two main parts to an FCC catalyst: the nonframework structure called matrix and the crystalline structure called zeolite. When FCC feed contacts the catalyst, the nickel in the feed deposits on the matrix. The nickel promotes

dehydrogenation reactions, which remove hydrogen from stable compounds and leave behind heavy hydrocarbon molecules. These reaction result in higher hydrogen and coke yields. The higher coke content will result in a higher regenerator temperature which lowers the catalyst-to-oil ratio and causes loss of conversion at constant preheat temperature.

High nickel level are normally encountered when processing heavy feed. Neither excess hydrogen nor excess regenerator temperature is desirable. Excess hydrogen is undesirable because it limits the capacity of the wet gas compressor, forcing a reduction in unit charge or lowering conversion.

A number of indices have been developed to relate metal activity to hydrogen and coke production. These indices predate the use of metal passivation in the FCC process. The most commonly used index is 4 x Nickel + Vanadium. This indicates that nickel is four times as active as vanadium in producing hydrogen. Other indices used are as follows:

$$\text{Jersey Nickel Equivalent index} = 1000 \times (\text{Ni} + 0.2 \times \text{V} + 0.1 \times \text{Fe})$$

$$\text{Shell Contamination Index} = 1000 \times (14 \times \text{Ni} + 14 \times \text{Cu} + 4 \times \text{V} + \text{Fe})$$

$$\text{Davison Index} = \text{Ni} + \text{Cu} + 0.25 \times \text{V}$$

$$\text{Mobil} = \text{Ni} + 0.25 \times \text{V}$$

$$\text{Mitchell} = \text{Ni} + 0.2 \times \text{V} \text{ (Mitchell, 1980)}$$

These indices convert all metals to a common basis, generally either vanadium or nickel.

Nickel and other metals are most active as soon as they deposit on the catalyst. With time, they lose their initial effectiveness through continuous oxidation-reduction

cycles. On the average, about one third of the nickel on the equilibrium catalyst will have the activity to promote dehydrogenation reactions.

On a wt% basis, the increase in hydrogen is negligible. It is the sharp increase in the volume of the gas that drastically impacts unit performance. The composition of cracking catalyst has a noticeable impact on hydrogen yields. Catalyst with an active alumina matrix tends to increase the dehydrogenation reactions. In addition, the presence of chlorides in the feed also reactivates the aged nickel and thus results in large hydrogen yield.

There are two common means of tracking effects of nickel on the catalyst. These are hydrogen/methane ratio and standard cubic feet of hydrogen per barrel of feed. Aside from dehydration reactions,  $H_2/CH_4$  is also more sensitive to reactor temperature and the type of catalyst than hydrogen yield alone. Therefore, measuring standard cubic feet of hydrogen per barrel of fresh feed is a better indicator of nickel activity than the  $H_2/CH_4$  ratio. The typical  $H_2/CH_4$  ratio for a gas oil having less than 0.5 ppm. nickel is between 0.25 to 0.35 mole ratio. The equivalent  $H_2$  make is between 30 and 40 scf/bbl of feed.

Frequently, it is more accurate to back-calculate the feed metals from the equilibrium catalyst inspection data than to analyze the feed randomly. Depending on the unit's constraints and economic margins, it is beneficial to use some type of passivation if the nickel on the equilibrium catalyst is greater than 1500 ppm.

Iron is usually present in FCC feed as tramp iron and is not catalytically active. Tramp iron refers to various iron oxides formed as part of corrosion by-products.



However, copper is as active as nickel but its magnitude in the feed is substantially lower than nickel.

### 2.3.3 Vanadium (Magee, et, al., 1993)

Some of the largest natural resources of vanadium are certain crudes from Mexico and Venezuela. However, vanadium is present to some extent in virtually all crudes. Vanadium compounds in crude oil are primarily porphyrin complexes or naphthenates. Naphthenates decompose fully below 525-530°C; however, porphorins decompose only after one-half hour at these conditions. Cracking may or may not be complete in the short contact time of the modern FCC riser. Whether or not complete decomposition occurs through riser cracking or by combustion in the regenerator, it is generally agreed that vanadium is deposited on the exterior of the catalyst particle due to the polar nature and size of the porphorin molecule. Since the coked catalyst is carried into the regenerator of the fluid catalytic cracker, a portion of vanadium present on the catalyst is oxidized to  $V^{+5}$ . ESCA studies of equilibrium and metal-impregnated fresh catalysts show vanadium only in the +5 valence state. Another study indicates that approximately 5% of the vanadium is present  $VO^{+2}$  species on a steamed Y zeolite. However, it is generally agreed that the primary species of vanadium is +5 after steaming. The vanadium oxidation state is independent of the vanadium source contained in the crude. As the cracking catalyst is repeatedly transported from the regenerator to the reactor and back again, the vanadium continually undergoes valence changes between +5 and +4. Once formed in the regenerator,  $V^{+5}$  does not readily reduce to a +3 valence under normal fluid catalytic cracking reactor conditions.

Vanadium deposition on the cracking catalyst results in substantial loss of catalyst surface area and activity. As the zeolite component is the highest surface area component of the modern cracking catalyst, a decline in surface area is primarily associated with loss of zeolite crystallinity. Catalytic activity is effected similarly by contamination by sodium or vanadium (Figure 1-5) although caused by zeolite acid site poisoning versus zeolite destruction, respectively. Vanadium has been reported to be less destructive to the zeolite in the presence of nickel.

Vanadium deposited on the catalyst exterior gradually migrates from the matrix surface to the zeolite crystal where it reacts destructively with the zeolite. The mechanism of this attack is a subject of considerable controversy. Several papers published in the early 1980's propose interaction of vanadium pentoxide ( $V_2O_5$ ) with the zeolite to form a low-melting eutectic. Vanadium pentoxide is known to have a low melting point,  $690^\circ\text{C}$ , which is lower than the average FCC regenerator temperature of  $720^\circ\text{C}$ . Hettinger and coworkers clearly demonstrated that an oxidative atmosphere is necessary for zeolite destruction. Therefore, a  $V^{+5}$  species is usually assumed to be responsible for the destruction of zeolite. Most of the damage to the zeolite is expected to occur in the regenerator. Further evidence is that the destructive properties of vanadium can be mitigated by using hydrogen as a reducing agent at high temperature. These conditions are thought to reduce the  $V^{+5}$  and, therefore, prevent its effect on the zeolite.

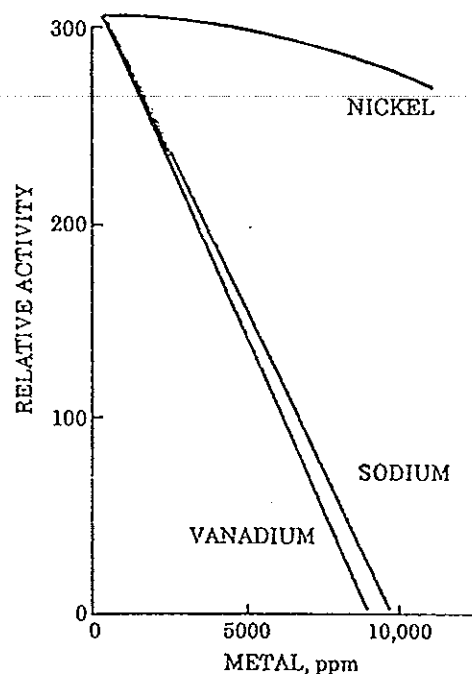


Figure 1-5 Relative activity loss due to metals.

Source: Richard and Patricia (Eds.: Magee and Mitchell Jr.), 1993: 344

Vanadates of rare earths or aluminum were identified in studies conducted using physical mixtures of catalyst or catalyst components and vanadium pentoxide powder. The mixtures were calcined to high temperatures and characterized. Studies using laser Raman spectroscopy, XPS, and X-ray diffraction (XRD) on equilibrium catalyst showed a variety of phase changes occur with the destruction of zeolite by vanadium. Calcined rare-earth-exchanged Y (CREY) collapsed with the formation of cerium orthovanadate ( $\text{CeVO}_4$ ) whereas HY formed mullite ( $\text{Al}_6\text{Si}_2\text{O}_{13}$ ) and silica (tridymite). Mullite formation was also observed in steam-aged V-load gels but not when nickel was present. These studies led to theories of zeolite destruction by the formation of

such compounds with abstracted atoms from the zeolite which lead to structural collapse. For example, Pompe proposed the destruction of REY resulted when  $V_2O_5$  attacked the rare earth component of the zeolite forming a low melting point RE-vanadate phase in which RE-ions were incorporated in varying proportions because of their chemical similarity. Although these compounds were formed, these studies did not establish whether their formation caused zeolite destruction or whether they were simply formed subsequent the zeolite destruction.

These theories were later questioned by researchers who found that  $V_2O_5$  did not cause zeolite structural damage in the absence of steam. If sintering were the operative mechanism, destruction should have taken place in dry air. In the absence of steam, no zeolite destruction occurred. In 1986, Wormsbecher, Peters and Maselli proposed vanadic acid as the vanadium species responsible for zeolite destruction. The acid,  $H_3VO_4$ , would be formed under FCC regenerator conditions by the reaction  $V_2O_{5(s)} + 3H_2O_{(v)} \rightarrow 2H_3VO_{4(v)}$ . This hypothesis incorporated both the oxygen and steam requirements. Since vanadic acid is a strong acid analogous to  $H_3PO_4$ , acid attack of the zeolite via hydrolysis of the  $SiO_2/Al_2O_3$  framework seemed plausible. The instability of zeolites to acid attack was well documented. However, these theory did not explain why catalysts which contain high sodium levels were even less vanadium tolerant than those with low levels. Sodium ions would be expected to have a neutralizing effect and to improve vanadium tolerance.

Vanadium was found to be equally destructive whether added to catalyst by naphthenate impregnation or by physical mixture of  $V_2O_5$  powder. X-ray adsorption spectroscopy (XAS) studies found the vanadium adsorption edges were identical for

steamed catalyst exposed to vanadium by impregnation or physical mixture, indicating the same oxidation state and coordination geometry. Electron microprobe studies showed that after steam treatment vanadium was evenly distributed throughout the catalyst particle in each case. Wormsbecher contended that a volatile species must be responsible for a small amount of  $V_2O_5$  powder to cause the same destruction as vanadium impregnation. Liquid wetting or solid-state reaction could not account for deactivation by small amounts of  $V_2O_5$  powder. To prove that zeolite destruction was caused by a volatile species, transport experiments were carried out in a flowing tube reactor. In these experiments, the zeolite containing catalyst was physically separated from a source of  $V_2O_5$  powder. High temperature water was injected above the  $V_2O_5$  in flowing air. Even though the vanadium source and the catalyst did not come into contact, after several hours the zeolite had completely lost crystallinity. Hence, the precursor for vanadium poisoning must involve  $H_2O$  vapor and  $V_2O_5$ ; the resulting species must be volatile. Compounds of vanadium with oxidation states lower than +5 were not considered as they did not exist at FCC regenerator conditions.

Recently Pine studies vanadium destruction using a solid-state kinetics approach. He proposed that pentavalent vanadium simply served as a catalyst for the steam destruction of zeolite. The rate constants for crystallinity loss were found to be directly proportional to the vanadium concentration. This would be true whether the role of vanadium was that of a reactant or of a catalyst. However, the fact that very small amounts of vanadium have a large effect on the reaction rate without being consumed was more consistent with a catalytic role. Pine extrapolated the rate constants obtained with vanadium to zero concentration and found agreement with

rate constants taken without vanadium. This fact was consistent with the conclusion that the reaction was the well known steam destruction of zeolite. To further understand the location of vanadium attack in the zeolite, rate constants were determined for silicalite, CREY and USY (ultrastable Y) in the presence and absence of vanadium. Silicalite was found to have a low vanadium tolerance. CREY and USY were found to have the same vanadium tolerance even though the CREY had almost 5 times as many framework aluminum atoms per unit cell. Based on these findings, the Si-OH bond was considered the more probable site of attack. This was consistent with lower steam stability of a small particle Y zeolite which would have a high surface area to volume ratio. In addition, contrary to another studies, sodium and vanadium independently were found to have the same catalytic activity for steam destruction of zeolite, and together they acted synergistically. From the kinetic results Pine concluded both materials enhance the rate of reaction of steam with the zeolite. However, Pine did not explain the mechanism of this synergistic effect.

### 3. FCC Passivation Additives (Magee, et, al.,1993)

Numerous strategies to deal with the deleterious effects of metals, primarily nickel and vanadium, have been developed. These include hydrotreatment to remove metals from the resid FCC feed, operational changes to alter the oxidation states of metals, and passivation agents. The use of metal passivation has become an established practice. A passivation agent is a compound which can be utilized in and FCC unit under normal operating conditions. Passivation additives can also include

metals traps or scavengers which are mixed with the catalyst or compounds which are incorporated in the catalyst during manufacture.

### 3.1 Nickel Passivation Agents

Nickel passivation agents are normally injected into the FCC feedstock to react with the contaminated catalyst. Although a large number of elements are claimed in the patent literature as effective agents for nickel passivation (as discussed later), only antimony, bismuth and cerium based compounds have been utilized commercially. Compounds are available with the active ingredients in an organic solvent or an aqueous solvent.

#### 3.1.1 Antimony

Research focused on heavy oil cracking and contaminant metals on cracking catalyst led Phillips Petroleum Company in the late sixties to mid-seventies to the discovery of several metals passivation agents. Antimony containing compounds discovered by Marvin M. Johnson and Donald C. Tabler consistently were outstanding metals passivation agents. The first commercially used additive was an oil-soluble compound containing antimony, phosphorus, and sulfur in a hydrocarbon solvent developed by Phillips Petroleum Company called Phi-Ad<sup>®</sup> CA. The active compound was antimony trisdipropyldithio-phosphate. The antimony content was typically 10.5 to 12.5 wt.%; sulfur, 17.5 wt.%, and phosphorus, 7.5 wt.% minimum.

Tests in bench scale, semi-batch, micro confined fluidized bed units demonstrated large decreases in hydrogen and coke yields accompanied by corresponding increases in gasoline yield. The relationship with antimony concentration at a constant metal loading was nonlinear (Figure 1-6). A similar

nonlinear relationship was observed in the hydrogen yield variation with antimony/nickel ratio in commercial tests. Pilot plant transfer line reactor tests confirmed the bench scale yield results and that multiple cracking-regeneration cycles could be run without a significant decrease in passivation benefits.

In a series of laboratory experiments with passivation agents impregnated on equilibrium catalyst, antimony trisdipropyldithio-phosphate was compared with triphenyl antimony, antimony trihallate, and colloidal antimony pentoxide dispersed in a hydrocarbon. Although passivation was observed with each compound, the antimony trisdipropyldithio-phosphate produced significantly more gasoline and less hydrogen and coke than the other compounds. This suggested sulfur or phosphorous or both improved the passivation. While this enhanced passivation is small, pilot plant studies have shown it to be economically significant.

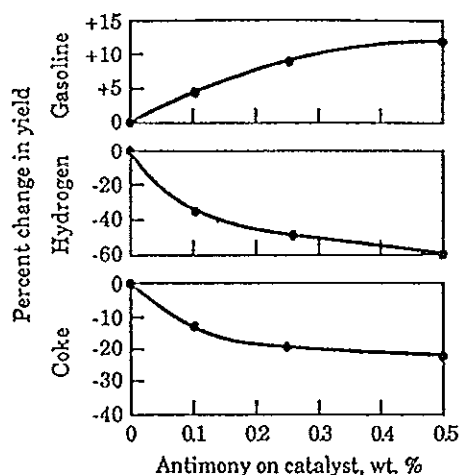


Figure 1-6 Antimony passivates metals on FCC catalyst. Data for 75 vol.% conversion of West Texas topped crude on equilibrium catalyst from HOC at 950<sup>o</sup>F.

Source: Richard and Patricia (Eds.: Magee and Mitchell Jr.), 1993: 348



An organo-antimony compound, antimony tricarboxylate, and a colloidal dispersion of antimony pentoxide in a hydrocarbon-based solvent were compared in a circulating pilot plant and three commercial units. In the pilot plant antimony was cracked onto an equilibrium catalyst containing 1000 ppm. nickel and 3100 ppm vanadium with gas oil. No significant differences in conversion or yield of gasoline, hydrogen or coke were found between the antimony tricarboxylate and the colloidal antimony pentoxide. However, the laydown efficiency was found to favor the antimony tricarboxylate which started with an efficiency near 100 % and declined to about 50% within 50 hours while the colloidal antimony started with about 80% efficiency and declined to about 40% during the same time period.

In commercial practice water-based antimony agents were found to be as effective as hydrocarbon based agents.

Despite the fact that, from an industrial point of view, antimony passivation of nickel is a well-known process, the influence of accompanying elements (co-catalyst) is less well understood. A recent laboratory study of antimony passivation with and without sulfur and/or phosphorus was conducted. XPS analysis found a decrease in the surface nickel atoms in those samples passivated with antimony compounds containing sulfur and phosphorus with respect to unpassivated catalyst. This was attributed to the fact that antimony complexes containing sulfur and phosphorus were more active for forming Ni-Sb alloys than antimony/sulfur or antimony alone. Nevertheless, the passivation of nickel was slightly more effective with the antimony organo complex containing only sulfur. At low levels of antimony, no differences in passivation were observed between the complexes studied. Therefore, the role of

sulfur and phosphorus as co-catalysts for antimony passivation of nickel remains unknown.

The Research Institute of Petroleum Processing, SINOPEC (RIPP) has developed and antimony-containing additive, MP-25, comparable in performance to an imported additive in a test at the Jiujiang Refinery. Before testing MP-25, the Luoyang Refinery tested an oil soluble passivator with low antimony content, MP-85, and found the hydrogen yield decreased 35%, the coke yield decreased, and the yield of light cycle oil increase slightly. Care was taken to avoid exposing the MP-25 to air. The MP-25 was charged at a high rate initially for four days and then set to the maintenance rate to build the antimony concentration from 500 ppm to 1500 ppm. The antimony laydown efficiency was 79%. The hydrogen content of the dry gas decreased after only one day of passivator injection. Comparing the before and after periods of MP-25 use, the hydrogen content of the dry gas decreased 38% from 51.3 to 32%. The yield of coke decreased slightly and the yield of slurry oil ("oil paste") decreased approximately 1%.

#### 3.1.1.1 Antimony-Nickel Interactions

Since the advent of commercial use of antimony additives, the interaction of antimony with nickel has been the subject of detailed studies. Dreiling and Schaffer examined catalysts having nickel loadings in the range of 1.9-4.4% in weight and Sb:Ni ratios varying from 0.0 to 0.41. From XRD results the authors suggested the formation of Ni-Sb solid solutions with a high level of Sb present on the nickel surface. Geometric and electronic effects were invoked to explain the results.

Parks et al., working with different types of Ni and Ni-Sb on catalyst at high levels, suggested the formation of an alloy. Hydrogen chemisorption on nickel was effectively poisoned by the presence of antimony. XPS showed that both antimony and nickel were present on surface sites. Three types of nickel and two types of antimony were found. On cracking catalyst with high metal levels, the antimony forms were: 1) a non-reducible antimony oxide, probably existing as a mixed metal oxide catalyst, 2) a reducible species, well dispersed on the catalyst and 3) reducible antimony which forms an alloy with nickel upon reduction. In view of their findings, the following was proposed: a) geometric blocking of nickel sites by the antimony present on the catalyst, b) alteration of the electronic properties of nickel surface atoms by the presence of Sb in such a way that their catalytic activity was significantly reduced and c) that the amount of antimony available to passivate the nickel is determined by the equilibrium between antimony interacting with the support and with nickel.

Goldwasser studied the effect of antimony addition on the structure and chemisorption properties of nickel. The addition of antimony substantially reduced the chemisorption properties of nickel. Complete reduction to metallic nickel and metallic antimony was found for the Ni- and Sb-rich samples. Nickel increased coke and hydrogen yields in isooctane cracking. The presence of antimony reduced the amounts of coke and hydrogen produced by nickel. Site blockage of nickel and weakening of the Ni-C bond by the addition of antimony was suggested to explain the results. Electronic effects were proposed to explain the strong Ni-Sb interaction. Due to these effects the back bonding capacity of the nickel was reduced by the presence

of antimony, producing a weakened Ni-C bond strength, thereby decreasing the amount of chemisorbed carbon monoxide.

### 3.1.1.2 Antimony Effects at High/Low Nickel Loadings

Antimony passivation is effect at low nickel levels (<6000 ppm 4Ni+V). The relative metal levels of the equilibrium catalyst in these tests ranges from 2100 to 5000 ppm 4Ni+V. Hydrogen yield decreases by 26 to 40 vol.%, even in two units producing only 40-55 SCF/BFF without pasivation. Two plant tests are briefly discussed below.

The first FCCU's catalyst contained 900 ppm nickel and 600 ppm vanadium for 4200 ppm 4Ni+V. A significant production of hydrogen caused the wet gas compressor to be operating at its limit. Passivation with antimony reduced the yield of hydrogen by 31%. The yield of coke decreased 5% and the yield of gasoline increased 1.5%. With the wet gas compressor unloaded, 2.5% of the gas oil fresh feed was replaced with lower value resid. The cost benefit ratio of the improvements was greater than 1:30.

The second example of passivation at low nickel level was a unit whose catalyst contained 3,160 ppm 4Ni+V with only 490 ppm nickel and 1200 ppm vanadium. The unit operated against both its air blower and process gas compressor limits. The 92 SCF/B of hydrogen caused difficulty in maintaining the governor on control as well as affecting the heat control of fuel gas users. When passivated of antimony (Table 1-1), the hydrogen production dropped 37% to 58 SCF/B, unloading the compressor, allowing the governor to function and stabilizing the fuel gas composition. Coke production was also reduced as indicated by a 17<sup>0</sup>F regenerator bed temperature

reduction. The decreased compressor loading was utilized by increasing the fresh feed from 31,000 B/D to 33,000 B/D with a poorer quality feed. The metals on the catalyst increased with the higher metals concentration in the feed. The yield of gasoline was lower due to a seasonal end point adjustment

Nickel passivation is particularly important when processing Chinese and other Pacific Rim crudes. For example, some major Chinese crudes are very high in nickel content and low in vanadium. A Shengli atmospheric resid contains 36.5 ppm nickel but not only 0.1 ppm vanadium. The percentage decrease in hydrogen production in commercial units is independent of the catalyst Ni/V ratio. Phillips laboratory studies showed antimony interacts with vanadium to reduce its dehydrogenation activity.

High nickel-containing catalysts were effectively passivated with antimony added to a pilot plant feed. The test was conducted by the Research Institute of Petroleum Processing, SINOPEC. An antimony concentration of 1000 ppm on 3800 ppm nickel on a 6000 ppm nickel catalysts resulted in a one half to one third reduction in the yield of hydrogen and a significant reduction in the yield of coke (Figure 1-7). The rate of increase of hydrogen and coke yields slowed down to a low rate above 6000 ppm nickel. However, the hydrogen-to-methane molar ratio continued to rise at about a constant rate. An 11,400 ppm catalyst required higher antimony levels (up to 4000 ppm Sb) and the extent of reduction in hydrogen and coke yields was significant, but not as great as with the lower nickel catalysts. Probably due to partial surface covering with antimony and antimony-nickel alloy, the MAT activity of the 11,400 ppm Ni catalyst decreased by 7 units with antimony addition. The pilot plant's yield of gasoline was still rising with antimony level, however. A loss of catalyst

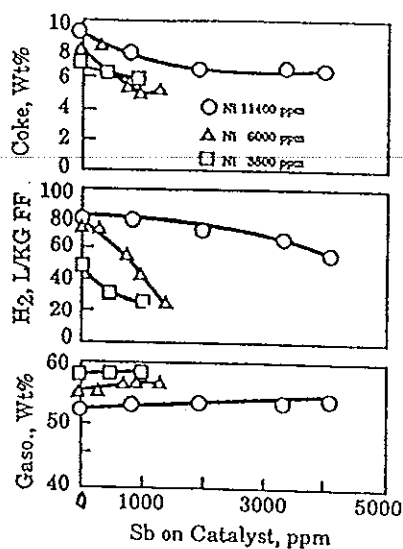
surface area and activity was also noted with 12,000 ppm nickel plus vanadium, but indications were that the vanadium was mainly the cause and that the nickel was not effective in reducing the surface area.

Table 1-1 Antimony Passivation at Low Nickel Level.

Source: Richard and Patricia (Eds.: Magee and Mitchell Jr.), 1993: 356

	Before	After Passivation
Charge, B/D	30,774	32,943
Feed API Gravity	28.2	27.5
Feed Carbon residue, wt. %	0.38	0.63
Regenerator Bed, °F	1,302	1,285
Metals on Catalyst, ppm		
Nickel	489	611
Vanadium	1,203	1,585
Hydrogen, SCF/BFF	92	58
C <sub>2</sub> & Lighter, LB/BFF	14.3	14.7
C <sub>3</sub> & C <sub>4</sub> Olefins, LV%FF	12.8	13.2
iC <sub>4</sub> , LV%FF	3.1	3.1
Gasoline, LV%FF	56.2	54.3*
LCO, LV%FF	24.2	26.5
Coke, LB/BFF	19.7	18.3

\* Separations conditions were changed to increase yield of LCO during the late fall and winter months.



**Figure 1-7** Effect of antimony on high nickel catalysts.

Source: Richard and Patricia (Eds.: Magee and Mitchell Jr.), 1993: 357

### 3.1.2 Bismuth

Bismuth (and manganese) compounds are reported as effective nickel passivating agents developed by Gulf (Chevron). Little has been published about the chemistry of the interaction of these materials with nickel. Varying reports are given of the commercial benefits of the additive compared to antimony and the Betz Dimetallic<sup>®</sup> 9P2. The main benefits of bismuth are it is less toxic than antimony and it currently is not listed by the United States Environmental Protection Agency as a hazardous chemical. The volatility and leachability of bismuth from the cracking catalyst is reported to be less than antimony.

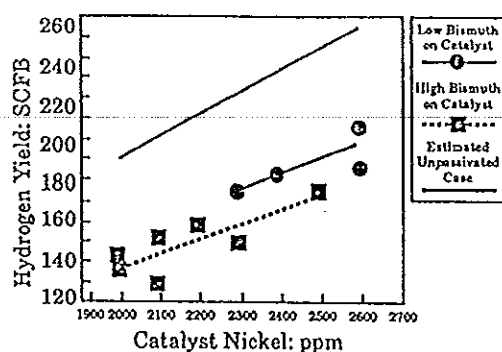


Figure 1-8 Effect of Bismuth Level.

Source: Richard and Patricia (Eds.: Magee and Mitchell Jr.), 1993: 360

### 3.1.3 Cerium

Certain cerium compounds were found unexpectedly to be effective passivators for nickel as well as for vanadium. The compounds included both cerous and ceric oxidation states from an array of organic and inorganic anions. Cerium was claimed to be less toxic than antimony. Water or organic solvents solubilized or suspended the compounds. The agent was injected into the cracker's fresh feed stream. Patent claims of the cerium levels on the catalyst ranged from 0.005-240 ppm or an atomic Ce:Ni ratio of 0.05-1 to 1:1. The mechanism of the cerium-nickel interaction was the more effective.

### 3.2 Vanadium Passivation Agents

Vanadium is the most damaging of the contaminant metals to the cracking catalyst resulting in high catalyst replacement costs to the refiner. For this reason, research efforts have been extended to develop an effective passivation agent for vanadium. Although a number of materials have been cited in the literature for



vanadium passivation, only tin additives are commercially available. Data from laboratory studies or short commercial trials are available for oil-soluble titanium and rare earth compounds. These vanadium passivation agents dissolved in a solvent are injected into the cracker feed stream to react with the incoming vanadium before it can destroy the zeolite.

### 3.2.1 Tin

Since catalyst activity appears to monotonically decrease with increasing vanadium levels due to zeolite destruction, passivation of vanadium to prevent catalyst damage is of prime commercial interest. While the passivation of vanadium has not been as successful as nickel, tin does reduce the deleterious effects of vanadium contaminants. Vanadium destroys the zeolitic component of the catalyst. Chevron claims the rate of zeolite destruction can be decreased by tin. While the interaction of tin with vanadium is thought to be rapid, the major benefits are not observable until the vanadium damaged the zeolite becomes depleted from the unit inventory. Although data on the effectiveness of tin are mixed, when correctly used, tin can effectively reduce the harmful effects of vanadium by 20-30 percent.

The mechanism of tin passivation was not well understood, except for the general assumption that inert compounds were formed on the FCC surface. Recently the effects of Sn on V-contaminated model catalysts were studied using Mossbauer spectroscopy and electron paramagnetic resonance (EPR) measurements. Tin-119 Mossbauer spectroscopy indicated that Sn-V interactions take place only during steam-aging. Mossbauer results indicated that tin was present as a  $\text{Sn}^{+4}$  species. Occelli proposed that  $\text{Sn}^{+4}$  formed ligands to vanadium through oxygen bridges. The

Sn/V complex formed in ( $V^{+5}$ -O- $Sn^{+4}$ ) units. V-Sn alloys were not observed. In laboratory studies the order of deposition of tin and vanadium had little effect on the nature of the resulting species.

Since tin forms oxides which are stable up to  $900^{\circ}C$ , it was reasonable to assume that tin oxides would form at FCC regenerator conditions. Based upon this assumption, recent studies have applied Lewis acid-base oxide reaction concepts to explain Sn passivation of vanadium. However, molten salt tests showed  $SnO_2$ , presumably because of its acidic nature, essentially nonreactive with  $V_2O_5$  or  $Na_2O$ - $V_2O_5$ . Since no chemical reaction between bulk  $SnO_2$  and  $V_2O_5$  was observed at FCC temperatures, the author concluded any tendency to form inert compounds between only Sn, V and O would be unlikely. A "three-way" complex between  $SnO_2$ ,  $V_2O_5$  and the zeolite surface was proposed. Although an interaction of oxide did not occur in the molten salts experiments, the effect of steam atmosphere was not investigated. Therefore, the study did not discount the possibility that interactions would occur in the presence of steam.

In another study, XPS experiments were conducted to scan only the surface layers of the catalyst. A strong tin signal was detected indicating tin remained predominantly on the catalyst surface. Measurements of surface vanadium concentrations were also made on samples containing vanadium only and vanadium plus tin. Results indicated about 2.5 times as much vanadium on the surface of the vanadium-only samples than with the vanadium-tin sample. This was despite the fact that equal amounts of vanadium were added to both samples. These data indicated tin formed a thin layer on the catalyst, coating a portion of the vanadium.

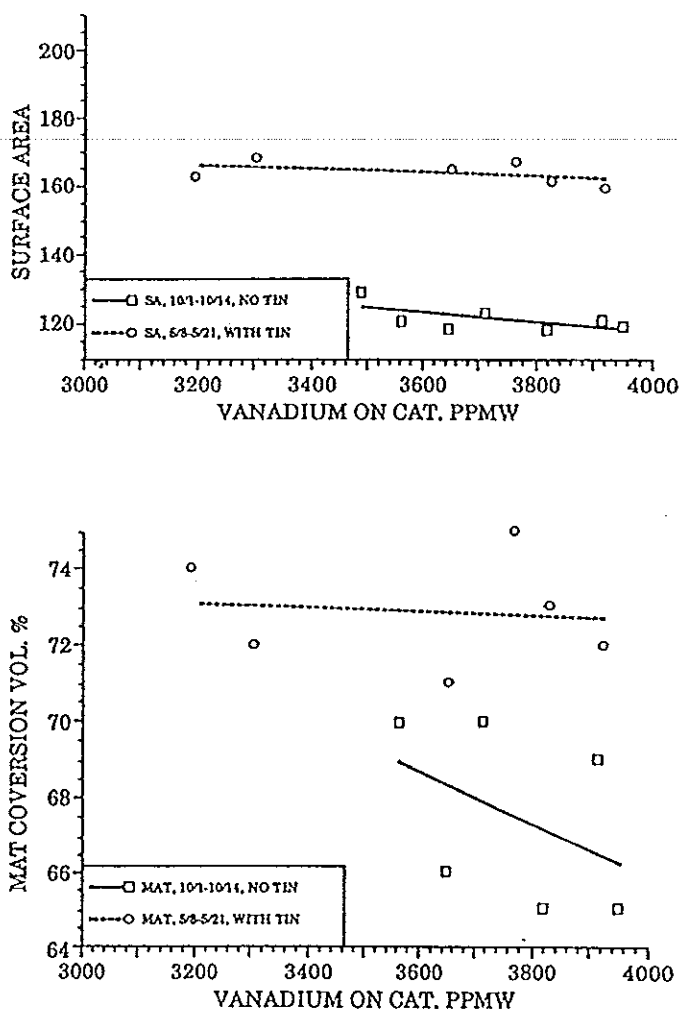


Figure 1-9 Tin maintains catalyst surface area and MAT activity.

Source: Richard and Patricia (Eds.: Magee and Mitchell Jr.), 1993: 367

### 3.2.1.1 Antimony and Tin

Combinations of passivation agents in the FCC unit have also been used successfully. In a test program, Phillips Petroleum Company evaluated an antimony-tin system. The raw results from the plant data indicated a 2.9% conversion increase, 2.2% increase in the yield of gasoline with only a 0.2% increase in the yield of coke.

The plant data was further evaluated using a model to account for variations in fresh feed properties, slurry recycle and other process conditions. Adjusted for process conditions, the results improved to a 4.4% increase in conversion, a 2.6% higher gasoline yield, and only a 0.3% increase in the yield of coke due to high conversion of lower quality oil charged. The unit fresh feed rate did not decrease.

By 1989, some FCC units having 1000-3000 ppm or higher concentrations of vanadium on the catalyst routinely used antimony-tin passivation. Tin concentrations ranged from 110 ppm to 460 ppm. Antimony:tin atomic ratios ranged from 3-11. Regenerator temperatures were 1200-1330<sup>o</sup>F. Incremental improvements over antimony alone were: conversion up to +3.0%, gasoline yield up to +2.4%, and yield of coke up to a 0.5% decrease.

The Department of Chemistry of Oil and Organic Catalysis of Moscow University, The All-Union Scientific Research Institute for Oil Refining and the Institute of Organic Chemistry, Academy of Science of the former USSR developed a one-step synthesis of nickel passivators from readily available reactants on the semi-industrial scale. Results were comparable to the best foreign additive. The water soluble passivator contain antimony and other elements. The agent was claimed as unique in that the ratio of ingredients could be varied to achieve optimum benefits for specific conditions. For example Formulation A maximized the yield of gasoline while Formulation B, with the same catalyst and vacuum gas oil, maximized the reduction in coke and hydrogen yields. Oil-soluble formulations based on antimony, bismuth and tin were also developed with the goal of low-toxicity and high efficiency.

### 3.2.2 Titanium and Zirconium

Metal additives such as titania and zirconia are reported to tie up vanadium through the formation of high melting point binary oxides with  $V_2O_5$ . With titanium and vanadium, no true compound could be identified. It is postulated that substitution of  $Ti^{+4}$  into the crystalline structure of  $V^{+4}$  occurs leading to the disappearance of the titania and the vanadium pentoxide X-ray patterns.

Limited commercial experience using TYZOR<sup>®</sup> titanium additive from DuPont showed an increase in equilibrium catalyst MAT activity with the titanium. The organo-metallic compound was introduced via the cracker feedstock. Studies conducted in circulating pilot units with TYZOR<sup>®</sup> feed addition did not show an improvement in catalyst activity. The riser time appears to be fast compared to the time required for titanium to interact and tie up vanadium on the catalyst.

### 3.2.3 Rare Earths

A number of studies have shown the benefits of rare earths in metal passivation. Feron reports that hydrocarbon soluble rare-earth compounds, dysprosium and samarium naphenate and lanthanum octoate, are efficient vanadium passivating agents. Treatment at a lanthanum:vanadium ratio of one preserved greater than 90% of the zeolite structure after high temperature-hydrothermal treatment (700°C, 20% steam). Using this practice, the catalyst composition would not require modification since the passivating agent is added in proportion to the concentration of vanadium in the feed. This permits a more flexible operation since cracker feedstocks of different vanadium content could be processed without a catalyst changeout. Since rare earths react readily with vanadium to form chemically stable compounds, lanthanum or other

rare earths are effective passivators. Rare earth vanadates are stable even at the high temperatures reached in the FCC regenerator. The rare-earth vanadium compounds are thought to be distributed homogeneously on the different components of the catalyst, avoiding clogged pore mouths on the external surface.

### 3.3 Additional Agents

Numerous passivating agents have been claimed in various patents to passivate nickel, vanadium or sodium. The more well-known commercially tested passivation

**Table 1-2** Ranking of Elements for reduction of Hydrogen.

Source: Richard and Patricia (Eds.: Magee and Mitchell Jr.), 1993: 371

Element	Hydrogen Reduction Relative To Antimony Passivation
Sb	1.0
Tl	0.8
Bi	0.7
P	0.6
Sn	0.5
In	0.4
Ca	0.4
Te	0.3
Ba	0.3
Ge	0.2
Al	0.2
Si	0.2

agents were discussed above. A list of other elements includes germanium, gallium, tellurium, indium, aluminium, barium, zinc, boron, phosphorous, tungsten, tantalum, lithium and cadmium.

A ranking of various passivation elements relative to antimony for hydrogen reduction is shown in Table 1-2. The agents were primarily organo-metal compounds or oxides of the elements. Arsenic did not effectively passivate the metals.

### **Objectives**

1. Evaluation of nickel/vanadium impregnation techniques to gain equilibrium catalyst from fresh catalyst.
2. Investigation of the effect of nickel and/or vanadium on catalytic cracking process.

### **Possible Achievement**

The possible achievement is to obtain the impregnation technique that suitable to make equilibrium catalyst from fresh catalyst. The equilibrium catalyst was used to study the influence of nickel and vanadium on yield, gasoline selectivity and coke formation from the catalytic cracking process.

## Content of Research

---

1. Evaluation of nickel/vanadium impregnation techniques.
2. Investigation of the effect of nickel or vanadium on cracking catalyst.
  - 2.1 Study of the effect of nickel on cracking catalyst
  - 2.2 Study of the effect of vanadium on cracking catalyst
3. Study of the effect of both nickel and vanadium.



## Chapter 2

### EXPERIMENTATION

#### 2.1 Feedstocks and Catalysts

##### - Feedstocks

In this research, redistilled diesel oil from Fang refinery (boiling range 260-340°C) was used as a feedstock for micro-activity test. The diesel oil from Fang refinery is too heavy (boiling range 241-380°C) and not suitable for analysis by column of Gas chromatograph used in this research. Therefore, it was redistilled to remove the heavy fraction. The distillation was performed by True boiling point distillation unit (see Appendix B). The properties of redistilled diesel oil was list in Table 2-1

Table 2-1 Properties of gas oil

Properties	Result
Boiling range	260-340°C
Viscosity at 40°C	4.6 centistoke
Refractive index at 20°C	1.459
Density at 40°C	0.801 g/m <sup>3</sup>

## - Catalysts

Table 2-2 Catalysts used in experiments

Catalyst	Treatment	Source
A	Fresh	Thai oil company Ltd.,Co.
E	Fresh	Thai oil company Ltd.,Co.
China	Fresh	RIPP
China-EQ	Equilibrium catalyst	RIPP

## 2.2 Equipment and Materials

1. Deionized water
2. Ethanol:  $\text{CH}_3\text{CH}_2\text{OH}$
3. Standard normal dodecane ( $n\text{-CH}_3(\text{CH}_2)_{10}\text{CH}_3$ )
4. Hydrogen peroxide solution 30% m/m in water ( $\text{H}_2\text{O}_2$ )
5. Nickel (II) nitrate hexahydrate ( $\text{Ni}(\text{NO}_3)_2 \cdot 6\text{H}_2\text{O}$ )
6. Ammonium metavanadate ( $\text{NH}_4\text{VO}_3$ )
7. Ice bath and glass receiver for liquid product from MAT unit
8. Quartz and Glass wool
9. Rubber tube
10. Porcelain ring
11. Crucible
12. Desiccator

13. Nitrogen gas (UHP Grade, Purity 99.99%for GC and Regular for MAT unit)

14. Hydrogen gas (UHP Grade, Purity 99.99%for GC)

15. Helium gas (UHP Grade, Purity 99.99%for GC)

16. Air (Regular Grade)

### 2.3 Instrument

1. Hydrothermal Aging Unit, Model CLY-1, RIPP (see appendix C)
2. Micro-Activity Test (MAT) Unit, Model WFS-1D, RIPP (see appendix D)
3. Gas Chromatograph (GC-14 A, SHIMADZU) and Integrater (HP3295, Hewlett Packard) (see appendix E)
4. Gas Chromatograph (GC-14 B, SHIMADZU) and Integrater (HP3295, Hewlett Packard) (see appendix F)
5. Surface area and pore size analyzer (SA3100, Coulter) (see appendix G)
6. True Boiling Point Distillation Unit (see appendix B)
7. X-Ray Fluorescence Spectrometer (XRF), Model PW2400, Philips
8. Inductively Coupled Plasma Atomic Emission Spectrometry (ICP-AES) Optimum, Model 4300 DV, Perkin Elmer
9. Thermogravimetric Analysis (TGA), Model TGA 7, Perkin-Elmer
10. Viscometer
11. Balance, Model TOLEDO PB153, Metler
12. Furnace

## 2.4 Experiment and Procedure

### - Impregnation Method (Mitchell B.R., 1980)

1. Fresh catalyst was heated at desired temperature for one hour.
2. The catalyst was immersed in the Nickel (II)-Nitrate Hexahydrate solution (water was used as solvent) for 2 hours.
3. The catalyst was dried in hot air oven at 120<sup>o</sup>C for 3 hour.
4. The catalyst was immersed in the Ammonium Metavanadate solution (H<sub>2</sub>O<sub>2</sub> solution was used as solvent) for 2 hours.
5. The catalyst was dried in hot air oven at 120<sup>o</sup>C for 3 hours.
6. The catalyst was steam-deactivated at 800<sup>o</sup>C for 6 hours (Angkasuwan A., 1998).

Remark In all cases, the catalysts were impregnated by two metals, nickel was first impregnated metal (David F. T. and Rodney L. M., 1988).

### - Experiment

1. Investigation of the appropriate condition for impregnation method.

The sequences of the impregnation method.

The synthetic contamination was prepared by impregnation method (Mitchell B.R., 1980). China fresh catalyst was heated at 600 °C and dried for 3 hours. The different sequences are as follows:

Sequence 1: Impregnation of nickel at 0, 800, 1600, 2400, 3200 ppm. on catalyst before steam deactivated.

Sequence 2: Impregnation of nickel at 0, 800, 1600, 2400, 3200 ppm. on catalyst after steam deactivated.

The catalysts from both sequences were analyzed for nickel content in the solution by inductively couple plasma atomic emission spectrometry (ICP-AES). The catalyst digestion process was prepared as explained in Appendix A.

2. Evaluation of the effect of Nickel, Vanadium, Nickel +Vanadium on catalyst surface area.
  - The optimal impregnation method, obtained from the first experiment was used. Catalyst A and E were impregnated by nickel at 0,1000, 2000, 3000, 4000 ppm., vanadium at 0, 1000, 2000, 3000, 4000 ppm., nickel and vanadium (only catalyst E) at 0/0, 1000/1000, 2000/2000, 3000/3000, 4000/4000 ppm.
  - The catalyst surface area was analyzed by surface area and pore size analyzer (see appendix G).
3. Investigation of the effect of nickel contamination on the catalytic properties.
  - Both nickel contaminated catalysts (A, E) from the second experiment were tested for catalytic properties by micro-activity testing unit.
  - Effect of nickel contamination on catalyst A and E was examined.
4. Effect of vanadium contamination on catalytic properties was studied.
  - Both vanadium contaminated catalysts (A, E) from the second experiment were tested for catalytic properties by micro-activity testing unit.
  - Effect of vanadium contamination on catalyst A and E was tested.
5. Effect of both nickel and vanadium on catalytic properties was investigated.

- Nickel+vanadium contaminated catalyst (E) from the second experiment was tested for catalytic properties by micro-activity testing unit.
- The catalytic property results were compared with nickel contaminated catalyst (E) and vanadium contaminated catalyst (E).

## 2.5 Test procedure and Test Conditions

### 2.5.1 Evaluation

The laboratory evaluation of cracking catalysts has evolved into a very common method for measuring performance characteristics of commercial or experimental catalyst samples. The Micro-Activity Test (MAT) is the primary tool in accessing the performance of catalyst samples. The schematic for MAT was shown in Figure 2-1.

#### 2.5.1.1 A Micro-Activity Test Method and Test Condition of MAT

(see MAT set up and operation in Appendix D)

Catalyst loading:	5	g
Oil weight:	1.56 ± 0.01	g
Catalyst/Oil:	3.2	
Feedstock:	Gas Oil (LCO, bp. 260-340°C)	
Weight hourly space velocity (WHSV):	16	hr <sup>-1</sup>
Feeding rate:	1.337	g/min
Feeding time:	70	sec
Temperature:	460 ± 1	°C
Purging time:	600	sec

Liquid produced from MAT was then analyzed by Gas Chromatograph.

$$\text{Microactivity (MA, \%)} = 100 - \left[ \left( \frac{100 - A}{C} \right) \times B \right]$$

where

A = Gasoline yield (wt%), analyzed by GC

B = Liquid produced from MAT, (g)

C = Feed oil, (g)

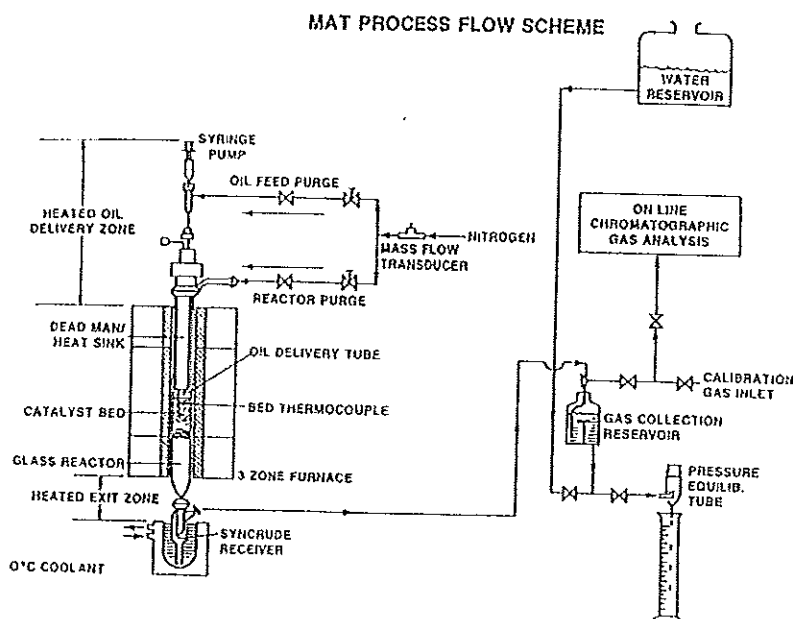


Figure 2-1 Schematic for typical MAT unit

Source: Moorehead, McLean and Cronkright (Eds.: Magee and Mitchell Jr),

1993: 226

**Condition for Gas Chromatograph (GC 14B)**

---

Column:	Packed Column (OVI, methylsilocane)
Detector:	Frame Ionization Detector (FID)
Carrier gas:	Nitrogen (Purity 99.99%, OFN), flow rate 35-40 ml/min
Combustion gas:	Hydrogen, flow rate 40 ml/min
Auxiliary gas:	Air, flow rate 400 ml/min
Sample injection volume:	1 $\mu$ l
Temperature of vaporization chamber (injector):	280 <sup>o</sup> C
Temperature of detector chamber:	280 <sup>o</sup> C
Temperature of column chamber:	35 <sup>o</sup> C to 80 <sup>o</sup> C with a rate of 15 <sup>o</sup> C/min, then raise from 80 <sup>o</sup> C to 235 <sup>o</sup> C with a rate of 8 <sup>o</sup> C/min and hold at 235 <sup>o</sup> C for 10 min.

**Condition for Gas Chromatograph (GC 14A)****Analyze H<sub>2</sub> in gas product**

Column:	Packed Column (Molecular sieve 5A)
Detector:	Thermal Conductivity Detector (TCD)
Carrier gas:	Helium (Purity 99.999%, UHP), flow rate 30 ml/min
Sample injection volume:	100 $\mu$ l
Temperature of vaporization chamber (injector):	90 <sup>o</sup> C



Temperature of detector chamber: 100°C

Temperature of TCD detector chamber: 100°C

Temperature of column chamber: 50°C.

Current : 60mA

### 2.5.1.2 Hydrothermal Treatment Procedure and Test Condition

The freshly catalysts have been deactivated by using hydrothermal aging unit. The primary objective is to deactivate a fresh catalyst such that its performance in the MAT is representative of what is observed when testing a commercially deactivated sample at the same catalyst. In this way, prediction of commercial performance for new catalysts can be made.

#### Condition for hydrothermal aging

Catalyst loading:	15-22 g
Aging temperature:	800°C
Aging time:	6 hr
H <sub>2</sub> O	0.41 ml/min

Catalysts are usually loaded at ambient temperature and the steaming of catalysts is generally done in the presence of 100 percent steam.

### 2.5.2 Characterization

Physicoproperties of catalyst have been performed by using several instruments according to ASTM standard. The instruments for characterization of catalysts and standard method used were listed in Table 2-3.

Table 2-3 Characterization Listed for Catalyst

No.	Characteristic	Instrument	Method
1	Chemical content, eg. Ni, V.	Inductively couple plasma atomic emission spectrometry	Typical standard
2	Specific surface area	Surface area and pore size analyze	ASTM D3663-78
3	Coke content	Thermogravimetric analysis	Typical standard

## Chapter 3

### RESULTS AND DISCUSSION

Microactivity test condition of this work was performed at standard conditions, as seen in section 2.5.1.1, page 52.

#### Definition

$$1. \%H_2 \text{ (Feed Basis)} = \frac{\text{Mole } H_2 \text{ from GC} * 2 * 100}{\text{Weight of feed oil (g)}}$$

$$2. \%Conversion \text{ (MAT)} = 100 - \{[(100-A)*B]/C\}$$

Where: A = Gasoline yield, analyzed by GC, %wt.

B = Liquid product from MAT, g

C = Weight feed oil, g

$$3. \%Coke \text{ (Feed Basis)} = A * \{B/[C*(1-(B/100))]\}$$

Where: A = Weight of fresh catalyst passing the MAT unit, g

B = Percentage of coke on spent catalyst,  $\Delta Y$ , %wt.

C = Weight of feed oil, g

$$4. \%Gas \text{ (Feed Basis)} = 100 - \%Coke - [(A/B)*100]$$

Where: A = Weight of liquid product, g

B = Weight of feed oil, g

$$5. \text{Coke selectivity} = \%Coke / \% \text{ Conversion}$$

$$6. \text{Gas selectivity} = \%Gas / \% \text{ Conversion}$$

$$7. H_2 \text{ Selectivity} = \%H_2 / \% \text{ Conversion}$$

### 3.1 Investigation of the appropriate condition for impregnation method.

#### The sequences of the impregnation method.

China catalyst was heated shock at 600°C for 1 hour before impregnation.

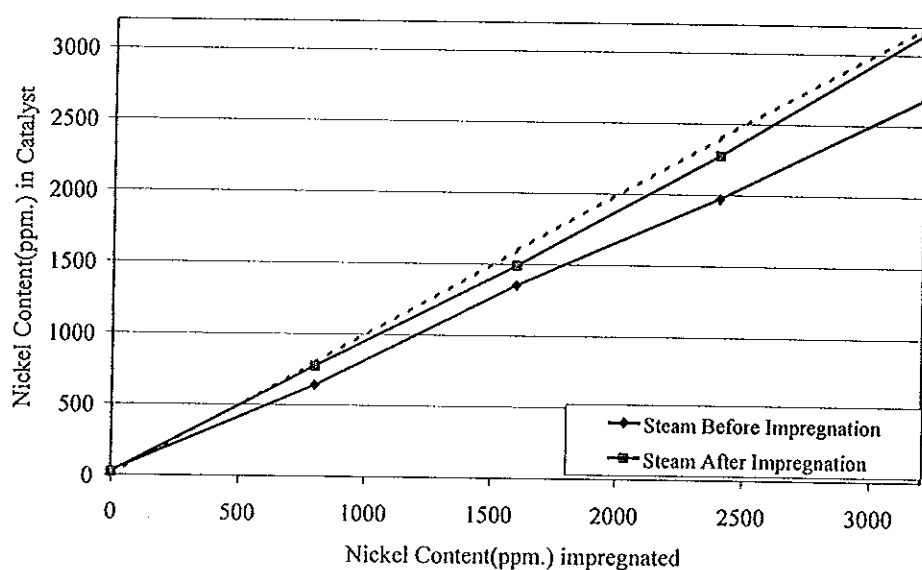


Figure 3-1 Effect of impregnation sequence on nickel content.

Figure 3-1 confirmed that the second sequence (Steam after impregnation) was better than the first sequence (Steam before impregnation). This result agreed with previous result by Mitchell B.R.'s (Mitchell, 1980). Nickel content by the second sequence was closer to a desired value than the first sequence. This might be because zeolite was dealuminated by steam, so its structure destroyed and surface area and pore size were decreased as shown in Table 3-1. The catalyst obtained by the first sequence had lower absorption surface area than the catalyst obtained by the second sequence. Therefore, the second sequence was chosen as an appropriate impregnation method.

Table 3-1 Surface area and pore volume of catalyst E from experiment 3.1.1

Catalyst	BET (m <sup>2</sup> /g)	Total Pore Volume (ml/g)	Micro Pore Surface Area (m <sup>2</sup> /g)	Micro Pore Volume (ml/g)
Fresh Catalyst	236.68	0.1984	166.06	0.076
Heat Shock Catalyst	224.22	0.2098	151.57	0.069
Steam and Heat Shock	126.73	0.1776	71.44	0.033

### 3.2 Evaluation of the effect of Nickel , Vanadium, Nickel +Vanadium on catalyst surface area.

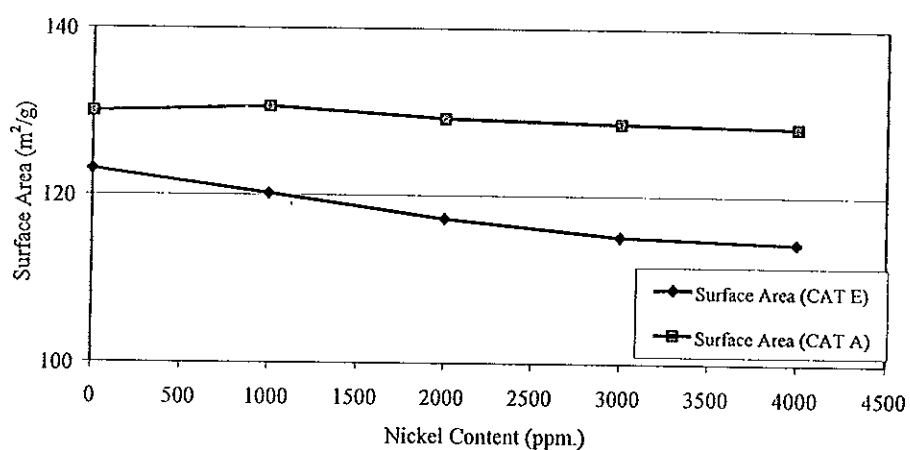


Figure 3-2 Effect of nickel content on surface area (m<sup>2</sup>/g).

Figure 3-2 shows that the surface areas of both catalysts were slightly decreased with increasing nickel content. Hettinger W.P.,*et.al.*,(1983) also reported that the zeolite structure was not affected by nickel content.

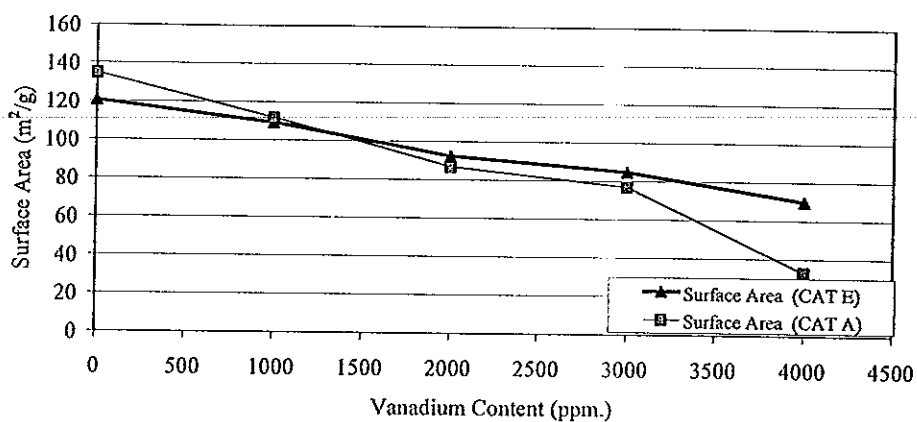
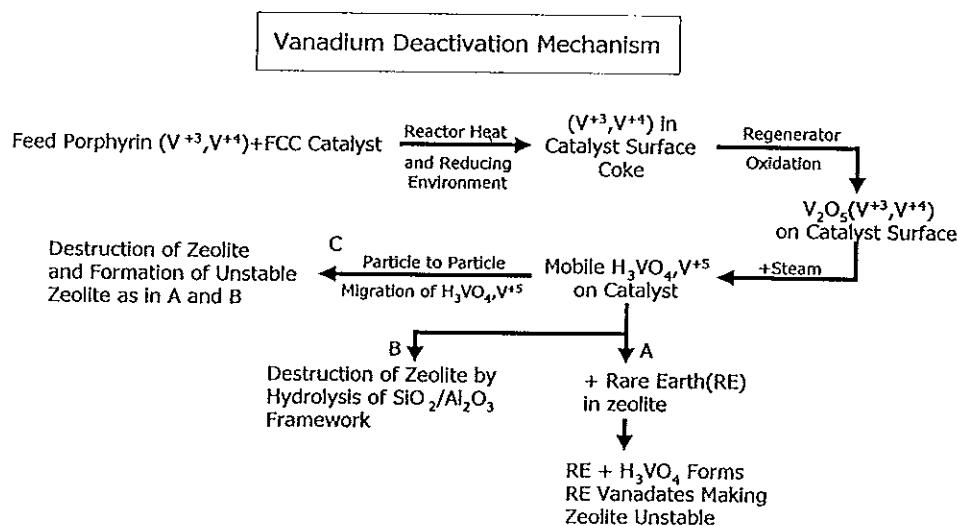


Figure 3-3 Effect of vanadium content on surface area (m<sup>2</sup>/g).

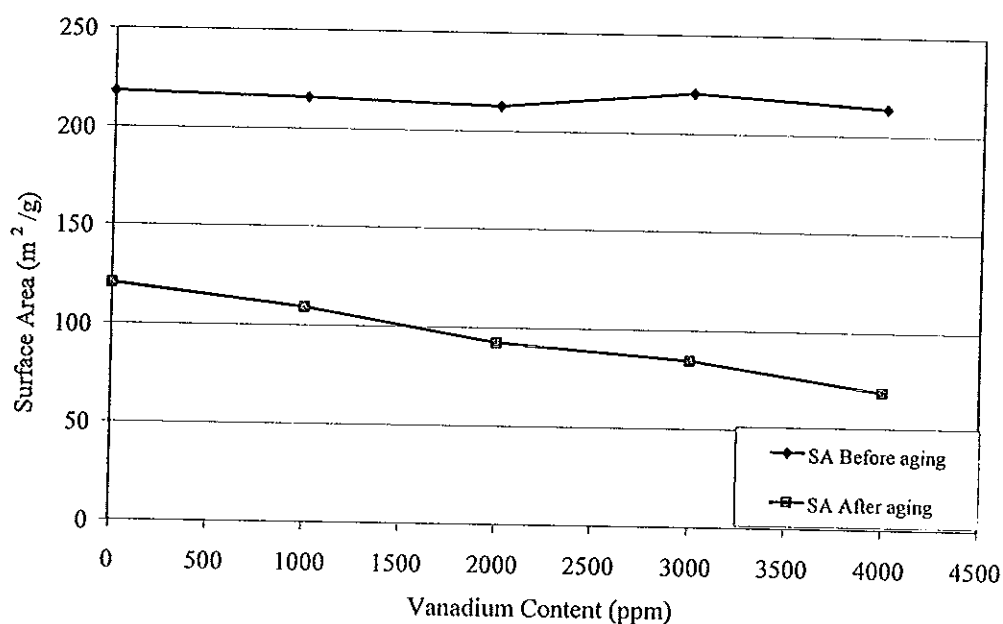
Figure 3-3 shows that vanadium deposition on the catalyst resulted in a substantial loss of the catalyst surface area. This is because of vanadic acid formed from reaction of vanadium and steam destroyed the zeolite structure as seen in Figure 3-8.



Grace Davidson, 1993

Figure 3-4 Vanadium Deactivation Mechanism.

Figure 3-5 can confirm that the surface area of catalyst E lost when vanadium reacted with steam. If there was no steam deactivates, vanadium could not destroy the zeolite structure. The surface area was decreased as the vanadium content increased.

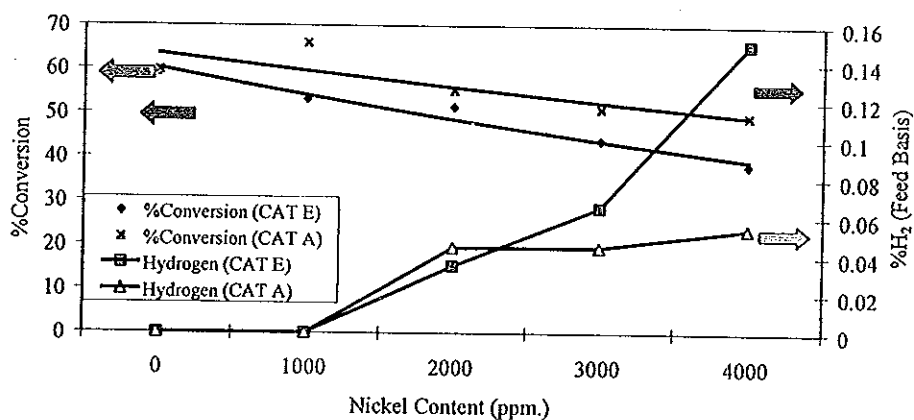


Figures 3-5 Effect of vanadium content on surface area (m<sup>2</sup>/g).

### 3.3 Investigation of the effect of nickel contamination on the catalytic properties.

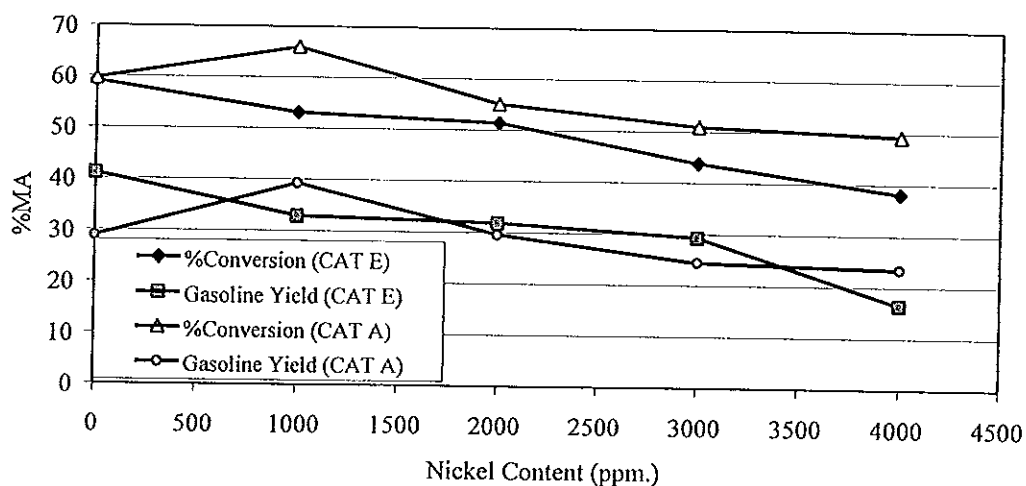
It was clearly observed from Figure 3-6 that H<sub>2</sub> gas was formed when nickel content is higher than 1000 ppm. There was some passivators in catalyst that passivated nickel, so it reduced dehydrogenation reaction. Passivators could not passivate all of nickel content when nickel content is more than 1000 ppm. Dehydrogenation reaction might be resulted from active alumina matrix which accelerated the reaction.

The occurring of dehydrogenation reaction could confirm by H<sub>2</sub> production. When nickel content increased, the percent conversion was decreased, coke yield and H<sub>2</sub> yield was increased, but gas yield was slightly decreased.



\*Test condition: see section 2.5.1.1, page 52

Figure 3-6 Effect of nickel content on %H<sub>2</sub> (feed basis) and %conversion.



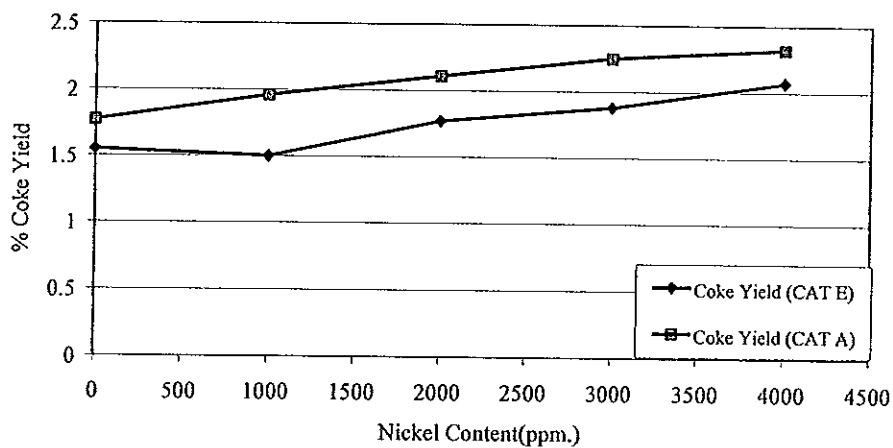
\*Test condition: see section 2.5.1.1, page 52

Figure 3-7 Effect of nickel content on %conversion and gasoline yield.



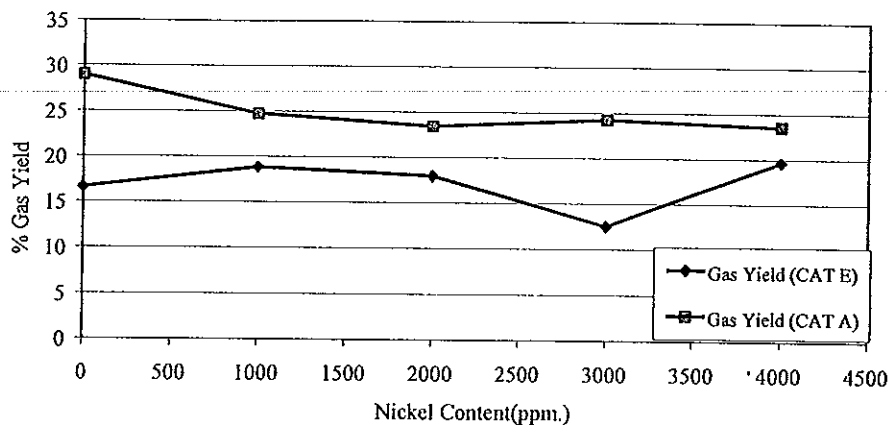
The percent conversion and gasoline yield trended to decrease with increasing of nickel content (Figure 3-7). The increasing of percent conversion and gasoline yield in catalyst A might be because of nickel acceleration, but when nickel content reached the tolerance limit percent conversion and gasoline yield still decreased. This might be caused from increasing coke deposit on the catalyst as seen in Figure 3-8.

In Figures 3-8 and 3-9, coke yield trended to increase when nickel content increased. Gas yield was just slightly changed. Gas yield of catalyst A was higher than catalyst E's because catalyst A was a resid cracking catalyst, so the secondary reaction occurred when used the low boiling point feedstock. From this reason, it caused high gas yield that also made high coke yield.



\*Test condition: see section 2.5.1.1, page 52

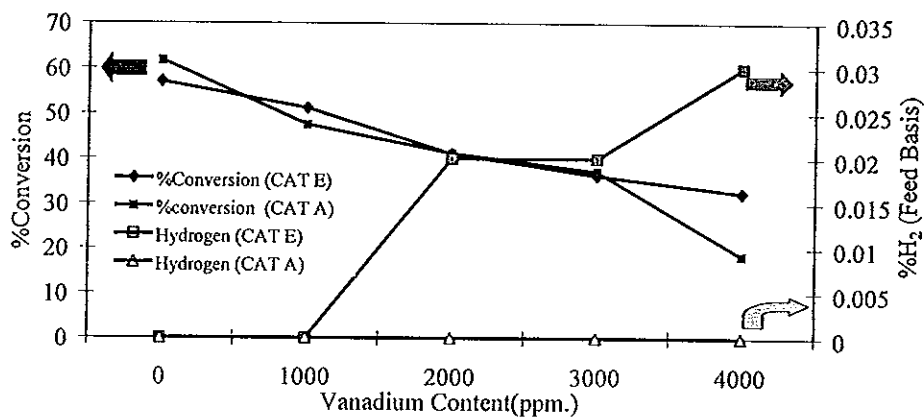
Figure 3-8 Effect of nickel content on coke yield.



\*Test condition: see section 2.5.1.1, page 52

Figure 3-9 Effect of nickel content on gas yield.

### 3.4 Investigation of the effect of vanadium contamination on the catalytic properties.

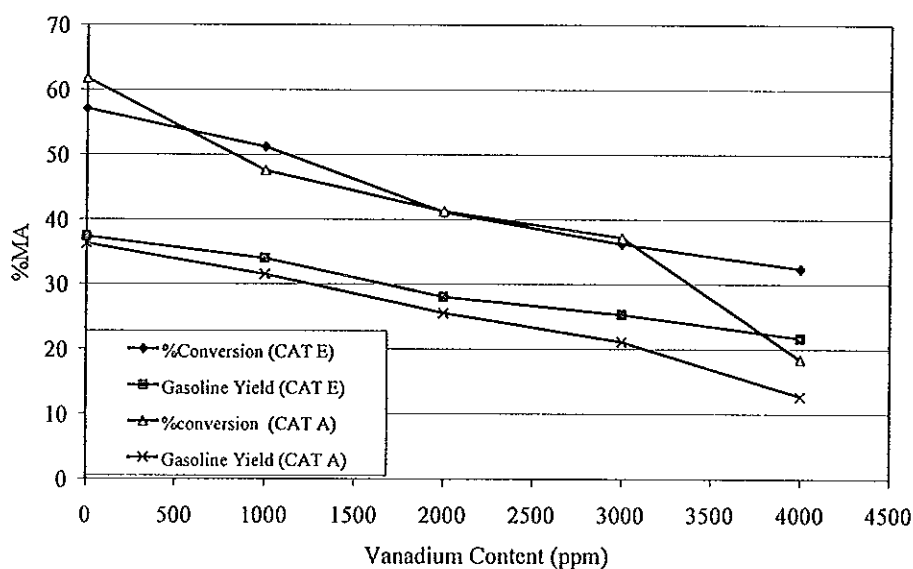


\*Test condition: see section 2.5.1.1, page 52

Figure 3-10 Effect of vanadium content on %H<sub>2</sub> (feed basis) and %conversion

The effect of vanadium on dehydrogenation reaction was 4-5 times less than the effect of nickel (Figure 3-10). Percent conversion and gas yield were sharply

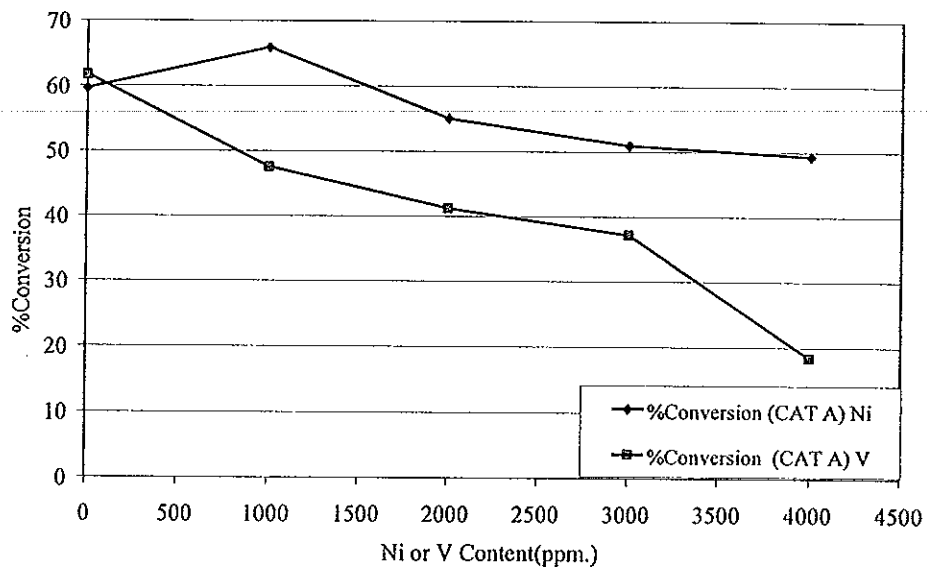
decreased with vanadium increasing because the zeolite structure was damaged. Catalyst A was severely destroyed by vanadium, so H<sub>2</sub> formation was lower than the detection limit. H<sub>2</sub> formed from vanadium contaminated catalyst E could be detected but it was 2-5 times less than nickel contaminated catalyst E.



\*Test condition: see section 2.5.1.1, page 52

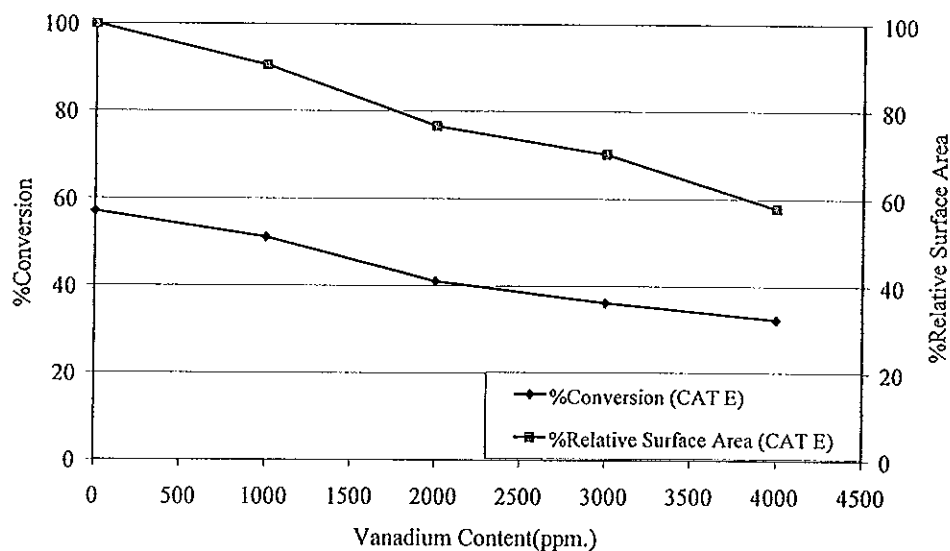
Figure 3-11 Effect of vanadium content on gasoline yield and %conversion.

Increasing of vanadium caused more reduction of percent conversion and gasoline yield when compared to increasing of nickel contamination (Figure 3-11). Structure of zeolite was destroyed by vanadium as clearly seen in Figure 3-12.



\*Test condition: see section 2.5.1.1, page 52

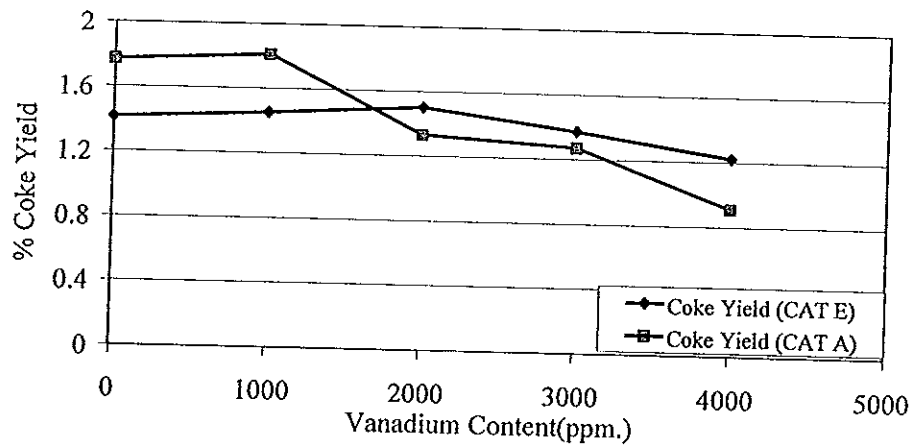
Figure 3-12 Effect of nickel/vanadium on %conversion (CAT A).



\*Test condition: see section 2.5.1.1, page 52

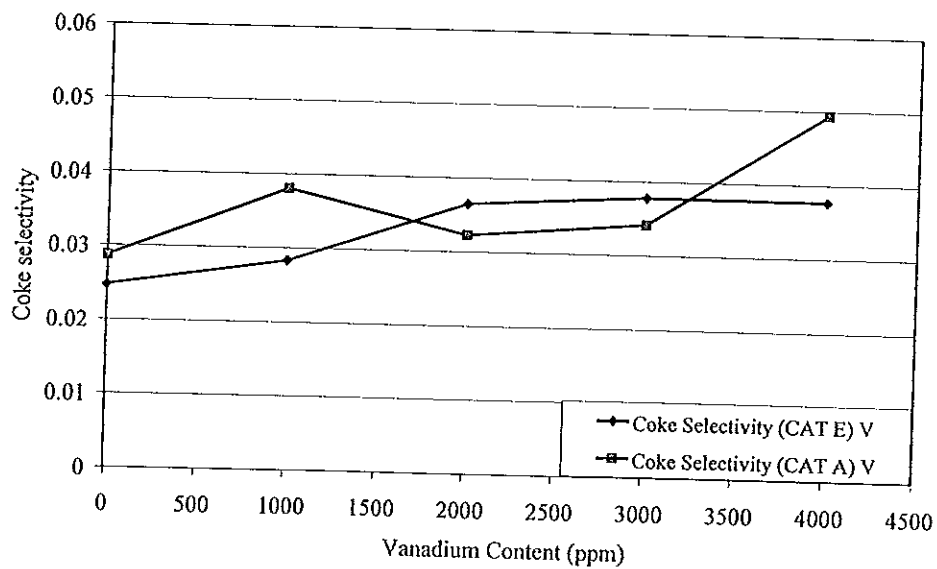
Figure 3-13 Effect of vanadium on %conversion and relative surface area.

Figure 3-13 confirms that when vanadium increased, catalyst was destroyed so the surface area for reaction was sharply decreased. Increasing of vanadium resulted in reduction of percent conversion and surface area.



\*Test condition: see section 2.5.1.1, page 52

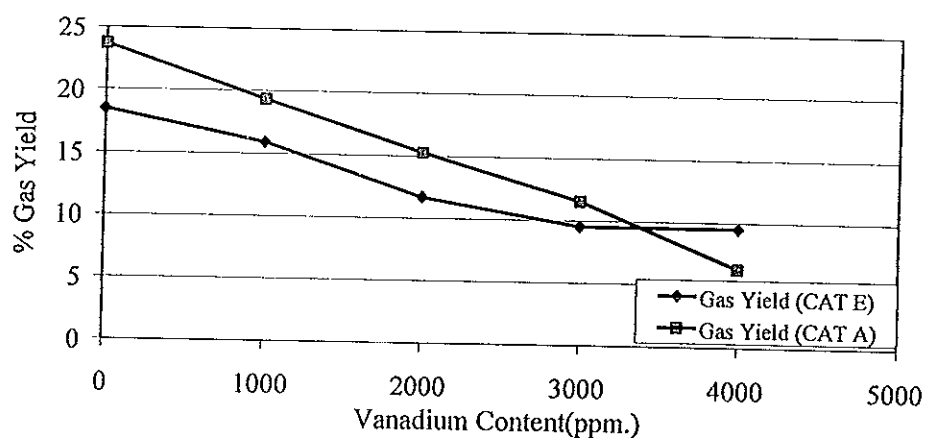
Figure 3-14 Effect of vanadium on coke yield.



\*Test condition: see section 2.5.1.1, page 52

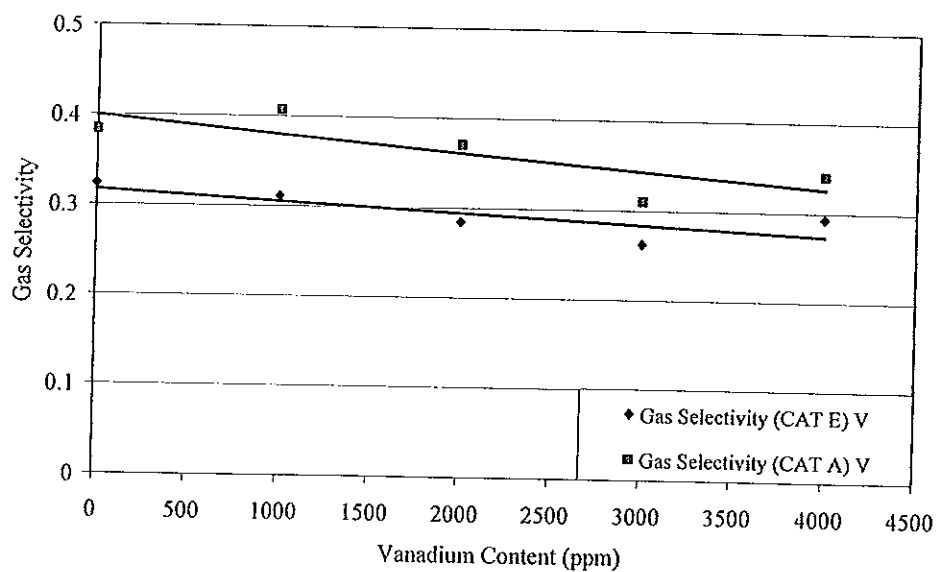
Figure 3-15 Effect of vanadium on coke selectivity.

The catalyst structure was destroyed by vanadium, therefore, the surface area, percent conversion, and coke yield were decreased (Figure 3-14). In Figure 3-15, coke selectivity increased with increasing of vanadium content. This was reported before that active metal could decrease gasoline yield, but increase H<sub>2</sub> and coke.



\*Test condition: see section 2.5.1.1, page 52

Figure 3-16 Effect of vanadium on gas yield.



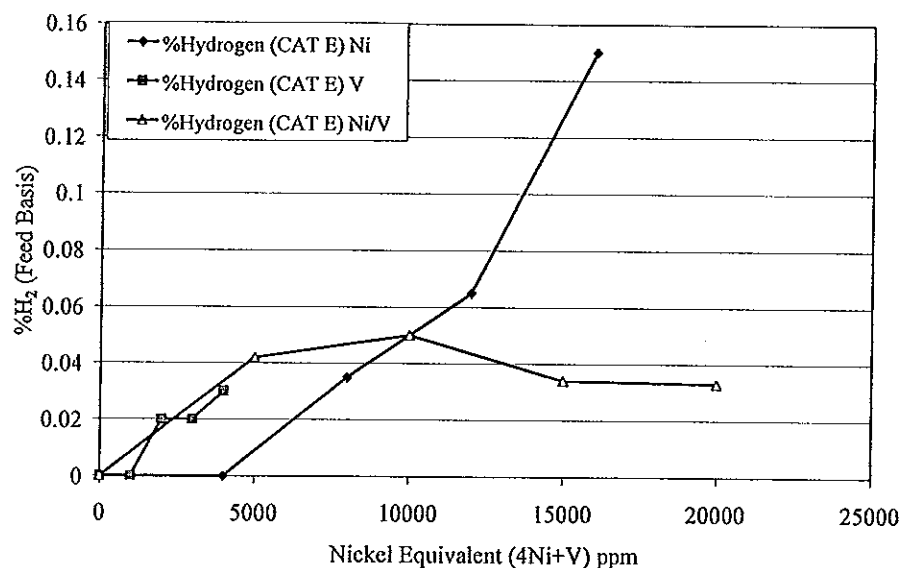
\*Test condition: see section 2.5.1.1, page 52

Figure 3-17 Effect of vanadium on gas selectivity.

In figure 3-16, gas yield and coke yield were decreased with vanadium increasing. This is because the zeolite structure was destroyed so surface area and percent conversion were decreased. Gas yield trended to decrease because percent conversion decreased. As seen in Figures 3-16 and 3-17, gas yield and gas selectivity trended to decrease as vanadium content increased.

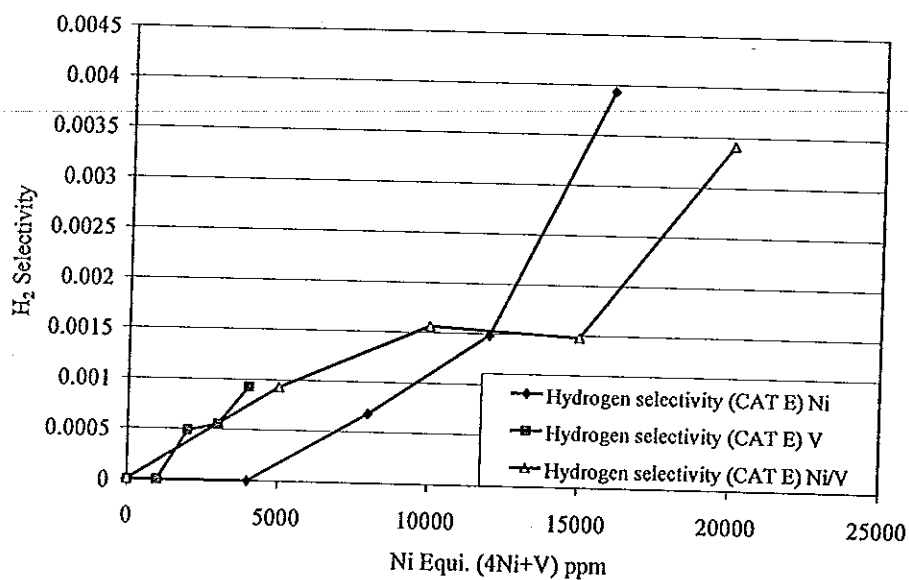
### 3.5 Effect of both nickel and vanadium on catalytic properties.

From experiments 3.3 and 3.4, the influence of nickel and vanadium contamination on catalyst E is better than catalyst A. So catalyst E was used in this experiment for testing effect of nickel and vanadium compared with catalyst E that had only nickel or vanadium.



\*Test condition: see section 2.5.1.1, page 52

Figure 3-18 Effect of nickel equivalent on percent H<sub>2</sub>.



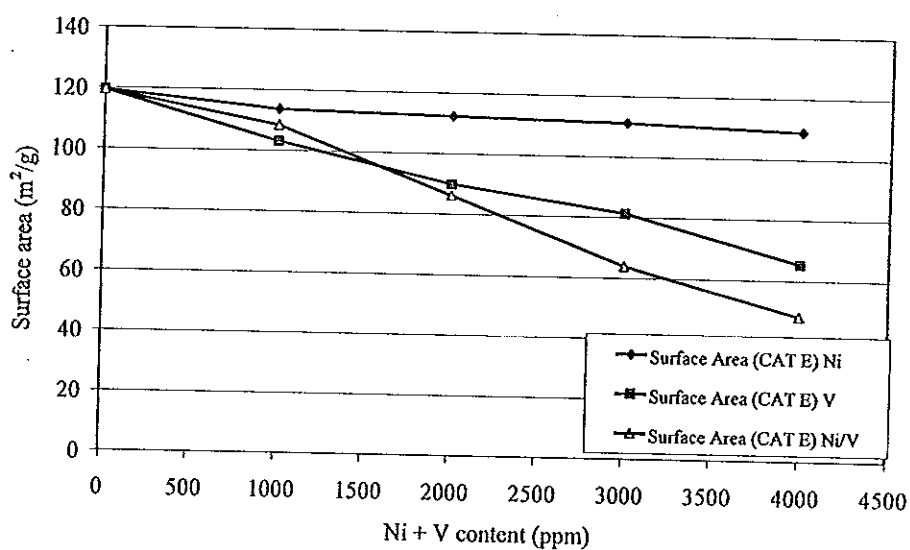
\*Test condition: see section 2.5.1.1, page 52

Figure 3-19 Effect of nickel equivalent on H<sub>2</sub> selectivity.

In Figures 3-18 and 3-19, percent H<sub>2</sub> and H<sub>2</sub> selectivity produced by the nickel contaminated catalyst, the vanadium contaminated catalyst, and nickel-vanadium contaminated catalyst were compared. Nickel equivalent shown in these figures were calculated from equation, Ni (equi) = 4Ni+V, for comparison in the same base. As seen, nickel equivalent increased as H<sub>2</sub> increased. This is possibly because dehydrogenation reaction was occurred. H<sub>2</sub> produced by nickel contaminated catalyst could be detected when nickel equivalent content was above 4000 ppm. The dehydrogenation reaction was stopped when nickel was lower than 1000 ppm. in the catalyst. H<sub>2</sub> produced by vanadium contaminated catalyst could be detected when nickel equivalent was above 1000 ppm. The dehydrogenation reaction was stopped when there was 1000 ppm. vanadium this is because the active metal as passivator passivated the catalyst surface. H<sub>2</sub> produced by the nickel-vanadium contaminated



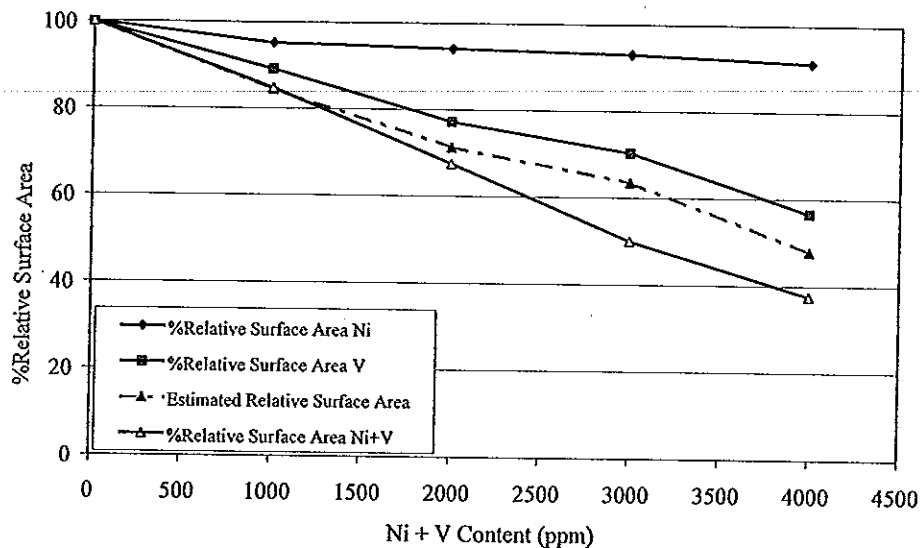
catalyst, decreased when high metals contaminated because of the decreasing of percent conversion caused from zeolite structure was damaged. However the  $H_2$  selectivity still increased as nickel equivalent increased.



\*Test condition: see section 2.5.1.1, page 52

Figure 3-20 Effect of nickel/vanadium on surface area.

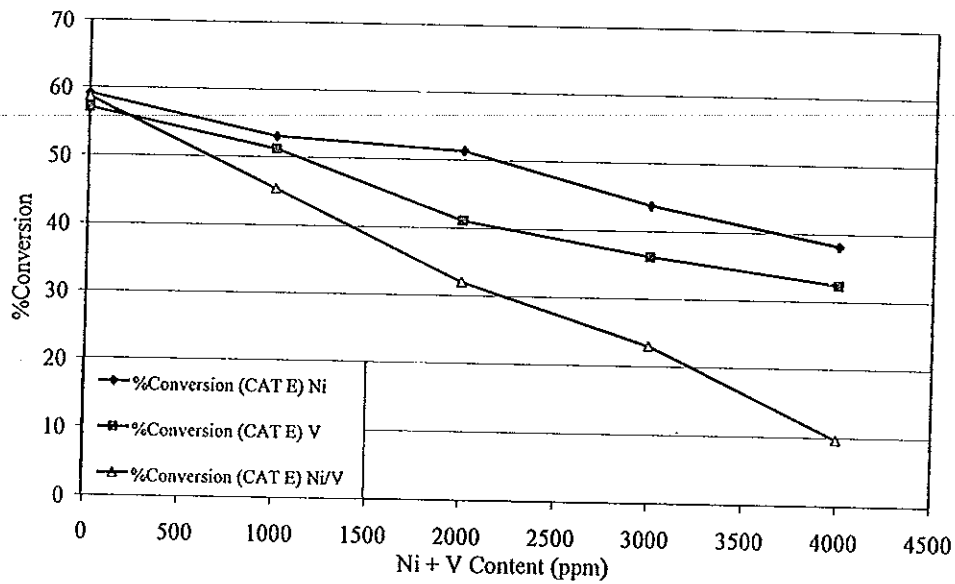
The catalyst contaminated with nickel+vanadium above 2000 ppm was severely destroyed, the surface area was dramatically decreased (Figure 3-20). Rapid decreasing of surface area caused  $H_2$  decreased, but  $H_2$  still remained constant with nickel contaminated. Nickel caused high  $H_2$  yield. Highly loss surface area from high nickel/vanadium contamination did not effect  $H_2$  yield.



\*Test condition: see section 2.5.1.1, page 52

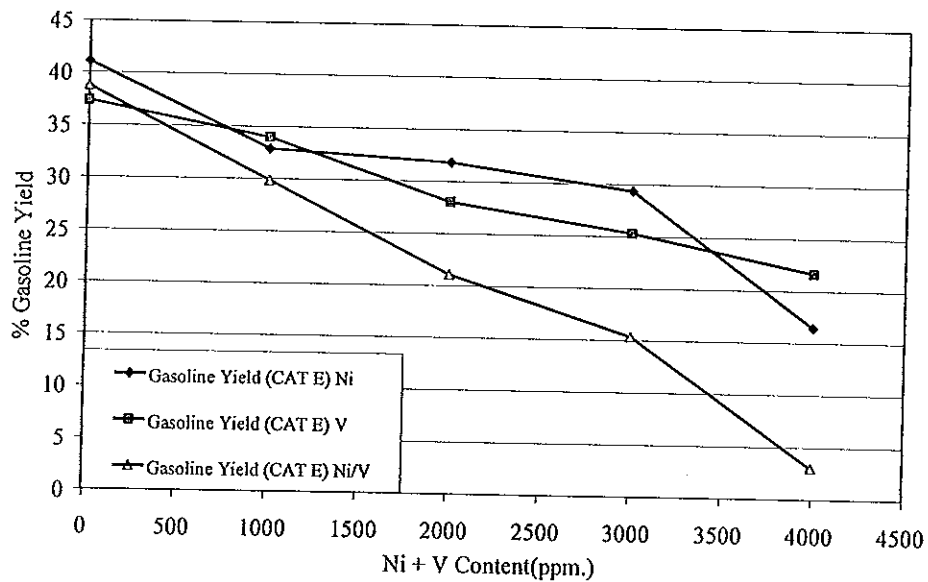
Figure 3-21 Effect of nickel/vanadium on percent relative surface area.

The percent relative surface area, decreased by content of nickel and/or vanadium in the catalyst (Figure 3-21). The relative surface area was greatest reduced by nickel/vanadium contaminated catalyst because nickel/vanadium contamination caused the synergistic effect. Surface area of nickel/vanadium contaminated catalyst was decreased more than only nickel or vanadium contaminated catalyst.



\*Test condition: see section 2.5.1.1, page 52

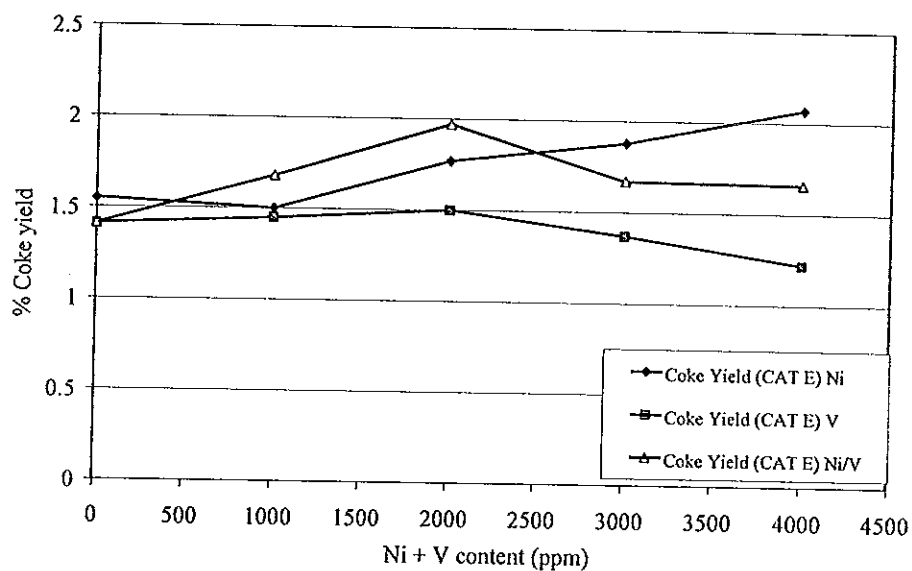
Figure 3-22 Effect of nickel/vanadium on percent conversion.



\*Test condition: see section 2.5.1.1, page 52

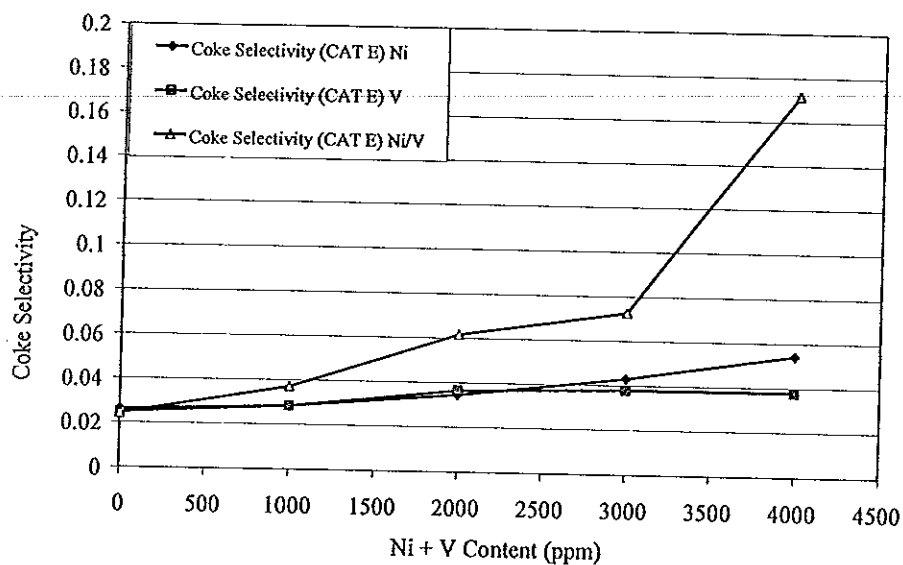
Figure 3-23 Effect of nickel/vanadium on gasoline yield.

In Figures 3-22 and 3-23, percent conversion and gasoline yield by the nickel/vanadium contaminated catalysts were shaper decreased than those by only nickel or vanadium contaminated catalysts because nickel and vanadium could support each other. When nickel content was above 2000 ppm,  $H_2$  would be increased as liquid product yield and surface areas were decreased. And this caused percent conversion and gasoline yield decreased.



\*Test condition: see section 2.5.1.1, page 52

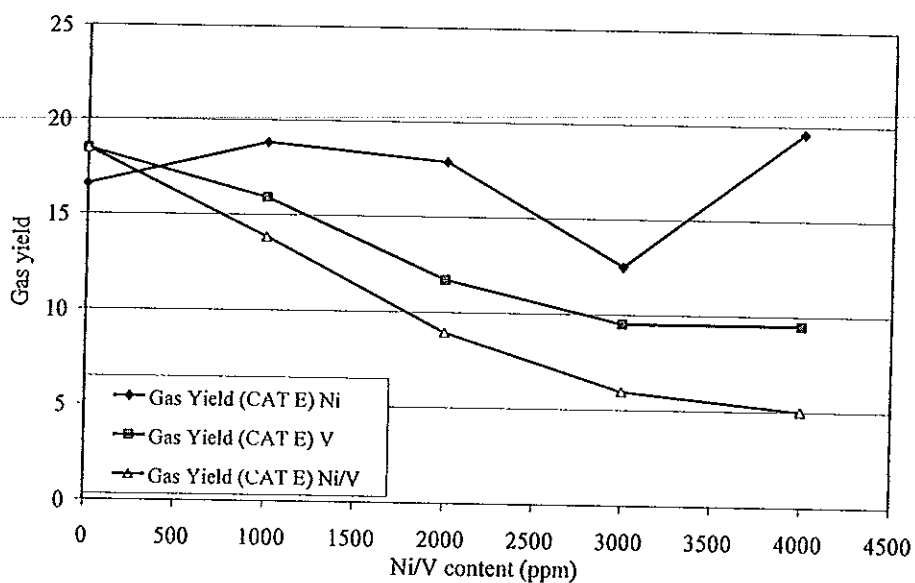
Figure 3-24 Effect of nickel/vanadium on coke yield.



\*Test condition: see section 2.5.1.1, page 52

Figure 3-25 Effect of nickel/vanadium on coke selectivity.

The structure of nickel/vanadium contaminated catalysts was destroyed by increasing of vanadium (Figure 3-24). Coke yield obtained by nickel/vanadium contaminated catalysts decreased. This is in contrast with increasing of coke yield obtained by nickel contaminated catalyst. In Figure 3-25, coke selectivity was increased as nickel/vanadium content increased.



\*Test condition: see section 2.5.1.1, page 52

Figure 3-26 Effect of nickel/vanadium on gas yield.

In Figure 3-26, gas yield gain by nickel contaminated catalysts trended to increase. This might be caused from increasing of  $H_2$  yield, produced from dehydrogenation reaction. In vanadium contaminated catalysts and nickel-vanadium contaminated catalysts vanadium damaged zeolite structure, so percent conversion and gas yield of the catalysts were decreased.

**Table 3.2** Percent of crystallinity reduction with metal content on catalyst E.

Vanadium content	Nickel content	%Crystallinity reduction
0	0	38.78
1000	0	34.48
2000	0	24.98
3000	0	21.95
4000	0	17.35

Vanadium content	Nickel content	%Crystallinity reduction
0	0	38.52
1000	1000	30.45
2000	2000	19.87
3000	3000	0*
4000	4000	0*

Remark: The percent crystallinity reduction was calculated by one Y zeolite peak method (fresh catalyst 100 percent crystallinity).

\* Can not detect the Y zeolite peak (23.6 deg. 2 $\theta$ )

Table 3-2 shows that the percent of crystallinity was decreased when vanadium contaminant increased. These results confirm that vanadium destroyed the zeolite structure. The crystallinity was rapidly decreased when nickel was simultaneously contaminated with vanadium. The combination of vanadium and nickel at high content level showed greater destruction of zeolite crystallinity than the summation of each separated effect. These results may come from the synergistic effect.

## Chapter 4

### CONCLUSIONS

In this work, synthetic Ni/V contamination on FCC catalyst was studied. The techniques for synthetic Ni/V contamination used in this work consisted of heat shock a fresh catalyst step at 600<sup>o</sup>C for 1 hour, then an impregnation treatment of Ni and/or V, after that a deactivation step by saturated steam at 800<sup>o</sup>C for 6 hours. For both depositions of Ni and V, the impregnation of Ni was carried out first. The catalytic activity of metal contaminated FCC catalysts was performed by micro-activity testing unit (MAT) at standard conditions (460<sup>o</sup>C, cat/oil ratio 3.2, WHSV 16 h<sup>-1</sup>) using Fang gas oil (boiling point range 260-340<sup>o</sup>C) as the feedstock.

The major effect of metal deposition on FCC catalyst is the dehydrogenation reactions. These reactions were evaluated by hydrogen and coke yields. The Ni contaminated FCC catalyst was predominantly affected by dehydrogenation. Hydrogen and coke selectivity were increased with increasing of Ni contamination. Percent conversion and percent gasoline yields were decreased as Ni content was increased. The loss of activity was possibly come from the loss of active sites by coke deposition. BET analysis showed that there was only slightly loss of catalyst's surface area by Ni contamination.

Vanadium contamination showed the major effect on zeolite structure destruction. The destruction of zeolite structure occurred under a severe condition of steam and high temperature at deactivation step. Vanadium content showed less effect on dehydrogenation than Ni (about 1/5 of Ni). Coke selectivity was increased with



vanadium content. The percent conversion decreased as vanadium content increased and this might be due to the loss of FCC catalyst's surface area.

The effect of both nickel and vanadium deposition on FCC catalyst showed similar results of dehydrogenation effect as explained above. In the relation of hydrogen yield with nickel and/or vanadium content, the nickel equivalent ( $4\text{Ni}+\text{V}$ ) content showed a good correlation of hydrogen yield. Nickel and vanadium content showed a synergistic effect on surface area and crystallinity loss at a high level of Ni and V. This may be the cause of rapidly decrease of percent conversion.

## Bibliography

American Society for testing and Material. 1997. Standard Test Method for Distillation of Petroleum Products at Atmospheric Pressure. ASTM Designation: D-86 Vol. 05. 03, The ASTM Committee of Standard, Easton, MD, U.S.A.

American Society for testing and Material. 1998a. Standard Test Method for Distillation of Crude Petroleum (15-Theoretical Plate Column). ASTM Designation: D-2892 Vol. 05. 03, The ASTM Committee of Standard, Easton, MD, U.S.A.

American Society for testing and Material. 1992. Standard Test Method for Surface Area of Catalysts. ASTM Designation: D-3663 Vol. 05. 03, The ASTM Committee of Standard, Easton, MD, U.S.A.

American Society for testing and Material. 1992. Standard Test Method for Testing Fluid Catalytic Cracking (FCC) Catalysts by Microactivity Test. ASTM Designation: D-3907 Vol. 05. 03, The ASTM Committee of Standard, Easton, MD, U.S.A.

American Society for testing and Material. 1991. Standard Test Method for Determining the Activity and Selectivity of Fluid Catalytic Cracking (FCC) Catalysts by Microactivity Test. ASTM Designation: D-5154 Vol. 05. 03, The ASTM Committee of Standard, Easton, MD, U.S.A.

Aurapun Angkasuwan. 1999. "Testing on Fluid Catalytic Cracking (FCC) Catalysts", Master of Engineering Thesis in Chemical Engineering, Prince of Songkla University. (Unpublished)

Bertus, et al. 1980. Passivation of Metals on Cracking Catalyst with Thallium. U.S.Pat. 4,238,367 Dec. 9, 1980.

Cadet, V.; Raatz, F.; Lynch, J. and Marcilly, Ch. 1991. "Nickel Contamination of Fluidised Cracking Catalysts A Model Study", Applied Catalysis, 68, 263-275.

Campagna, R.J. et.al. 1986. "Fresh FCC Catalyst Tests Predict Performance", Oil & Gas Journal, (Mar 24, 1986), 85-96.

Chester, et.al. 1981. Steam Passivation of Metal Contaminants on Cracking Catalysts. U.S.Pat. 4,276,149 Jun. 30, 1981.

Forester, 1991. Method of Passivating Alkali Metals on Fluid Catalytic Cracking Catalysts Using Aluminum Containing Compounds. U.S.Pat. 5,109,241 May 28, 1991.

Grace Davison, 1996. Guide to Fluid Catalytic Cracking: Part II, W. R. Grace & Co.-Conn.

Hollander, M.A.D.; Makkee, M. and Moulijn, J.A. 1998. "Coke Formation in Fluid Catalytic Cracking Studied with The Microriser", Catalysis Today, 46, 27-35.

Itoh, et.al. 1977. Method for Preparing Hydrocarbon Conversion Catalyst Using Acid Amide Solutions to Impregnate A Tin Component. U.S.Pat. 4,049,581 Sept. 20, 1977.

Kritsana Kritsanaphak. 2001. "Preparation of REY-Zeolite Catalyst", Master of Engineering Thesis in Chemical Engineering, Prince of Songkla University. (Unpublished)

McKay, 1977. Passivating Metals on Cracking Catalysts. U.S.Pat. 4,025,458 May 24, 1977.

McEVOY, J.E.; Milliken, T.H. and Mills, G.A. 1957. "Distribution of Metal Contaminants on Cracking Catalysts", Industrial and Engineering Chemistry, May, Vol. 49, 865-868.

Mitchell, B.R. 1980. "Metal Contamination of Cracking Catalysts. 1. Synthetic Metals Deposition on Fresh Catalyst", Industrial Engineer Chemistry Product Research Development, 19, 209-213.

Moorehead, E.L.; Maclean, J.B. and Cronkright, W.A. 1993. "Microactivity Evaluation of FCC Catalysts in the Laboratory: Principles, Approaches and Applications", In Fluid Catalytic Cracking: Science and Technology, p. 226. Magee, J. S. and Mitchell Jr., M. M., eds. Amsterdam: Elsevier Science Publishers B. V.

Nielsen, R.H. and Doolin, P.K., 1993. "Metals Passivation", In Fluid Catalytic Cracking: Science and Technology, p. 339-386. Magee, J. S. and Mitchell Jr., M. M., eds. Amsterdam: Elsevier Science Publishers B. V.

Oudar, J. and Wise, H., 1985. Deactivation and Poisoning of Catalysts, Newyork: Marcel Dekker, Inc.

Petti, T.F.; Tomczak, D.; Pereira, C.J. and Cheng, Wc. 1998. "Investigation of Nickel Species on Commercial FCC Equilibrium Catalysts-Implications on Catalyst Performance and Laboratory Evaluation", Applied Catalysis A: General, 169, 95-109.

Research Institute of Petroleum Processing, SINOPEC, 1997 (a) CLY-1 Hydrothermal Aging Unit Manual Instructions.

Rothrock, J.J.; Birkhimer, E.R. and Leum, L.M. 1957. "Fluid Cracking Catalyst Contamination Development of a Contaminant Test", Industrial and Engineering Chemistry, February, Vol.49, 272-282.

Sadeghbeigi, R., 1995. Fluid Catalytic Cracking Handbook, Taxus, Houston: Gulf Publishing Company.

Scherzer, J. and McArthur, D.P. 1988. "Catalytic Cracking of High-Nitrogen Petroleum Feedstocks: Effect of Catalyst Composition and Properties", Industrial Engineer Chemical Research, 27, 1571-1576.

Sutha Onka. 2001. "Preparation and Characterization of a Catalytic Cracking of REY-Zeolite", Master of Engineering Thesis in Chemical Engineering, Prince of Songkla University. (Unpublished)

- Tangstad, E.; Myhrvold, E.M. and Myrstad, T. 2000. "A Study on The Effect of Sodium Chloride Deposition on An FCC Catalyst in A Cyclic Deactivation Unit", Applied Catalysis A, 193, 113-122.
- Tatterson, D.F. and Mieville, R.L. 1988. "Nickel/Vanadium Interactions on Cracking Catalyst", Industrial Engineer Chemical Research, 27, 1595-1599.
- Venuto, P.B. and Thomas, H.E.JR., 1979. Fluid Catalytic Cracking with Zeolite Catalysts, Newyork: Marcel Dekker, Inc.
- Vreugdenhil, W. and Mao, M. 1999. "Calcium Contamination in FCC Catalysts", <http://www.akzonobel-catalysts.com/html/catalystcourier/courier37/c37a2.htm>, Akzonobel-Catalysts, Oct. 1999.
- Wallenstein, D. and Alkemade, U. 1996. "Modelling of Selectivity Data Obtained from Microactivity Testing of FCC Catalysts", Applied Catalysis A General, 137, 37-54.
- Wallenstein, D. and Haas, B.K. 2000. "Influence of Coke Deactivation and Vanadium and Nickel Contamination on The Performance of Low ZSM-5 Levels in FCC Catalysts", Applied Catalysis A: General, 192, 105-123.

Wilson, J.W., 1997. Fluid Catalytic Cracking Technology and Operations, Oklahoma  
Tulsa : Pennwell Publishing Company.

---



## Appendix A

### The acid digestion process for zeolite

1. Grinding the samples into fine powers and drying at 120°C.
2. Weighing 0.2 g of sample treated under step 1, putting it into a Teflon vessel and then adding 5 ml HF, 4 ml HClO<sub>4</sub> and 10 ml HCl (1:1 HCl:H<sub>2</sub>O v/v).
3. Heating the Teflon vessel under the low temperature (<180°C), until the fog of HClO<sub>4</sub> vapors was observed.
4. Cooling the vessel and putting 2 ml H<sub>2</sub>O<sub>2</sub>. After waiting a few minutes, heat the vessel again until see the fog of HClO<sub>4</sub> vapors appears again.
5. Cooling it to the room temperature.
6. Adding 20 wt% HCl into the vessel to 25 ml.

## Appendix B

### True Boiling Point Distillation Unit (TBP)

This work used gas oil feedstock, boiling point rang 260-340<sup>o</sup>C that was redistilled from Fang Diesel Oil by true boiling point distillation unit (TBP).

TBP is designed mainly according to ASTM D-2892. The pot volume is 15 liters and the charge volume is 5-10 liters. The reflux ratio is fixed to 5:1. The unit can provide 15 theoretical plates.

It is mainly used to evaluate the crude oil. By this unit the crude oil is distilled at atmospheric pressure, 100 mmHg. and 10 mmHg. absolute pressure. The distilled is collected into glass tubes that are analyzed by other methods.

TBP is controlled by a computer. The distillation pressure, temperature, the distillation rate, distilled collection etc. are automatically controlled by a computer.

#### B-1 Specification and condition requirements.

- Distillation pot volume : 15 L.
- Charge of crude oil : 5-10 L.
- Theoretical plates : 15
- Distillation temperature : < 350<sup>o</sup>C (AET)
- Accumulative repeatability : 1%
- Weight loss : <0.4%

- Distillation stage : 3
  - a. Atmospheric distillation;
  - b. 100 mmHg. (95 mmHg.) distillation;
  - c. 10 mmHg. Distillation;
- Collecting bottles : 10 x 3
- Collecting bottle volume : 950 ml.
- Power supply : three phase, 3 x 220 V AC
  - frequency : 50 or 60 Hz.
- Power consumption : 6 kW (one of the three phase require 3.5 kW)
- Environment temperature : <35°C
- Air compressor or air supply : 0.3 MPa
- Tap water
- Dry ice

## B-2 Equipment introduction

### 1. Distillation pot

The volume of distillation pot is 15 liters that can load 5-10 liters of crude oil. There are two heaters with it, one at the bottom of the furnace, another is around the furnace wall. There are three holes at the top, 1. use for insetting the pot thermocouple (T4), 2. use for draining out residual oil, 3. use for feeding crude oil and measuring the differential pressure. The pot is connected with the distillation column by flange.

## 2. Distillation column

The column is 875 mm. Long with inner diameter 50 mm. It is packed with semi-ring feedings. There is stainless steel cylinder jack cover the column that quickly cool down after distillation.

## 3. Top condenser

It is on the top of the column. There are 5 slots surround the inner condenser wall. Five part of condensed oil go back to the column. Another one part of condensed oil go out of the column, so the reflux ratio is 5:1. The oil stream is condensed by water jacket around the condenser.

## 4. Conduct tube

The distillate from the column passes through a conduct tube to the collector. Further condensation occurs there. There are two condensers, one uses a cold water, another use the cold medium from the cool bath.

## 5. Glass collector and gas collector

When the distillation temperature lower than  $65^{\circ}\text{C}$  in the atmospheric distillation, the distilled oil should be collected in the glass collector which is cooled down by the cool bath and gas should be collected in the metal gas collector which is in a bath filled with alcohol cooling down by dry-ice.

## 6. Automatic collector

Ten collecting bottles that automatically or manually control in the distillation process.

## 7. Vacuum system

Vacuum pump is used for decreasing pressure in the distillation process.

#### 8. Cool bath

It uses to condense oil vapor in the atmospheric distillation. In the vacuum distillation, it uses for well condensing in vacuum pump.

#### 9. Control system

The temperature, the distillation vacuum pressure and the column differential pressure (or distillation rate) are controlled or measured by West controllers, while the heating power contractor etc. are controlled by Simatic S7-200 programmable logical controller. The West controller and PCL are controlled by a PC computer. West controllers can set in automatic or manual mode.

#### B-3 Operation procedures

For the true boiling point distillation of crude oil usually need following steps:

- 1) Put the crude oil in the pot and lift the pot's heater.
- 2) Execute atmospheric distillation, the cut points are usually 80, 100, 120, 135, 145, 150, 165, 180 and 200<sup>o</sup>C.
- 3) Down the pot heater then cool down the pot and column until the column temperature (T1) below 100<sup>o</sup>C and the pot temperature (T4) below 150<sup>o</sup>C.
- 4) Execute vacuum distillation at 100 mmHg., the cut points are 220, 230, 240, 260, 280 and 300<sup>o</sup>C (AET).
- 5) Down the pot heater then cool down the pot and column until the column temperature (T1) below 100<sup>o</sup>C and the pot temperature (T4) below 150<sup>o</sup>C.  
Then stop the vacuum pump.
- 6) Vacuum distillation at 10 mmHg., the cut points are 320, 350 and 360<sup>o</sup>C (AET).

7) Down the pot heater then cool down the pot and column until the column temperature (T1) below 100°C and the pot temperature (T4) below 150°C.

8) Drain out the residual oil from the pot by a drainpipe through the pot's outlet by applying air or nitrogen pressure to the pot's oil inlet.

**Caution:** Before doing this, the V2 and V3 must be closed, otherwise, the expensive vacuum pressure transducer would be damaged.

9) Wash the distillation system by putting 2 liters of light oil into the pot, manually start heating as atmospheric distillation until about one liter of oil distill.

10) Drain off resident oil like step 8, close the instrument.

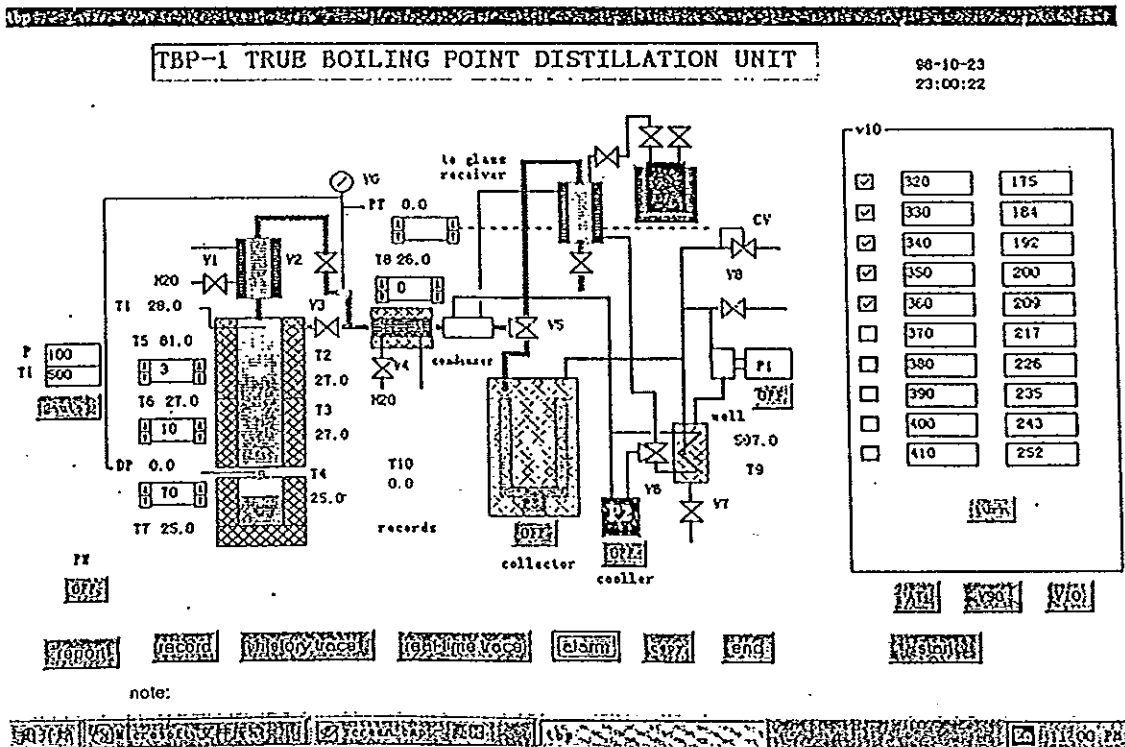


Figure B-1 True boiling point distillation unit.

## Appendix C

### Hydrothermal Deactivation (by CLY-1 Hydrothermal Aging Unit)

#### C-1 Installation and Preparation

##### C-1.1 Power Supply

It is better to have a three-phase electrical power. Each L-N voltage is 220 V, AC, 20A, If the lab isn't equipped with three-phase power supply, the three lines should be shorted in the power switch. The water pump and the recorder is lined to AC 220 V.

##### C-1.2 Air Supply

There has to be an air supply, with a pressure of about 0.4 MPa. It can be from a pipe line or a small air compressor. On the aging unit the air pressure is adjusted to 0.3 MPa, Regulator pressure is adjusted to 0.1 MPa and the air flow is adjusted to 30 ml/min.

##### C-1.3 Water

The water used for aging should be demonized water. Before starting aging, the water is to be filled in the water tank to the full scale.

##### C-1.4 Temperature Adjustment

The furnace must have a long enough isothermal length (~10 cm). If the isothermal length is not long enough, you can adjust the furnace temperature as follows. Fill the aging tube with porcelain rings or sand. Set the three temperature controller of the furnace at nearly 800°C, start heating and air stripping. When the

temperature is stable, start water pump at a rate of 25 ml/min. After 40 min gradually adjust the three temperature controllers for the furnace until the isothermal length reaches its maximum at 800°C.

## **C-2 Aging Procedure**

### **C-2.1 Load Catalyst**

The catalyst is to be loaded in the middle of the isothermal section of the aging tube as follows.

- 1) Fill porcelain rings at the bottom of the aging tube up to the isothermal section (about 17 cm. From the bottom). And at its top, put some broken rings, the thickness is about 1-2 cm.
- 2) Put a quartz cotton layer of about 1-2 cm on its top.
- 3) Better to fill 40 ml. Catalyst inside the tube.
- 4) Put a quartz cotton layer of about 1-2 cm. Thick on the top of the catalyst bed.
- 5) Put some broken porcelain chips in.
- 6) Put in the tube with porcelain rings.
- 7) Put the tube in the furnace and line up.

### **C-2.2 Pre Air Stripping and Start Heating**

- 1) Open the air-in valve on the unit panel, adjust the air pressures to 0.3 MPa, regulated pressure be 0.1 MPa, and adjust the air flow to 30 ml/min.
- 2) Turn the "power" switch on.
- 3) Set the heating time for 2 hrs.



- 4) Set the aging time for 4, 6, 8, 12, 17, (16) hrs. respectively.
- 5) Set the alarm time at aging time minus 1 min.
- 6) Push the button "heat" to start heating.
- 7) Turn on pump power and set pump rate at 0.41 ml/min.

### **C-2.3 Start Hydrothermal Aging**

When the aging temperature stays at 800°C for about 10-20 min, push the "start" button to start aging. (use water-pump to start pump water, water valve open and the air valve close, and aging time start going on automatically)

### **C-2.4 Post Air Stripping**

When the aging time has passed, the water-pump stops, water valve closed and the air valve opened automatically by LOGO, the post air stripping begins.

### **C-2.5 Finish**

After about 10 minutes post air stripping, you can turn off the power and close the air supply, take out the aging tube and cool it down in the air, and then take out the catalyst and separate it from porcelain rings.



Figure C-1 Hydrothermal aging unit

## Appendix D

### Micro-Activity Unit

In this work we used MAT unit model WFS-1D produced by Research Institute of Petroleum Processing (RIPP), SINOPEC. WFS-1D is designed according to the standard method developed by RIPP and mainly used to test the activity index of cracking catalyst. The standard test method of cracking catalyst micro-activity index in China is RIPP 92-90, the conditions are:

Standard feed gas oil: Straight-run light oil, boiling range of 235 - 337°C

Reaction temperature :  $460 \pm 1^\circ\text{C}$

Feed oil weight :  $1.56 \pm 0.01$  g

Feeding time : 70 sec

Post stripping time : 10 min

Stripping nitrogen flow-rate : 20-30 ml/min

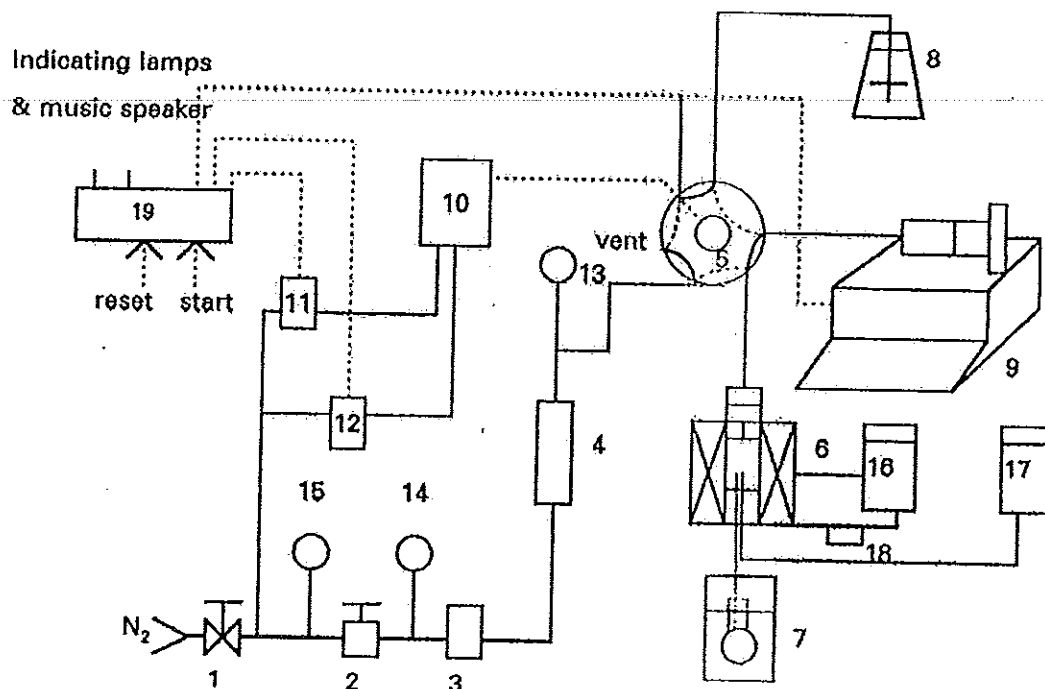


Figure D-1 The process diagram of MAT unit.

- |                               |  |  |
|-------------------------------|--|--|
| 1 : valve                     | 8 : feed oil bottle                        | 15 : inlet pressure gauge<br>0-0.16 MPa  |
| 2 : pressure                  | 9 : injection pump                         | 16 : temperature controller<br>(furnace) |
| 3 : flow regulator            | 10 : six-port valve driver                 | 17 : temperature monitor<br>(reactor)    |
| 4 : rotary flow meter         | 11 : solenoid valve                        | 18 : solid relay                         |
| 5 : six-port valve            | 12 : solenoid valve                        | 19 : programmable logic<br>controller    |
| 6 : reactor & heater          | 13 : reaction pressure<br>gauge 0-0.16 MPa |  |
| 7 : ice bath & collect bottle | 14 : regulated pressure<br>gauge 0-0.4 MPa |  |

### D-1.1 Reaction and Collection System

The system includes the reactor, the heating furnace, the condenser well and the collecting bottle. The reactor is the heart of the reaction system where the reaction takes place. The screw bar is at the reactor's upper section, around which the feed oil is vaporized. Under the bar there is an isothermal section, the length is about 7 cm.

Where the catalyst is to be loaded. At the bottom, liquid product is collected in a receiver bottle by passing through a long needle that is joined with the receiver bottle by a rubber tube. The bottle is immersed in the condense well filled with ice and water. A medical syringe needle sticks into the rubber tube, through it the cracking gas exits.

#### **D-1.2 Feed Oil Injection System**

This includes the injection pump, the six-ways valve and the feed oil bottle. It is used to smoothly inject  $1.56 \pm 0.01$  g feed oil into the reactor within 79 seconds.

#### **D-1.3 Stripping System**

It includes the pressure regulator, the gas-flow regulator, pressure gauge and rotary flow-meter. The functions of this system are:

- 1) Pre-stripping : The nitrogen stripping before oil injection can ensure the catalyst is in the nitrogen atmosphere and water-free
- 2) Post-stripping: After oil injection the nitrogen stripping can get residual oil in the tube into the reactor and strip out all reaction production from reactor.

#### **D-1.4 Measurement and Control System**

The system includes the temperature controllers, the solenoid valves and the programmable logic controller (PLC). The two temperature controllers are the same, one indicates the catalyst bed temperature, and the other one controls the temperature of the furnace. They are intelligent controllers produced by Shimandan (Shimadzu), Japan, with PID self tuning, automatic cold conjunction temperature compensation, thermocouple linearisation and deviant correction. Due to the uniqueness of the

furnace manufacture technology, the reactor has more than 7 cm. Long isothermal catalyst bed with only one heater.

The PLC controls the injection pump and the six-port valve. The operating procedures are as follows (refer to figure B-1):

- 1) Preparation step: If the nitrogen source is supplied, when the power switch turns on the PLC will draw the six-port valve to the position shown by the dotted lines. That is the pre-stripping.
- 2) Oil injection step: After the reactor bed temperature has stabilised, push the “start” button, then the six-ways valve will turn to the position shown by the solid lines, the syringe plug goes forward, the feed is injected into the reactor through the six-way valve.
- 3) Oil suction step: After 70 seconds of oil injection, the six-way valve turns back to the dotted line position. Then post-stripping begins and syringe plug goes backward, the feed oil is sucked into the syringe from the feed oil bottle.
- 4) Squeezing step: When the oil-suction has lasted for 70 seconds the syringe plug goes forward again for 20 seconds to squeeze out the gas bubbles.
- 5) Post-stripping: When post-stripping lasts about 10 min (the speaker song music), the system goes back to the preparation step again. In order to keep the syringe plug always stay at a certain position, only in this period the reset button is enable.

## **D-2 PC Work Station (Optional)**

### **D-2.1 Functions**

PC workstation is designed to work with WFS-1D to change and save test parameters, remote control, print report, display the history or real time trace of process variables. It is linked to the test unit through a serial communication card, but the test unit can work independently.

### **D-2.2 Operations**

#### **1) Start up**

- 1.1) Enter Window 3.11
- 1.2) Double click Group WFS-1D
- 1.3) Double click the icon WFS-1D of the group
- 1.4) Input the operator's name and click "OK" then go into the working window

#### **2) Operations in the main working window:**

- 2.1) To change the temperature controller's parameter: There are two temperature controllers. The upper one is used to indicate the reaction temperature, The lower one is used to control the furnace's temperature. The set value can be changed on its window, click "SV" to send it to the controller. The PID parameters can be changed by click the "PID", click the PID diagram blank place can close the PID window.
- 2.2) To change the operation time parameters: There is operation timetable on the right of the main working window. The feeding time

(T1), sucking time (T2), preparing time (T3) and purging time (T4) all can be changed. The ranges are:

$$0 \leq T1 \leq 150s$$

$$T1 \leq T2 \leq T1 + 30s$$

$$T3 = T2 - T1 (s)$$

$$T4 \leq 991 - T1 (s)$$

After they are set or changed, click "OK" then click "SEND", these parameters can be sending to PLC of the test unit.

### D-2.3 Commands

There are several command blocks at the main working window button:

1. "RUN" : begin to run
2. "RESET" : to reset the system
3. "EXIT" : to quit from the main working window
4. "SAVE" : to save the parameters onto the system's hard disk
5. "LOAD" : to load the parameter from the system's hard disk
6. "QUIT" : to quit from the WINDOWS
7. "CALCULATOR" : to use system's calculator
8. "REPORT" : to print test report. Each report can contain two test

reports. According to the prompt input parameters, and then click "OK", the computer can calculate out the needed parameters, and then click "PRINT" and the report can be print out Click "EXIT" to quit from the window.

9. "TRACE" : to display the temperature's trace. In this window there are several command blocks.



- "HISTORY" : to display history traces, the test number can be selected by click "SELECT" and "TIME"

- "SET SCALE": to set the temperature's scale by input the minimum/maximum temperature.

- "EXIT" : to quit from this window

### **D-3 Préparation before Operation**

#### **D-3.1 Reactor's Temperature**

In order to have reactor's catalyst bed temperature correctly indicated, its thermocouple should be calibrated regularly (half or one year) with standard or recently calibrated thermocouple and standard differential potential meter. The deviation value should input into the temperature controller.

The catalyst bed temperature of the reactor should be controlled at  $460 \pm 1^\circ\text{C}$ . It can be obtained by adjusting the furnace temperature controller's set value.

#### **D-3.2 Tested Catalyst**

In order to have the test catalyst correctly weighted, before loading it into the reactor it should be dried in an oven for an hour at  $110 - 120^\circ\text{C}$ .

#### **D-3.3 Feed Oil**

Heavy oil isn't suitable for this apparatus

#### **D-3.4 Feed Oil Weight Calibration**

In order to have a correct injected oil weight, it is suggested to calibrate the weight every day before starting the experiment. The method is to insert the joint in to a small bottle, then push the "start" button. When the squeezing step is finished, push

the “reset” button and weigh the bottle. If the oil weight is not  $1.56 \pm 0.01$  g, adjust the pump’s speed and calibrate again.

Example: Calibration of the syringe pumps.

**Table D-1** Feed oil: gas oil (Light Cycle Oil, LCO) obtained from RIPP

Flow rate MI/min	1.52	1.52	1.52	1.52	1.52	1.52	1.52
Measured Value (g)	1.569	1.571	1.563	1.557	1.556	1.556	1.559
average = 1.562 g							

### D-3.5 Material Balance Test:

In this test the cracking gas is not collected and the coke deposit is not detected either, so in practice test the material balance is not done. The material balance test here is like this: Instead of using catalyst, use quartz sand to do the same process as with catalyst, weight the collected oil, it should be more than 98% of the injected feed.

Example:

**Table D-2** Blank test for checking liquid recovery

<b>Feeding amount (g)</b>	1.562	1.562	1.562	1.562
<b>Liquid Recovery (g)</b>	1.547	1.567	1.558	1.537
<b>Balance (loss, g)</b>	0.015	-0.005	0.004	0.025
<b>% recovery</b>	99.0	100.32	99.7	98.4

#### D-4 Operation Steps

1. Adjust the gas tank pressure to 0.30-0.35 MPa and then turn on the power switch, WFS-1D goes stripping status automatically.

2. Put some quartz fiber, at the reactor's bottom, weight 5 g of catalyst and load it into the reactor. Put the reactor into the furnace and link it to the six-port valve.

3. Link the collect bottle to the reactor with rubber tube and then put the bottle into the ice bath well.

4. When the reactor's temperature has been stable for 5 min, push the "start" button then the unit works in automatic for injection, suction, squeezing and post-stripping. After 10 minutes stripping, the speaker sings music indicating that the test has finished.

5. Take off the collection bottle and wipe out the water on the bottle, weigh the bottle and note down the collected oil weight, put it in a refrigerator for G.C. analysis.

6. Take out the reactor from the furnace and take out the catalyst.

#### D-5 Analyses of Reacted Product and Data Disposal

The liquid product is analyzed with G.C. and then calculated the MAT with program WFS-1D

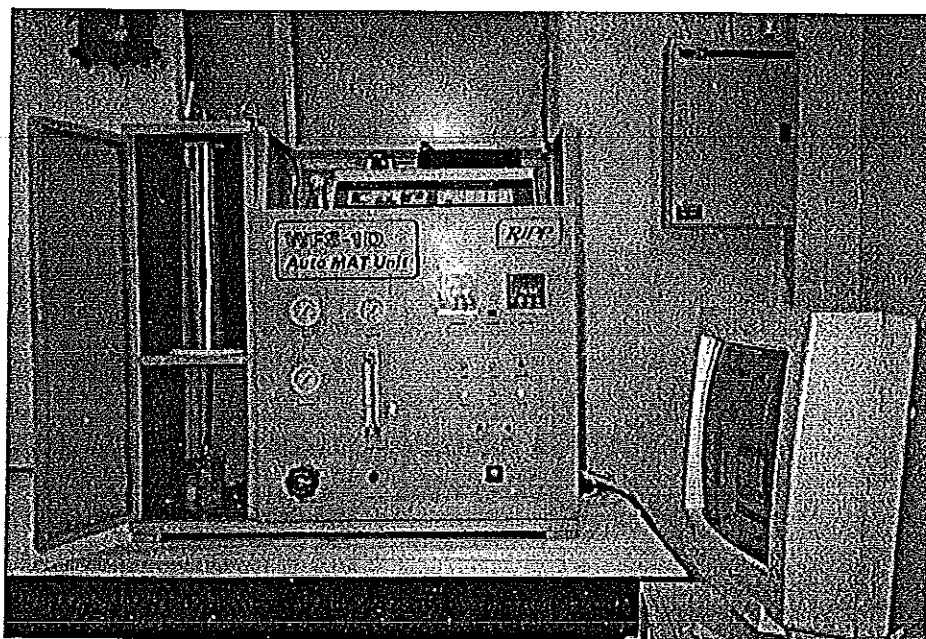


Figure D-2 Micro-Activity Test Unit

## Appendix E

### Gas Chromatography set and Integrator

The G.C. is Shimadzu GC-14B, the integrator is Shanghai HP 3295. For the use of detecting cracking catalyst microactivity index, the conditions in analysis are

Carrier gas : nitrogen (OFN), flow rate: 35-40 ml/min

Combustion gas : hydrogen, flow rate: 40 ml/min

Auxiliary gas : air, flow rate: 400 ml/min

Temperature of vaporization chamber (injector): 280°C

Temperature of column chamber : 280°C

Temperature of column chamber : rises from 35°C to 80°C by rate of 15°C/min, then rises from 80°C to 235°C by rate of 8°C/min, hold at 235°C for 10 min.

Sample injection volume : 1  $\mu$ L

Range : set to 10

The recommended integrator's parameters are:

Attenuation : 8

Half-pack width: 0.04 min. after 1.5 min. changes to 0.16 min

Use Integrate function 14 to sum up all the peak areas (%wt) before C<sub>12</sub> (including C<sub>12</sub>). It is the cut point of gasoline and feed oil (gas oil or diesel oil).

Use integration function 5 to set the base line horizontally.

## E-1 Operations steps

### E-1.1 Preparation

- 1) Open the carrier gas and the ignition gas until pressure 4 Mpa.
- 2) Adjust air and hydrogen flowrate to design value
- 3) Set column, injector, detector temperature that show above.

### E-1.2 Operation

- 1) Open nitrogen, air and hydrogen.
- 2) On the power switch of gas chromatography then press the start bottom.
- 3) On the power switch of integrator, feed paper then press the ESC bottom.
- 4) When column, injector, detector temperature are constant (green light at ready position is bright), inject 0.5  $\mu\text{l}$ . of sample into the injection port 1 and press the start bottoms of both gas chromatography and integrator immediately.
- 5) When the set time program is complete, GC will stop and cool down the column to initial column temperature (green light at cool position is bright)
- 6) When the green light is change to ready position, GC. can analyze another sample or close.

## E-2 Calibrate the retention time of n-dodecane

Put a little standard n-dodecane ( $\text{CH}_3 (\text{CH}_2)_{10} \text{CH}_3$ ) into the mixture of gasoline and the standard feed oil or used only standard n-dodecane, Analyze the sample with G.C., The n-dodecane retention time is the cut pint (n-dodecane belong to the gasoline)

### E-3 Calculation the microactivity index

Put weight of feed oil, weight of liquid product, gasoline area (%wt) in program WSF-1D in report command, it will calculate the MAT index.

$$\text{Microactivity (MA, \%)} = 100 - \left[ \left( \frac{100 - A}{C} \right) \times B \right]$$

Where

A = Gasoline yield, analyzed by GC, %wt

B = Liquid product from MAT, g.

C = Feed oil, g

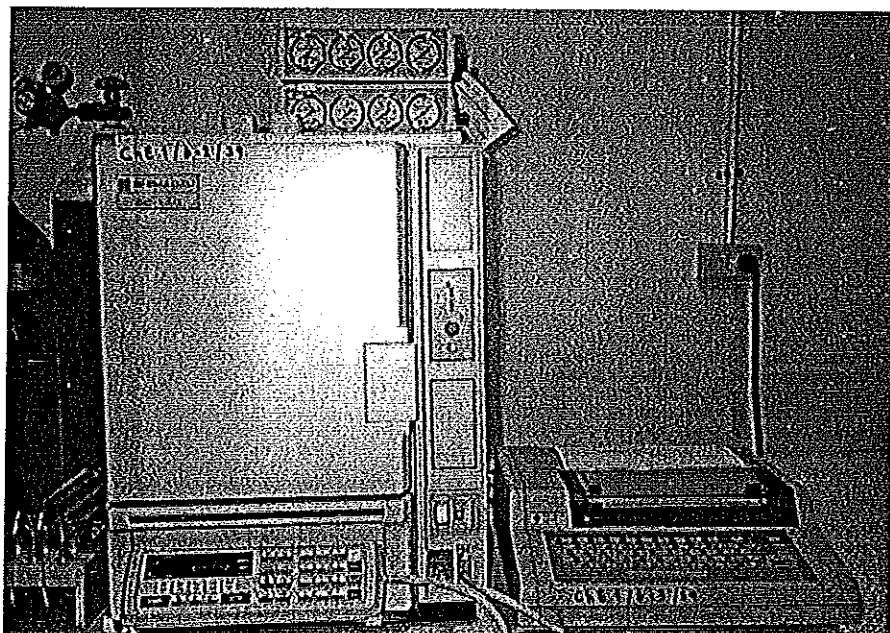


Figure E-1 Gas Chromatograph unit

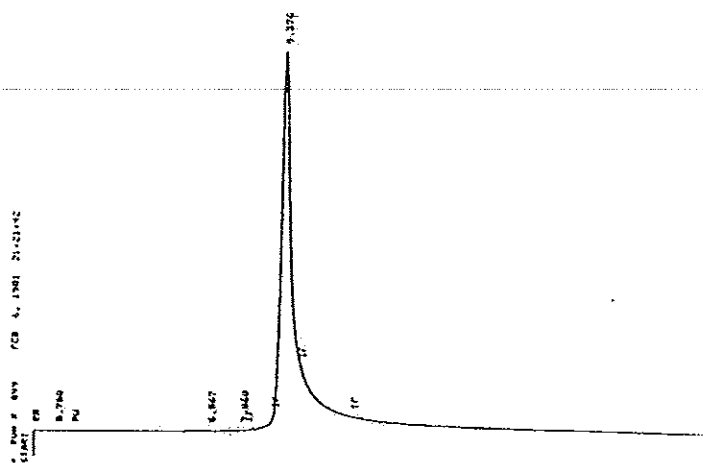


Figure E-2 Chromatogram of n-dodecane (n-C<sub>12</sub>)

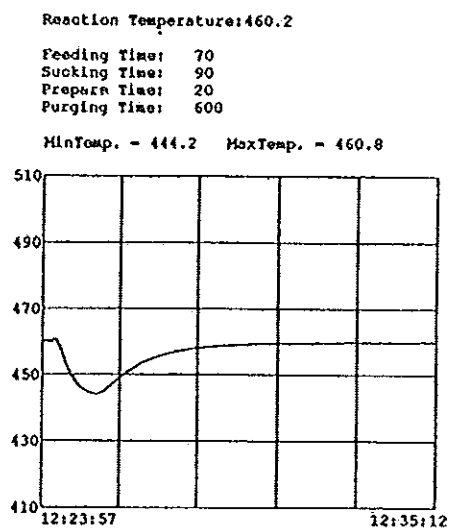


Figure E-3 Temperature profile during catalytic cracking.



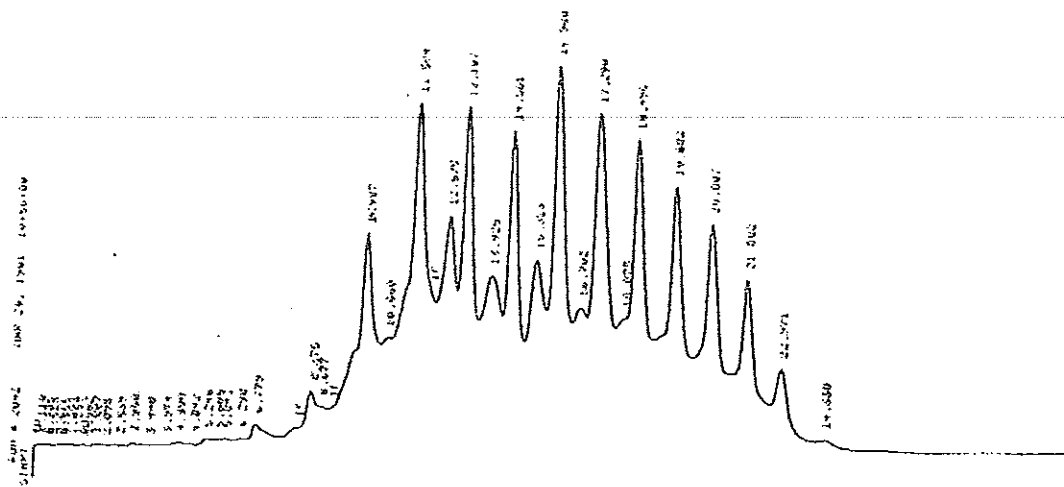


Figure E-4 Chromatogram of gas oil (LCO) before reaction with catalyst.

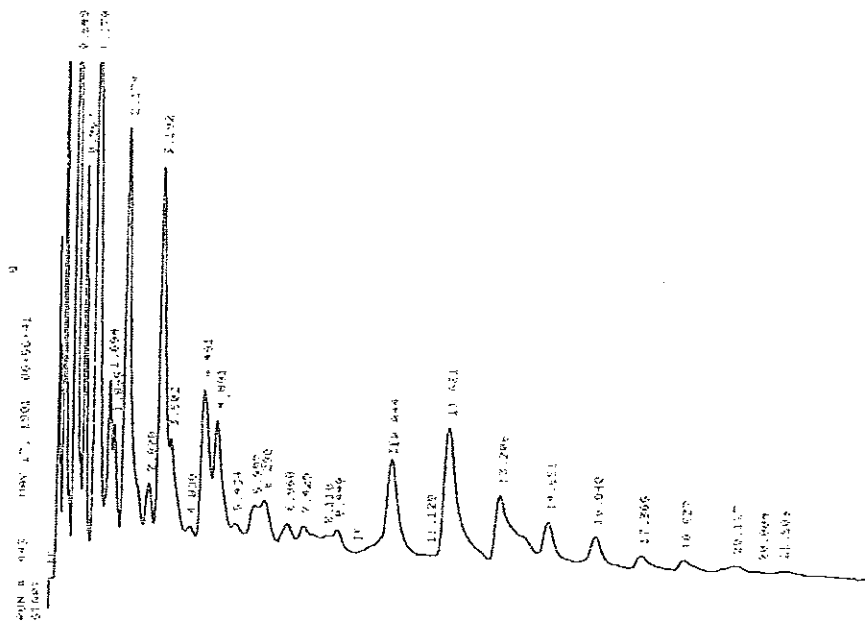


Figure E-5 Chromatogram of liquid after reaction.

Table E-1 MAT operation report

Test Date	10-05-1998
Operator	Aurapun
<b>Test Condition :</b>	
Reaction Temp. (C)	460
Feeding Time (S)	70
Space Velocity Weight (/h)	16
Feed oil (g)	1.56
Catalyst No.	A8.1
Reaction No.	2
<b>Item :</b>	
Feeding Time (S)	70
Reaction Temp. (C)	460.2
Catalyst Load (g)	5.004
Feed oil Quantity (g)	1.565
<b>Liquid Product Weight :</b>	
Oil and Receiver weight (g)	1.332
Receiver weight (g)	0
Oil weight (g)	1.332
Light oil yield	0.4823
Micro Activity	55.938
Average Value	55.938
<b>Note</b>	

## Appendix F

### Gas Chromatography set and Integrator (GC-14A)

The G.C. is Shimadzu GC-14A, the integrator is Shanghai HP 3295. For the use of detecting hydrogen content in gas product that produces from microactivity test, the conditions in analysis are

Carrier gas : Helium (UHP), flow rate: 25-30 ml/min

Temperature of vaporization chamber (injector): 90°C

Temperature of column chamber : 50°C (constant temperature)

Temperature of detector chamber : 100°C

Temperature of TCD detector chamber : 100°C

Current : 60mA

Sample injection volume : 100  $\mu$ L

The recommended integrator's parameters are:

Attenuation : 0

Threshold : -2

Chart speed : 0.5

Area rejection value : 0

Half-pack width: 0.04 min. after 1.5 min. changes to 0.15 min

Use Integrate function 0 to set base line now. Use integration function 5 to set the base line horizontally.

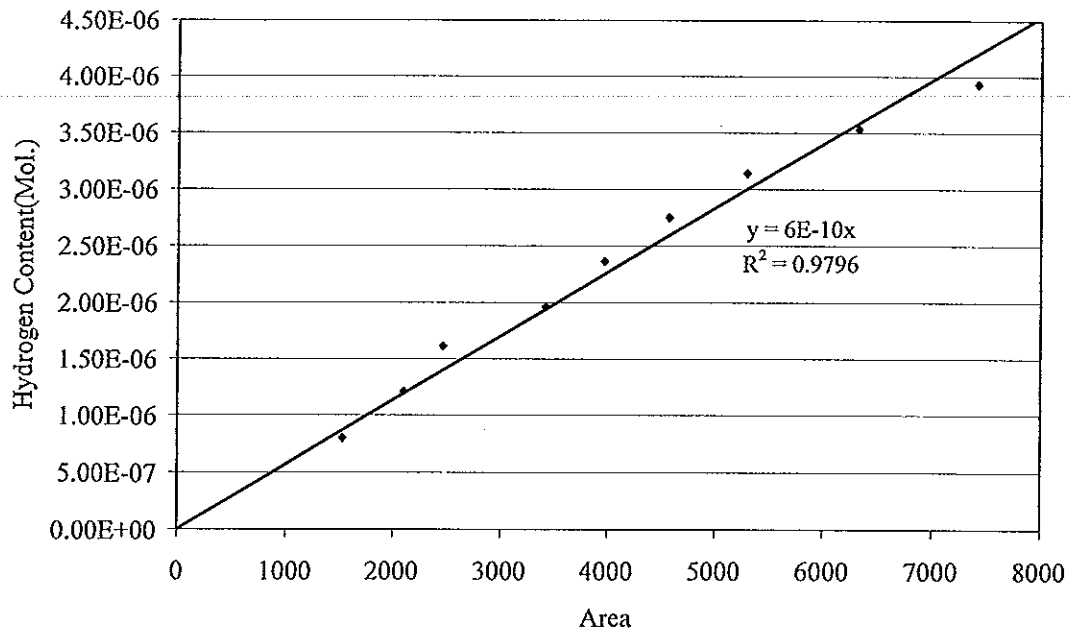
## **F-1 Operations steps**

### **F-1.1 Preparation**

- 1) Open the carrier gas through pressure 4 Mpa.
- 2) Adjust helium flowrate to design value
- 3) Set column, injector, detector temperature that show above.

### **E-1.2 Operation**

- 1) Open helium gas 10 minutes before opening the instrument.
- 2) On the power switch of gas chromatography then press the start bottom.
- 3) On the power switch of integrator, feed paper then press the ESC bottom.
- 4) When column, injector, detector temperature are constant (green light at ready position is bright), inject 100  $\mu\text{l}$ . of gas sample, collect from microactivity test, into the injection port 1 and press the start bottoms of both gas chromatography and integrator immediately.
- 5) Wait for all of gas sample leave out the column. Generally wait for 20 minutes. Then GC. can analyze another gas sample or close.



\*Test condition: see page 111

Figure F-1 Calibration curve of hydrogen gas

## Appendix G

### Surface Area and Pore Size Analyzer

#### G-1 System overview

The COULTER SA 3100 analyzers are bench-top Surface Area and Pore Size Analyzers with built-in vacuum pumps. It measures surface areas, pore size distributions, and pore volume parameters of powdered, pelleted or solid piece samples.

The instrument is very easy to learn and use due to the simple, graphical touch screen user interface. The interface allows you to create analysis profiles which store the run parameters you use most often. Run setup is therefore streamlined. In addition, isotherms for commonly run materials can be stored and used by the instrument to speed analysis through the use of a special algorithm.

#### G-2 System function

The SA 3100 analyzer is a completely integrated sample preparation, sample analysis, and data processing system. This section gives a brief overview of system operation.

##### G-2.1 Control

The instrument is controlled by a simple touch screen user interface. The interface displays the real-time status of all instrument functions, provides touch-key operation, and allows you to customize the SA 3100 analyzer for your application.

### **G-2.2 Sample preparation – outgassing**

Samples are prepared for surface area or pore size analysis on the SA 3100 analyzer by outgassing. Outgassing removes adsorbed gases and moisture from the sample surface. Outgassing is performed by evacuating gases from the sample tube(s) with the vacuum pump. The sample tube (s) are heated for outgassing by the outgassing furnace. Three samples can be simultaneously outgassed at the three outgassing ports. Sample analysis can proceed independently of and simultaneously with outgassing.

### **G-2.3 Sample analysis**

#### **General**

Many types of analyses can be performed with the SA 3100 analyzer, Principles of Operation, for further details. All analyses, however, involve the adsorption of a gas (called the adsorbate gas) onto the surface and into the pores of a sample prepared by outgassing. (Adsorption is the condensation of gas molecules onto the surface of a material.) The adsorbate gas is added in known doses into an evacuated tube containing the sample, incrementally increasing the quantity of adsorbed gas and the pressure in the sample tube. The pressure readings are used, in turn, to calculate the volume of gas adsorbed.

The volume of gas adsorbed is measured as a function of relative pressure. Relative pressure is the ratio of the pressure in the sample tube to saturation vapor pressure of the adsorbate gas (The pressure of which the adsorbate gas liquefies). The saturation pressure measured for every sample tube pressure data point. During the measurement, the sample is maintained at a temperature where liquefaction of

adsorbate gas can take place on the sample. To maintain this temperature, the sample tube is immersed in a dewar of liquid cryogen (usually nitrogen) during analysis.

Some types of analysis measure the desorption of gas from the surface and pores of the sample.

The surface area, pore size distribution, and pore volume parameters are calculated from the isotherm data. Depending on the type of analysis required, and adsorption and desorption isotherm may consist of as few as three points or as many as 100 to 200. Analysis time is a function of the number of points required.

#### **Fast BET analysis**

The SA 3100 Analyzer has a special fast BET mode which permits accelerated surface area analysis when increased throughput is required.

### **Output**

#### **General**

Result from analyses are automatically written to the diskette, and may be printed automatically at the completion of analysis if a printer is installed and configured. Output to the diskette is in ASCII format. The COULTER SA-VIEW microsoft windows-based program can be used for reviewing and comparing data files, printing data, and copying data to other windows applications.

#### **G-3 Components**

Figure G-1 (front view) and G-2 (back view) illustrate the SA 3100 system. The main components are called out in the figures and described below.



### **G-3.1 Control Components.**

#### **Power switch**

The red rocker switch is the power switch. To turn the instrument on, press the top of the switch (labeled I) until it clicks and is flush with the instrument case. To turn the instrument off, rock the switch back to its original position by pressing the bottom of the switch (labeled O).

#### **Touch screen**

When the instrument turned on, the touch screen lit and displays an interface screen with touch keys. All instrument control is accomplished by the touch screen. The keys are activated by touching with your finger or other soft blunt object (such as a pencil eraser). If the screen is not touched for 15 minutes, a screen saver becomes active, displaying only the status of the instrument. Touch the screen to restore the full display.

### **G-3.2 Measurement and outgassing components**

#### **Measurement manifold (internal)**

The measurement manifold is the heart of the SA 3100 analyzer. It consists of a gas manifold, valves, and pressure transducers, and connects the adsorption port, the vacuum pump, and the gas inputs.

#### **Analysis port**

The sample tube is attached to the analysis port for sample analysis.

**Saturation port**

The saturation tube is attached to the saturation port. The saturation tube is used to measure the saturation vapor pressure of the adsorbate gas, functioning as a vapor pressure thermometer.

**Outgassing manifold (internal)**

The outgassing manifold consists of gas valves and connections to the measurement manifold.

**Outgassing ports**

Sample tubes are attached to the outgassing ports for outgassing. Three samples can be outgassed simultaneously. Sample analysis can proceed while other samples are being outgassed.

**Outgassing furnace**

The outgassing furnace heats the samples to the required temperature for outgassing. You set the temperature appropriate for your sample.

**Dewar**

The dewar holds liquid for a constant temperature bath to keep the sample tube and saturation tube at the temperature required for analysis.

**Vacuum pump**

The vacuum pump achieves the low pressures necessary for outgassing and sample analysis.

**Gas lines**

Helium and the adsorbate gas lines connect to the respective gas cylinders. Gas must be supplied to the SA 3100 analyzer at the pressure of 12 psig to 15 psig.

### G-3.3 Output components

#### Floppy disk drive

The high density floppy disk drive is provided for data storage. Preformatted diskettes (IBM format) must be used.

#### Printer port

This is a standard parallel printer port. Coulter offers a rang of dot-matrix, inkjet, or laser printers compatible with the SA 3100 analyzer.

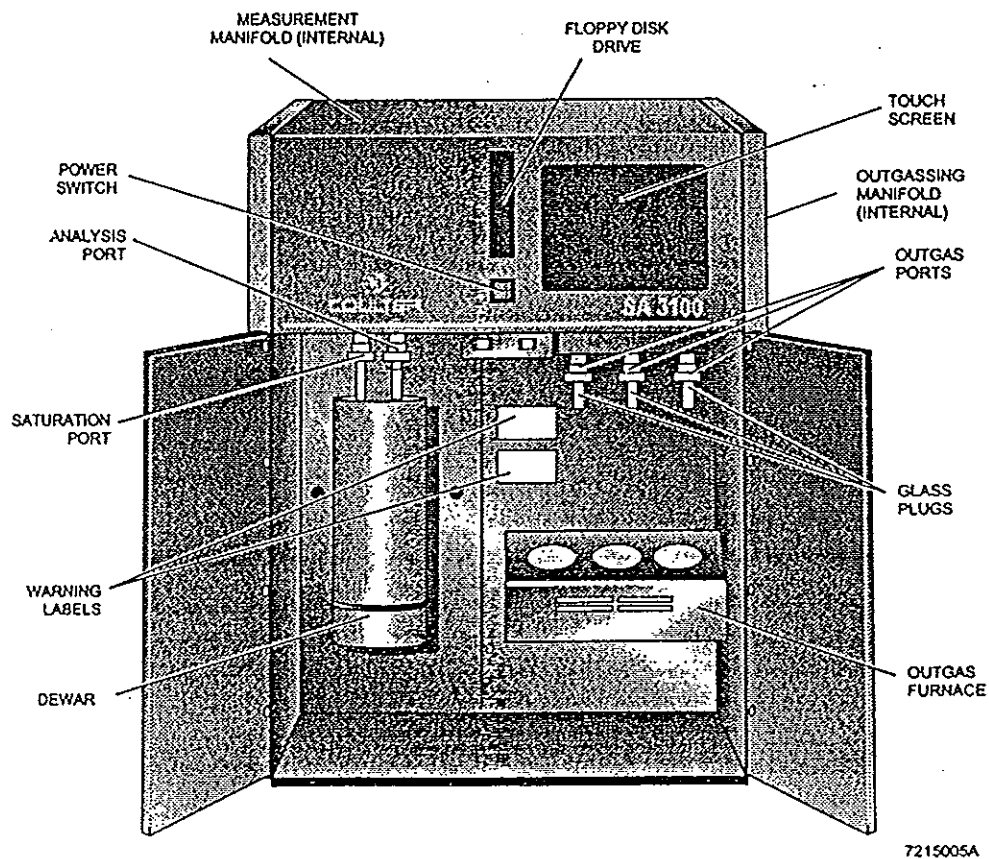


Figure G-1 SA 3100 analyzer front view.

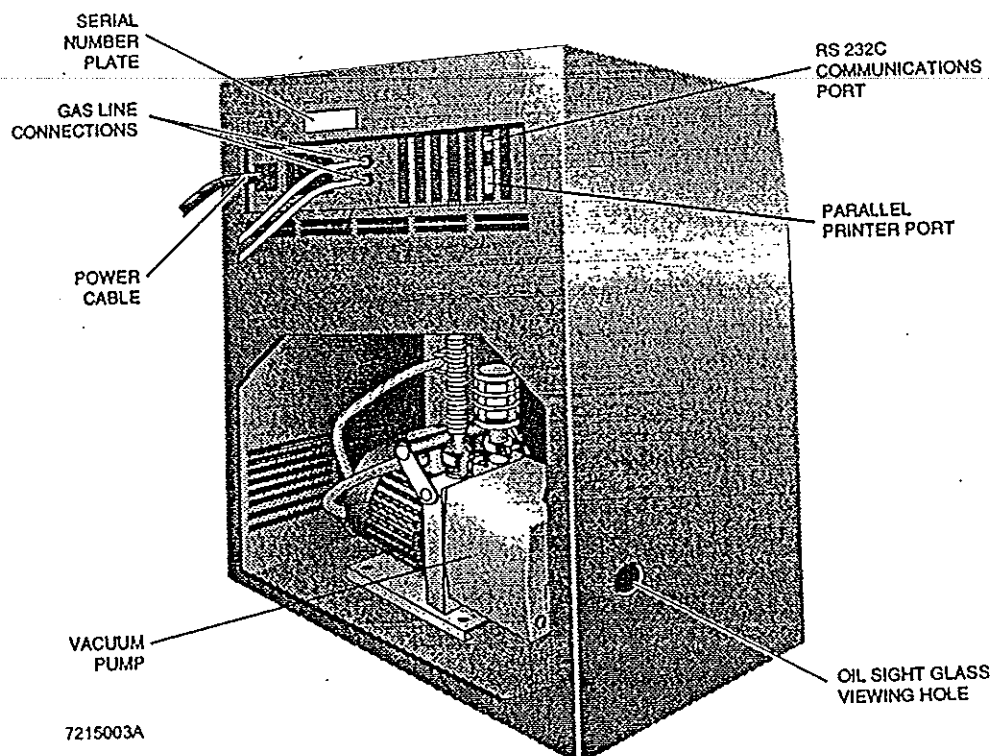


Figure G-2 SA 3100 analyzer back view.

#### G-4 Procedure

##### G-4.1 Weighing the sample tube assembly

Weigh the tube (including the tube insert) on the analytical balance to at least 0.001g precision. Make sure the following conditions are met before weighing the sample tube assembly.

- The sample tube is at room temperature.
- The sample tube is clean, dry, and without fingerprints. Use a lint-free laboratory tissue to remove fingerprints.
- The weighing pan on the analytical balance is clean.

- The sample tube is not charged with static electricity. Use an anti-static device to discharge the tube.

Make a note of the weight. It will need later. Interchanging parts after weighing introduces significant weight errors. Spaces are provided on sample tubes for marking, and indelible lab markers can be used on tube inserts to identify them uniquely, Don't make marks after weighing, however, as this changes the weight of the parts.

#### G-4.2 Adding sample to sample tube

The amount of sample added to the sample tube should be written certain limits to ensure the fastest and most accurate analysis.

- Remove the tube insert from the sample tube, then pour the weighed sample (0.1-0.2 g) into the sample tube using the sample loading funnel.
- Replace the tube insert in the sample tube.

#### G-4.3 Logging-in the sample

Logging in sample information allows the SA 3100 analyzer to keep track of sample status, and perform the desired analysis. In the following procedure will enter the proper parameters for outgassing and analysis.

- If no keys have been pressed since the unit was turned on, the **Analysis** screen is displayed. Press the **Outgas** key to move to the **Outgas** screen. If the **outgas** screen is displayed, go to next step.
- If no samples are currently outgassing, the instrument is ready to outgas the sample, indicated by the following message at the bottom of the **Outgas** screen

### LOAD AND LOG SAMPLES

Press Start Outgas when loaded

- In the central area of the **Outgas** screen, the three circles at the bottom of the vertical lines represent the three outgas ports; press the left-hand circle-this corresponds to the outgas port on which you will attach the sample tube. The **Sample Information** screen is displayed.
  - a. The only field that must be correct at this stage is the one on the **Profile** key. If 'BET 5' is not displayed on this key. Press the **profile** key, press the bottom labeled 'BET 5' on the **Profile** screen, and then press **OK**.
  - b. To enter an appropriate Sample ID for this sample, press the **Sample ID** key, use the displayed QWERTY keypad to enter characters, then press **Enter**.

#### G-4.4 Outgassing the sample

- Attaching the sample tube to an outgas port
  1. Loosen the knurled nut on the left-hand outgas port.
  2. Remove the cap from the sample tube, then insert the tube into the outgas port until it stops against the manifold.
  3. Tighten the knurled nut until finger-tight.
- Outgassing
  1. Set the outgas time and outgas temperature. Generally used 300°C for 60 minutes. After editing values, press **Enter** to confirm the change and return to the **Outgas** screen.

2. Press **Strat** on the **Outgas** screen. This initiates the outgassing procedure. For 60 minutes of outgassing at 300 °C, the entire procedure takes approximately 1 hour and 15 minutes. When outgassing is complete, the message *Outgassed* is displayed below the graphic for the outgassing port used. In addition, the following message is displayed at the bottom of the **Outgas** screen:

*REMOVE SAMPLES*

Press OK when removed

3. Remove the sample tube from the outgas port:
  - a. Have a sample tube cap ready.
  - b. Loosen the knurled nut and pull the tube out of the fitting.
  - c. Promptly place the cap on the sample tube (the tube is filled with nitrogen, so waiting too long will allow the gas to mix with air).
  - d. Press **OK**.

The sample is ready to be weighed and analyzed.

#### G-4.5 Weighing the outgassed sample

The outgassed sample weight is the weight used to determine the analysis results, and is therefore critical.

1. Weigh the tube (including the tube insert and sample) on the analytical balance to at least 0.001g precision. Remove the cap just before weighing and promptly replace it after weighing. Make sure the following conditions are met before weighing the sample tube after outgassing:

- The sample tube is at room temperature
  - The sample tube is clean and without fingerprints. Use a lint-free laboratory tissue to remove fingerprints.
  - The weighing pan on the analytical balance is clean.
  - The sample tube is not charged with static electricity. Use an anti-static device to discharge the tube.
2. Subtract the weight found earlier for the tube assembly without sample to determine the outgassed sample weight, and make a note of the result.

#### G-4.6 Analyzing the sample

1. Selecting the sample from the outgassed sample list
  - Press the **Analysis** key to move the **Analysis** screen.
  - Press the **Next Analysis** key. The **Outgassed Samples** screen is displayed.
  - Select the control sample by pressing the key marked with the Sample ID that entered, then press **OK**. The **Sample Information** screen is displayed.
2. Entering the outgassed sample weight
  - Enter the exact sample weight in the sample weight field
    - a. Press the **Sample Weight** key.
    - b. Enter the sample weight on the numeric keypad and press **Enter**.
  - Press **OK** on the **Sample Information** screen to confirm entries and return to the main **Analysis** screen. The following message is displayed on the screen:



*LOAD SAMPLE*

Press OK when loaded

3. Loading the sample

- Attach the sample tube to the analysis port:
  - a. Loosen the knurled nut on the analysis port.
  - b. Remove the cap from the sample tube, then promptly insert the tube into the port until it stops against the manifold.
  - c. Tighten the knurled nut until finger-tight.

The tube does not have to feel rigid in the fitting to be sealed. If a gentle downward pull on the tube does not pull it out of the fitting, it is installed properly.

- Press **Start**. The status message on the screen reads.

*WAIT*

Sample Evacuating.

4. Filling and loading liquid nitrogen dewar

- If the dewar is new, temper the dewar by swirling a small quantity of liquid nitrogen in the dewar.
- Add liquid nitrogen to the dewar until it is half-full.
- When the message

*LOAD DEWAR*

Press Start Analysis when loaded

Appears, load the half-full dewar into the dewar into the dewar rack.

- Using the dewar funnel fill the dewar to within 2-3 cm. of the top with liquid nitrogen.

---

- Install the insulating dewar lid.
- Press **Start Analysis**. The sample analysis proceeds automatically.

## Appendix H

### Table of result

#### H-1 Test the appropriate condition for impregnation method.

Table H-1 Test the sequence of impregnation method

Nickel Impregnated	Nickel Content in Catalyst Steam Before Impregnation	Nickel Content in Catalyst Steam after Impregnation
0	28	21
800	641	774
1600	1355	1491
2400	1973	2274
3200	2688	3153

#### H-2 Test the effect of nickel , vanadium, nickel+vanadium on surface area.

Table H-2 Effect of Nickel on surface area

Nickel Content (ppm)	Surface area (m <sup>2</sup> /g)	
	Catalyst A	Catalyst E
0	129.94	119.41
1000	130.57	113.73
2000	129.18	112.39
3000	128.6	111.22
4000	123.24	109.02

**Table H-3** Effect of vanadium on surface area

Vanadium Content (ppm)	Surface area (m <sup>2</sup> /g)	
	Catalyst A	Catalyst E
0	134.68	119.41
1000	111.68	103.11
2000	86.683	89.917
3000	76.621	81.3
4000	33	65.28

**Table H-4** Effect of nickel/vanadium on surface area of catalyst E

Nickel/Vanadium Content (ppm)	Surface Area (m <sup>2</sup> /g)
0/0	119.41
1000/1000	108.39
2000/2000	86.147
3000/3000	63.818
4000/4000	47.935

**H-3 Test the effect of nickel contamination on catalytic properties.****Table H-5 Effect of nickel on catalytic properties (Catalyst A)**

Nickel Content (ppm)	Percent Hydrogen (Feed Basis)	Percent Conversion	Gasoline Yield	Coke Yield	Gas Yield
0	0	59.6	28.86	1.77	28.97
1000	0	65.91	39.24	1.96	24.71
2000	0.0445	55.06	29.55	2.11	23.41
3000	0.0445	50.925	24.45	2.25	24.23
4000	0.054	49.305	23.445	2.32	23.54

**Table H-6 Effect of nickel on catalytic properties (Catalyst E)**

Nickel Content (ppm)	Percent Hydrogen (Feed Basis)	Percent Conversion	Gasoline Yield	Coke Yield	Gas Yield
0	0	59.09	41.07	1.55	16.59
1000	0	53.05	32.88	1.5	18.82
2000	0.035	51.35	31.83	1.77	17.91
3000	0.065	43.76	29.37	1.88	12.51
4000	0.15	38.14	16.47	2.07	19.6

**H-4 Test the effect of vanadium contamination on catalytic properties.****Table H-7** Effect of vanadium on catalytic properties (Catalyst A)

vanadium Content (ppm)	Percent Hydrogen (Feed Basis)	Percent Conversion	Gasoline Yield	Coke Yield	Gas Yield
0	0	61.72	36.27	1.77	23.68
1000	0	47.53	31.51	1.81	19.34
2000	0	41.21	25.54	1.33	15.27
3000	0	37.18	21.12	1.27	11.55
4000	0	18.41	12.73	0.91	6.27

**Table H-8** Effect of vanadium on catalytic properties (Catalyst E)

vanadium Content (ppm)	Percent Hydrogen (Feed Basis)	Percent Conversion	Gasoline Yield	Coke Yield	Gas Yield
0	0	57.06	37.34	1.41	18.46
1000	0	51.2	33.98	1.45	15.92
2000	0.02	41.07	28.04	1.5	11.7
3000	0.02	36.22	25.32	1.37	9.52
4000	0.03	32.37	21.66	1.22	9.49

H-5 Test the effect of nickel/vanadium contamination on catalytic properties.

Table H-9 Effect of nickel/vanadium on catalytic properties (Catalyst E)

vanadium Content (ppm)	Percent Hydrogen (Feed Basis)	Percent Conversion	Gasoline Yield	Coke Yield	Gas Yield
0/0	0	58.59	38.72	1.41	18.46
1000/1000	0.042	45.36	29.85	1.68	13.83
2000/2000	0.05	31.97	21.07	1.97	8.93
3000/3000	0.034	22.98	15.35	1.67	5.96
4000/4000	0.033	9.67	3.01	1.66	5.01

## Vitae

---

**Name** Mr. Thanong Hongdul

**Birth Date** March 12, 1976

### **Educational Attainment**

<b>Degree</b>	<b>Name of Institution</b>	<b>Year of Graduation</b>
B.Eng. (Chem.)	Mahidol University	1998